Micromorphology and Genetic Interpretations of Selected Colombian Andosols

By

FRANK GILBERT CALHOUN, JR.

A DISSERTATION PRESENTED TO THE GRADUATE COUNCIL OF
THE UNIVERSITY OF FLORIDA IN PARTIAL
FULFILLMENT OF THE REQUIREMENTS FOR THE DEGREE OF
DOCTOR OF PHILOSOPHY

UNIVERSITY OF FLORIDA
1971

UNIVERSITY OF FLORIDA
3 1262 08552 4873

ACKNOWLEDGMENTS

The author wishes to express his sincere appreciation to Dr. Victor W. Carlisle for his guidance, encouragement, and assistance during the progress of this investigation. Appreciations are extended to Drs. R. E. Caldwell, H. L. Popenoe, F. N. Blanchard, and A. E. Lugo for their interest and participation on the Supervisory Committee and review of this manuscript.

Supreme gratitude is expressed to Dr. Carlos Luna for his hospitality and guidance during the Colombian portion of this research. The author is grateful to Ingeniero Agronomo Victor Vega and Dr. Francisco Silva for laboratory facilities they most kindly made freely available. Appreciation is expressed to Instituto Geografico "Agustin Codazzi" for travel arrangements, both logistic and financial within Colombia. Gratitude is extended to Sr. Leonidas Mejía for his assistance in micromorphological analyses during the embryonic stage of this investigation. Sincere thanks are expressed to the laboratory technicians in the "Laboratorio de Suelos" for helping conduct many of the routine chemical and physical analyses. The author also cannot fully express his deep appreciation to the agronomists and other Colombian citizens for the many kindnesses they extended to him.

The author is indebted to Dr. C. F. Eno for awarding the NDEA Title IV Fellowship which facilitated this study. Gratitude is extended to the Center for Tropical Agriculture for providing additional financial support for this work both in Colombia and at the University of Florida.

Thanks are extended to Dr. D. H. Hubbell for access to photographic equipment and laboratory space during micromorphological investigations. Appreciation is expressed to Dr. L. W. Zelazny for operational assistance in X-ray diffraction techniques and helpful consultation pertaining to this study.

A special thanks to Sr. Julian Velez for occasional Spanish translation assistance.

The author wishes to express special commendation to Mrs. Lillian S. Ingenlath for excellent typing and proofing of this dissertation.

Above all, the author takes this opportunity to express deepest gratitude to his wife, Nancy, whose unyielding encouragement, labor, and understanding contributed beyond measure to the successful completion of this dissertation.

TABLE OF CONTENTS

	Page
ACKNOWLEDGMENTS	ii
LIST OF TABLES	viii
LIST OF FIGURES	ix
ABSTRACT	xiii
INTRODUCTION	1
LITERATURE REVIEW	3
Andosols	3
Definition	3
Occurrence	3
Morphology	4
Physical	5
Chemical	6
Mineralogy	7
Microfabric	8
Allophane	9
Introduction	9
Structure and Composition	10
X-Ray Diffraction Data	12
Electron Microscopy	13
Differential Thermal Analysis	13
Infrared Spectroscopy	14
Dehydration and Rehydration	15
Surface Area	16
Optical Properties	16
Ion Exchange and Sorption	17
Allophane-Organic Reactions	19
Pedogenetic Weathering	20
Definition	23
MATERIALS AND METHODS	24
Site Selection	24
Field Procedures	26

Page

Physical Methods 26

Particle Size Distribution 26
Bulk Density 27
Fifteen-Atmosphere Water Content 27

Chemical Methods 27

pH Determination 27
Cation Exchange Capacity 27
Exchangeable Calcium and Magnesium 27
Exchangeable Potassium 27
Exchangeable Sodium 28
Organic Carbon 28
Exchangeable Aluminum 28
Free Iron Oxides 28

Mineralogical Methods 28

Dispersion and Fractionation of Clay 28
X-Ray Diffraction 30
Differential Thermal Analysis 32
Infrared Spectrometry Analysis 33
Sodium Fluoride Test for Allophane 34
Sand Mineralogy 34

Micromorphology - Thin Section Techniques 35

Impregnation 35
Preparation of Thin Sections 35
Analysis 36

DESCRIPTION OF MARIÑO STUDY AREA 37

Location 37

Physiography 37

Bedrock and Surficial Geology 39

Climate 43

Plant Ecology 45

Dry Sub-Tropical Forest 45
Dry Lower Montane Forest 46
Humid Lower Montane Forest 47
Humid Montane Forest 47
Sub-Alpine Grasslands 49

Page

RESULTS AND DISCUSSION 51

Methodology 51

Organic Matter Oxidation 51
Dispersion of Andosol Clays 51

Morphology 56

Chemical Properties 60

Soil Reaction 60
Organic Carbon 65
Exchangeable Bases 65
Exchangeable Aluminum 66
Cation Exchange Capacity 67
Free Iron Oxides 67
Sodium Fluoride Test for Allophane 67
Genetic Interrelationships of Chemical Properties 67

Physical Properties 69

Sand Mineralogy 72

Light Minerals 72
Heavy Minerals 77
Genetic Relations of Sand Mineral Distributions 78

Clay Mineralogy 79

X-Ray Diffraction 79
Infrared Analysis 102
Differential Thermal Analysis 117

Micromorphology 119

Descriptive Features 124
Genetic Interpretations 128

SUMMARY 133

CONCLUSIONS 139

APPENDIX 143

Page

LITERATURE CITED 190

BIOGRAPHICAL SKETCH 197

LIST OF TABLES

Table		Page
1.	Climate-vegetation relationships in Departamento Nariño, Colombia	44
2.	Fe, Si, and Al amounts in extracts after treatment of certain Andosol horizons by NaOCl or H_2O_2	52
3.	Effect of pretreatment and dispersing agent on particle size distribution	55
4.	Chemical properties of selected Colombian soils	61
5.	Physical properties of selected Colombian soils	70
6.	Sand (50-500 μ fraction) mineralogy of selected Colombian soils	73
7.	Crystalline minerals recognized from X-ray diffraction patterns of the fine clay ($<0.2\ \mu$) and coarse clay ($0.2 - 2\ \mu$) fractions of selected Colombian soils	92
8.	Detailed field descriptions of selected Colombian soils	143
9.	The d/n spacing of crystalline minerals recognized from X-ray diffraction patterns of the fine clay ($<0.2\ \mu$) fraction of selected Colombian soils	157
10.	The d/n spacing of crystalline minerals recognized from X-ray diffraction patterns of the coarse clay ($0.2\text{-}2\ \mu$) fraction of selected Colombian soils	161
11.	Micromorphology of selected Colombian Andosols	166

LIST OF FIGURES

Figure		Page
1.	Departamento of Nariño located in southwestern Colombia	25
2.	Colombia, South America, showing location of the Departamento of Nariño	38
3.	Cross-section of Nariño, Colombia, study area showing locations of profiles 1-6 relative to Volcano Galeras	41
4.	Pumice beds 1 km north of Ecuadorian border	42
5.	Typical vegetation of sub-alpine grassland near profile 6	50
6.	Color photographs of profiles 1-4 representing altitudinal sequence of 2,000 - 2,730 m . . .	58
7.	Color photographs of profiles 5 and 6 representing altitudinal sequence of 3,120 - 3,510 m and ancillary profiles 8 and 9 at 3,020 and 3,060 m	59
8.	X-ray diffraction patterns of Mg-saturated air dry, K-saturated 100C, and K-saturated 500C treated coarse clay of horizon A3 profile 7 demonstrating identification of metahalloysite, hydrated halloysite, illite, and vermiculite by changes in d-spacings	80
9.	X-ray diffraction patterns of Mg-saturated coarse clay (0.2 - 2 μ) and fine clay (<0.2 μ) fractions of profile 1	82
10.	X-ray diffraction patterns of Mg-saturated coarse clay (0.2 - 2 μ) and fine clay (<0.2 μ) fractions of profile 2	83
11.	X-ray diffraction patterns of Mg-saturated coarse clay (0.2 - 2 μ) and fine clay (<0.2 μ) fractions of profile 3	84

Figure Page

12. X-ray diffraction patterns of Mg-saturated coarse clay (0.2 - 2 μ) and fine clay (< 0.2 μ) fractions of profile 4 85

13. X-ray diffraction patterns of Mg-saturated coarse clay (0.2 - 2 μ) and fine clay (< 0.2 μ) fractions of profile 5 86

14. X-ray diffraction patterns of Mg-saturated coarse clay (0.2 - 2 μ) and fine clay (< 0.2 μ) fractions of profile 6 87

15. X-ray diffraction patterns of Mg-saturated coarse clay (0.2 - 2 μ) and fine clay (< 0.2 μ) fractions of profile 7 88

16. X-ray diffraction patterns of Mg-saturated coarse clay (0.2 - 2 μ) and fine clay (< 0.2 μ) fractions of profile 8 89

17. X-ray diffraction patterns of Mg-saturated coarse clay (0.2 - 2 μ) and fine clay (< 0.2 μ) fractions of profile 9 90

18. X-ray diffraction patterns of Mg-saturated coarse clay (0.2 - 2 μ) and fine clay (< 0.2 μ) fractions of profile 10 91

19. Infrared spectra of coarse clay (0.2 - 2μ) and fine clay (< 0.2 μ) fractions of profile 1 103

20. Infrared spectra of coarse clay (0.2 - 2 μ) and fine clay (< 0.2 μ) fractions of profile 2 104

21. Infrared spectra of coarse clay (0.2 - 2 μ) and fine clay (< 0.2 μ) fractions of profile 3 105

22. Infrared spectra of coarse clay (0.2 - 2 μ) and fine clay (< 0.2 μ) fractions of profile 4 106

23. Infrared spectra of coarse clay (0.2 - 2 μ) and fine clay (< 0.2 μ) fractions of profile 5 107

24. Infrared spectra of coarse clay (0.2 - 2 μ) and fine clay (< 0.2 μ) fractions of profile 6 108

Figure		Page
25.	Infrared spectra of coarse clay (0.2 - 2 μ) and fine clay (< 0.2 μ) fractions of profile 7	109
26.	Infrared spectra of coarse clay (0.2 - 2 μ) and fine clay (< 0.2 μ) fractions of profile 8	110
27.	Infrared spectra of coarse clay (0.2 - 2 μ) and fine clay (< 0.2 μ) fractions of profile 9	111
28.	Infrared spectra of coarse clay (0.2 - 2 μ) and fine clay (< 0.2 μ) fractions of profile 10	112
29.	Infrared spectra of coarse clay (0.2 - 2 μ) and fine clay (< 0.2 μ) fractions of Km 119 buried argillic horizon; Ward's halloysite No. 12; and KBr blank	113
30.	Differential thermal patterns of coarse clay (0.2 - 2 μ) fraction of selected horizons from profiles 1 and 10	118
31.	Photomicrograph of A11 horizon, profile 3 showing two fecal pellets set against matrix of interconnected ortho-craze planes and orthovughs	120
32.	Photomicrograph of A11 horizon, profile 3 showing organan on andesite lithorelict and subrounded blocky secondary structural unit set against matrix of interconnected orthovughs	120
33.	Photomicrograph of A11 horizon, profile 3 showing isotic plasmic fabric	121
34.	Photomicrograph of A12 horizon, profile 3 showing feldspar grain with weathering fractures perpendicular to twins	121
35.	Photomicrograph of [B] horizon, profile 3 showing weakly silasepic and undulic plasmic fabric	122
36.	Photomicrograph of [B] horizon, profile 3 showing hornblende grain with thin, siliceous isotropic border	122

Figure Page

37. Photomicrograph of [B] horizon, profile 3 showing large sesquioxidic (hematitic) nodule and several smaller ones 123

38. Photomicrograph of C horizon, profile 3 showing hornblende grain with thin, discontinuous sesquan (hematan) set against matrix of interconnected orthovughs 123

Abstract of Dissertation Presented to the
Graduate Council of the University of Florida in Partial Fulfillment
of the Requirements for the Degree of Doctor of Philosophy

MICROMORPHOLOGY AND GENETIC INTERPRETATIONS
OF SELECTED COLOMBIAN ANDOSOLS

By

Frank Gilbert Calhoun, Jr.

August, 1971

Chairman: Dr. Victor W. Carlisle
Major Department: Soil Science

Ten soil profiles from the Andean highlands of Departamento Mariño, Colombia, were investigated by use of chemical, physical, mineralogical, and micromorphological techniques in order to elucidate pedogenetic processes in soils derived from andesitic volcanic ash and similar parent materials. Six Andosol profiles were selected in an altitudinal sequence from 2,000 m to 3,510 m as representative of maximum range of weathering severity experienced by aeolian pyroclastic materials in the altiplano of Mariño. Four additional soil profiles, developing in parent materials with varying degrees of ash influence, provided supplementary pedogenetic information. All of the soils were influenced by annual rainfall range of 500-2,000 mm and an annual isothermal temperature range of 6C to 18C which was closely related to altitude.

The following parameters were determined on selected horizons of each soil: (a) particle size distribution, (b) bulk density, (c) fifteen atmosphere water content, (d) pH in water and N KCl, (e) exchangeable cations, (f) cation exchange capacity, (g) organic carbon, (h) free iron oxides, (i) X-ray diffraction of fine clay (< 0.2μ) and coarse clay (0.2 - 2μ), (j) infrared analysis of fine clay and coarse clay, (k) NaF test for allophane, and (l) light and heavy mineral contents of the sand

(50 - 500 μ) fraction. Thin sections were prepared from selected horizons of Andosol profiles 1-6 (2,000 - 3,510 m) and described in detail.

The above mentioned analyses of Andosol profiles 1-6 revealed the following trends with increasing elevation: (1) increases in exchangeable K and Al; organic carbon; volcanic glass, pyroxenes, and andesite lithorelicts in the 50 - 500 μ sand fraction; allophane in <2 μ clay fraction; and isotropism of plasmic fabrics in subsurface horizons; (2) decreases in pH values; exchangeable Ca and Na; free iron oxides; quartz, feldspar and hornblende in 50 - 500 μ sand fraction; hydrated halloysite in the < 2 μ clay fraction; sesquioxidic nodules; and birefringence of plasmic fabrics in subsurface horizons.

Varying amounts of hydrated halloysite, metahalloysite, vermiculite, cristobalite, gibbsite, feldspar, and quartz were identified by infrared and X-ray analyses of the coarse clay fraction of Andosol profiles 1-6. Hydrated halloysite, metahalloysite, and possibly allophane A were identified in the fine clay fraction.

Andosol surface horizons generally had isotic plasmic fabrics while subsurface horizons exhibited weakly undulic and silasepic plasmic fabrics which were replaced by isotic plasmic fabrics at higher elevations. The term "Andic" was proposed as a modifier for this sequence of fabric types.

A clay mineral weathering sequence of allophane $\rightarrow$ metahalloysite $\rightarrow$ hydrated halloysite was postulated. The maturation of this sequence increased with profile depth and with increasing altitude. Coarse clay vermiculite was hypothesized as being transient or insufficient time has elapsed for it's transformation to other 2:1 phyllosilicates. It was

further postulated that vermiculite pedogenesis occurred rather rapidly with some modification from a primary mineral source.

INTRODUCTION

Opportunities have been all too rare for genetic investigations in the tropics involving soils derived from materials in an initial state of weathering. Research in temperate regions such as New Zealand and Japan has disclosed that unique weathering products occur during the early stages of primary mineral degradation in pyroclastic materials. Soils derived from such comminuted aeolian pyroclastic materials (usually andesitic) have been referred to as Andosols. Andosols present very real management challenges due to their aberrant physical, chemical, and mineralogical properties. These aberrations are in large part due to the presence of allophane which is a primitive weathering product of volcanic glass.

There is reason to believe that the genesis of tropical Andosols is to some degree thermal dependent. Wright (1964) noted a "thermal progression" in morphology of low latitude Andosols in South America. There was every reason to assume that morphological changes were related to chemical and mineralogical differences; however, laboratory data were unavailable for substantiation of this potential relationship. This investigation provides such analytical data. It also may be considered as an addition to the general reservoir of knowledge regarding the nature and properties of tropical soils.

Colombia is one of the worlds' largest coffee exporters. This crop is grown primarily and most efficiently on volcanic ash soils of the highlands. Additionally these soils hold an important role in small

grain and vegetable production for local consumption. The populace of Colombia is concentrated in the Andean highlands. It's economy is still primarily agrarian and population expansion will continue to apply considerable pressure on soil resources, especially the comparatively fertile Andosols.

A dire need evolves, then, for an accurate inventory and characterization of Andosols, especially in the tropics where they most commonly occur. Genetic interpretation of these data can add to understanding of Andosols with concomitant implications to their efficient management. It would behoove the temperate climate oriented pedologists to participate in and contribute to these programs in order to broaden their scope and understanding of soils derived from a wide spectrum of parent materials. Selection of study sites in close proximity to areas of historical volcanism would facilitate pedological investigation of soils dominated by easily weatherable primary minerals. With this in mind, arrangements were made with the Instituto Geografico "Agustin Codazzi" in Bogotá, Colombia, to participate in their program of characterizing and classifying the Andosols of Colombia.

The intent and objective of the study presented herein was to elucidate pedogenetic processes occurring in selected Colombian Andosols. This was expedited by use of chemical, physical, mineralogical, and heretofore seldom used micromorphological parameters.

LITERATURE REVIEW

Andosols

Definition

During summary and technical discussions of a "Meeting on the Classification and Correlation of Soils From Volcanic Ash" held in Tokyo, Japan (Anonymous, 1964), the following definition was proposed for Andosols: "Mineral soils in which the active fraction is dominated by amorphous material (minimum about 50%). These soils have a high sorptive capacity, a relatively thick friable dark "A" horizon, are high in organic matter, have a low bulk density and a low stickiness. They may have a (B) horizon and not show significant clay movement. These soils occur under humid and sub-humid conditions."

With the advent of a new soil classification system in the United States (U. S. Soil Survey Staff, 1970), an important suborder referred to as "Andepts" was developed which, according to Fiach (1969), encompassed many of the soils that had been called Andosols. Andepts are described as "more or less freely drained inceptisols that have low bulk density and appreciable amounts of allophane with a high exchange capacity, or that have mostly pyroclastic materials in the silt, sand, and gravel fractions."

Occurrence

According to the U. S. Soil Survey Staff in Soil Taxonomy (1970), Andepts occur in or near mountains with active volcanoes from the

equator to high latitudes. Andosols, therefore, occur widely throughout the Pacific ring of volcanism and in volcanic regions of the East Indies and Africa.

Luna (1969a) reported that in Colombia typical Andosols occur most commonly on gentle, slightly undulating topography between 1,300 m and 3,000 m above sea level in the Andes mountain range. Luna further stated that studies on volcanic ash soils and volcanism in general were very limited in Colombia. The implication was that expanded programs in these areas would be quite desirable.

Varela (1963) completed a general study of soils in the Pasto-Rio Mayo sector in Departamento Nariño, southern Colombia. He reported chemical, physical, and morphological properties for several profiles collected from six major soil areas in the sector. The dominant group of the six were soils derived from andesitic volcanic ash. Varela suggested that a large group of soils derived from volcanic tuff had "hardpans" cemented by carbonates and/or calcareous clay. Field observation of these soils by the author affirmed that the "hardpan" is actually a duripan as the primary cementing agent was silica.

Morphology

Wright (1964) stated that, even though Andosols occur under a wide range of climatic conditions from low to high latitudes, the gross morphology of the soil profiles remains rather uniform. He listed several properties as common to Andosols throughout the world:

(a) deep profiles often with distinct depositional stratification,

(b) thick dark surface horizons high in negligibly biodegradable humic compounds,

(c) prominent yellowish-brown subsoil colors and "smeariness" (thixotropism),

(d) low bulk density and high water-holding and retention capacity,

(e) weak structural aggregation and lack of cutans on ped surfaces, and

(f) lack of stickiness or plasticity when moist.

Wright also discussed, in detail, properties of both high and low latitude Andosols. He indicated that at low latitudes there is a thermal sequence with altitude which imparts only faint morphological trends to the soil profiles. The following differences with increasing temperature were noted:

(a) horizonation progressed from AC to A1-A3-C to A-(B)-C as moisture increased,

(b) topsoil colors changed from black to dark brown,

(c) weak granular structure progressed to moderate blocky in the surface horizons,

(d) subsoil colors became redder along with some plasticity development, and

(e) organic matter content decreased.

Physical

Very high natural moisture contents (measured on a weight basis) and associated low dry bulk densities are common features of volcanic ash soils (Swindale, 1969). Both total water and 15-bar water contents are high, however, and when measured on a volume basis, the values for available water are not markedly different from other soils. When these soils are dried to 15 atmospheres or beyond, the shrinkage becomes increasingly irreversible. Gradwell and Birrell (1954) dis-

covered that if soil samples have been previously air-dried there was a marked decrease in liquid limit and plastic limit values as the allophane content increased.

Andosols, in general, have a very high total porosity. Yamazaki et al. (1963) reported a figure of 80% for Kanto loam, a predominant soil around Tokyo. Swindale (1969) stated that associated with this high porosity is a high saturated permeability, although these soils are notoriously difficult to rewet after they are dried because the organic substances adhering to particle surfaces are generally hydrophobic and the contact angles are large. Youngberg and Dyrness (1964) published a range of 68-85% pore space for some Oregon Andosols.

According to Swindale (1969), the particle size range in Andosols is quite often very large. He further stated that particle size distribution data are difficult to obtain due to poor dispersion characteristics of these soils.

Chemical

In general, pH values of Andosols range above 5.0 (Müller et al., 1968, and Flach, 1964).

Cation exchange capacity values for these soils are quite high. Birrell and Gradwell (1956) have shown that this parameter varies with concentration of leaching solution, nature of ions in solution, and volume of water content of the washing alcohol. Birrell (1964) and Frink (1964) pointed out that conventional CEC determination may be subject to considerable error when applied to soils containing amorphous mineral colloids and all such determinations must be interpreted with caution.

Base saturation covers a wide range of values although pH values

can remain comparatively high when base saturation values are low. According to Swindale (1969), this can be attributed to the pH-dependent charge of amorphous mineral colloids.

Andosols are known to fix large quantities of phosphate, molybdate, and other similarly structured anions. Saunders (1959) and Müller et al. (1968) have shown for New Zealand and Costa Rican soils, respectively, that phosphate is bound to alumina. Blasco (1969) reported data for upland soils in Departamento Nariño, Colombia, and claimed that inert phosphorus represented about 50% of the total P with rather low values for other P fractions.

Andosols invariably contain relatively large amounts of organic matter in their surface horizons. Kosaka et al. (1962) and Aomine and Kobayashi (1964a, 1964b) demonstrated the negligible biodegradability of organic materials in these soils.

Mineralogy

Besoain (1969b) presented an extensive review of literature on the mineralogy of volcanic ash soils. The sand mineralogy of these soils is composed mainly of primary minerals such as ferromagnesiums (olivines, pyroxenes, and amphiboles), quartz, feldspars, magnetite, and various silicate complexes. The silt fraction may be constituted of primary and secondary minerals. The secondary minerals, especially in high allophane soils, may be aggregates of clay occurring as pseudomorphs of silt. Gibbsite and hydrated iron oxides frequently tend to accumulate in the fine silt fraction (5-2 μ).

Besoain (1969b) went into considerable detail regarding the occurrence and formation of various secondary minerals in the clay fraction of volcanic ash soils. Allophane and halloysite were the

most prevalent species. Weathering sequences involving these two members were especially interesting and will be discussed in greater detail later. Under special environmental conditions, such secondary mineral species as kaolinite, gibbsite, bohemite, imogolite, montmorillonite, hissingerite, vermiculite, chlorite, sericite, palagonite, amorphous silica, amorphous alumina, iron oxides, and amorphous and crystalline titanium oxides have been identified in the clay fraction of Andosols.

Microfabric

There is a dearth of published information on the micromorphological properties of Andosols. Frei (1964) described the microfabric of a black Andean or "Paramo" soil and a brunizem soil located in the central Andes of Ecuador. The black Andean soil was derived from andesitic volcanic ash and was characterized by having highly stable crumbs which formed a spongy and very porous matrix. He speculated that black cutans on ped surfaces in the lower epipedon resulted from precipitation of dispersed organic matter migrating downwards by percolation. Below the epipedon in the B/C horizon, organans occurred on all the primary sand-sized minerals. Frei also suggested that perhaps colloidal silica acted as a complexing and mobilizing agent for organic colloids with subsequent precipitation on mineral surfaces at lower depths in the profile.

Mejía (1971) concluded from fabric analyses of a profile of the Corzo series (an Andosol on the "Sabana de Bogotá") that these data provided valid additional criteria for the classification of ash-derived soils. He outlined several unique characteristics the most important of which was the presence of an isotic plasmic fabric (see

Brewer, 1964, for discussion of this and subsequent terminology on fabric analysis) in the A and B horizons grading to undulic plasmic fabric in the deepest horizons. This feature along with characteristic void patterns, cutan mineralogy and arrangement, and sand mineralogy suggested a unique fabric type peculiar to Andosols. Mejía proposed the generic name "Fabrica Andica" (Andic Fabric) for this fabric class. Mejía maintained, however, that rigorous statistical studies over a wide range of Andosols was needed before precise definition and adoption of this fabric type could be realized.

Luna (1969a) mentioned the existence of a fabric formed by a plasma of porous aspect and of isotropic character in a Typic Dystrandept of Departamento Antioquia, Colombia. The fabric type was tentatively designated as Amorphic.

Allophane

Introduction

As mentioned earlier, Andosols are characterized by low bulk densities and low base saturations in addition to high organic carbon contents and high phosphate and water retention capacities. These properties are to a considerable degree due to high quantities of allophane (a disordered hydrous alumino-silicate) in the clay fraction. The unique qualities of allophane in contrast to the more common ordered alumino-silicates present special management problems involving these soils.

Due to the widespread distribution of volcanic ash soils and a well-developed science of pedology in Japan and New Zealand, considerable research on allophane has been undertaken in these two countries

in the past 20 years. This review will outline and discuss a major portion of this research in addition to accomplishments in other areas of the world. Use of the term "allophane" will be restricted to pedogenetic disordered hydrous alumino-silicates derived from volcanic ash, generally of an andesitic type.

Structure and Composition

Ross and Kerr (1934) were probably the first workers to present significant data on allophane. They reported for geologic allophane: (a) variable chemical composition, (b) variable index of refraction, (c) no definite crystal structure (lack of sharp X-ray powder peaks), and (d) no regular molecular arrangement as interpreted from infrared spectroscopy. Ross and Kerr referred to allophane as an amorphous alumino-silicate and little more was ascertained as to its structure until the 1950's when Japanese and New Zealand pedologists began to explore more closely the weathering sequences of volcanic ash clays. Advances in structural knowledge of allophane came about through the increased use of techniques such as X-ray and electron diffractometry, differential thermal analysis, infrared spectroscopy, and electron microscopy.

Throughout the 1950's and early 1960's, several investigators discovered that allophane in volcanic ash soils could exist in a structural continuum below the "relative crystalline purity" of halloysite or kaolinite. Fieldes (1955) indicated a weathering sequence of increasing crystallinity: allophane B ⟶ allophane A ⟶ metahalloysite. Yoshinaga and Aomine (1962a) claimed to have discovered a more crystalline alumina-rich species with fibrous morphology which they called "imogolite." Later Aomine and Miyauchi (1965) through the use

of clay mineralogical techniques reported that they were able to isolate two types of "imogolite:" A and B. "Imogolite B" was supposed to represent a more crystalline stage than "imogolite A."

Wada (1966) began to increase the specificity of allophane structure through the use of infrared absorption with deuterium (D_2O) exchange of hydroxyl groups (OH---> OD) at room temperature to 100C. This was done on a comparative basis with montmorillonite and hydrated halloysite. He found that all the OH groups in allophane could be replaced by OD, while very minor and partial replacements resulted for montmorillonite and halloysite. Wada concluded that a sharp line exists between structural OH groups and absorbed H_2O in allophane.

Wada (1967) then summarized chemical, infrared spectroscopy, and morphological data for soil allophane and suggested two end-members with chemical composition $2SiO_2 \cdot Al_2O_3 \cdot 3H_2O$ (allophane) and $SiO_2 \cdot Al_2O_3$ $2H_2O$ ("imogolite") along with a structural scheme for the two end-members and intermediate compositions. He proposed a structure for allophane with a 1:1 Si/Al ratio composed of a silica tetrahedral chain and an alumina octahedral chain sharing a corner of the respective tetrahedron and octahedron. Addition of another alumina octahedral chain to the silica tetrahedral chain results in formation of allophane with a 1:2 Si/Al ratio ("imogolite"). Wada reported that noncrystalline and poorly crystalline X-ray patterns of allophane with a Si/Al ratio 1:1 and 1:2 could be interpreted in terms of the differences in the ease with which the respective unit chains are aligned.

Apparently there can be considerable substitution of Al for Si in tetrahedral co-ordination in allophane which definitely segregates it from halloysite and kaolinite. Wada's (1967) scheme claimed to predict

the transformation of Al co-ordination from 6 to 5 upon dehydration and further to 4 upon dehydroxylation.

Russell et al. (1969) presented supporting evidence for the uniqueness of "imogolite" which they believed warranted its classification as a distinct mineral species. They interpreted electron diffraction patterns in terms of repeat units 8.4A parallel and 23A perpendicular to the fiber axis. They proposed an alternate structure to that of Wada's (1967) for "imogolite" consisting of discontinuous distorted chains of Al-O octahedra linked through isolated Si_2O_7 groups. They contended that the existence of the Si_2O_7 groups was supported by an infrared absorption band near 930 cm^{-1}. They reported compositions of $3\ SiO_2 \cdot 2Al_2O_3 \cdot 5H_2O$ and $SiO_2 \cdot Al_2O_3 \cdot 3H_2O$ for "imogolite" and allophane, respectively, somewhat different from Wada's formulae.

X-Ray Diffraction Data

The presence or absence of X-ray diffraction peaks for allophane would, of course, be highly dependent upon its stage of crystallinity between partially weathered volcanic glass and hydrated halloysite. X-ray data have been presented in numerous papers generally as a subordinate analysis.

Separation of the clay fraction ($< 2\mu$) into smaller size ranges has usually facilitated diffraction investigations of allophane. Yoshinaga and Aomine (1962a) showed that the 2-1 μ fraction of a Uemura soil exhibited several distinct diffraction peaks indicating the presence of quartz, cristobalite, feldspar, and gibbsite. They were able to isolate "imogolite" and allophane using differential dispersion properties. In the $< 0.1\ \mu$ fraction, allophane displayed no diffraction peaks or bands (X-ray amorphous) while "imogolite" gave distinct diffraction bands at 14.5, 7.6, and 5.5A.

Electron Microscopy

Grim (1968) indicated that electron micrographs of allophane generally showed fluffy aggregates with a rounded nodular appearance. Yoshinaga and Aomine (1962a) described "very minute globoids" while Miyazawa (1962) observed many "fibrous matters" which would in retrospect probably be identified as "imogolite." Yoshinaga and Aomine (1962b) observed thread-like particles of relatively uniform size which they tentatively identified as "imogolite." Wada (1967) summarized several observations by indicating that a fairly good correlation existed between morphology and development of structural order. He stated that "imogolite" developed smooth, curved and often branched threads with diameter 50-200A and extending as long as several microns. With an increase in the Si/Al ratio, the thread-like tendency gradually diminished and minute particles (50 to 500A) in aggregated masses or thin films became dominant. The fibrous morphology of "imogolite" strongly suggested one dimensional regularity in structural organization.

Differential Thermal Analysis

Yoshinaga and Aomine (1962a) published thermal data on several soil allophanes. They revealed no marked thermal reactions with the exception of a strong endotherm between 150-170C (adsorbed H_2O) and a sharp exotherm between 910-915C (formation of gamma-alumina). A sluggish exotherm was noted just after the endotherm which was assumed to be due to tightly bound peroxide-resistant organic matter.

Thermal analysis of "imogolite" by Yoshinaga and Aomine (1962b) displayed the early endotherm and late exotherm of allophane, only they occurred at temperatures 20 to 40C higher along with a more intense

exotherm. In addition, "imogolite" exhibited an endotherm between 425-435C, indicating dehydroxylation.

Miyazawa (1962) reported a sharp exotherm at 850C for clay from a humified allophanic soil of Japan. This appeared to be a somewhat low nucleation temperature for allophane.

Miyauchi and Aomine (1966) indicated that DTA curves varied considerably with exchangeable cations, especially for the high temperature exotherm. They ranked the cation effect of this exotherm from highest temperature to lowest in the following order:

$$Ca > K > H > Mg > Na$$

Campbell et al. (1968) revealed that particle size, pH, and organic matter content had considerable effect on the thermal analysis of allophane. They found that the area of the low temperature endotherm and the height and temperature of the high temperature exotherm increased with decreasing particle size. With increasing pH, there was a considerable reduction in height and sharpness of the exotherm. Removal of organic matter had the same effect. The authors concluded that considerable changes in the high temperature exothermic peak of allophane could be produced by treatments often used in the separation of amorphous colloids from soils.

Infrared Spectroscopy

Infrared absorption spectra maxima for clay minerals have been generally identified as follows (Grim, 1968):

Frequency (cm^{-1})	λ (μ)	Absorption due to:
3,500 - 3,700	~4	OH groups
1,300 - 1,900	6-10	adsorbed H_2O
400 - 1,150	8-25	lattice vibrations

Several investigators such as Lai and Swindale (1969), Yoshinaga

and Aomine (1962a, 1962b), and Fieldes and Furkert (1966) reported infrared absorption maxima at approximately 3,500 cm^{-1}, 1,650 cm^{-1}, and 980 cm^{-1} due to hydroxyl groups, absorbed H_2O, and Si-O or Si-O-Al bond vibrations, respectively.

Wada (1966) was able to ascertain basic differences between "imogolite" and allophane in the Si-O stretching band. Allophane with Si/Al ratios of 1:1 to 1:1.3 displayed broad absorption maxima at 1,010 and 945 cm^{-1} while "imogolite" (Si/Al = 1/1) had rather well-defined absorption maxima at 990, 955, and 925 cm^{-1}.

Lai and Swindale (1969) reported that for four Andosols of Hawaii and one from Japan the main infrared absorption band shifted from 1,100 to 900 cm^{-1} with increasing weight ratio of $Al_2O_3/Al_2O_3 + SiO_2$. This apparently reflected a change in state of Al coordination. Cation exchange capacity and infrared data together suggested that some stabilized $Al^{IV} - O - Al^{IV}$ bonds occur in allophane minerals.

Dehydration and Rehydration

Integral dehydration curves of allophane have generally been observed to be quite smooth (Grim, 1968, Yoshinaga and Aomine, 1962a, 1962b); however, Yoshinaga and Aomine (1962b) reported an inflection for "imogolite" indicating rapid dehydration between 275-350C which was attributed to structural H_2O.

Schalsa et al. (1965) reported that air-drying of Chilean volcanic ash soils produced significant irreversible changes in CEC, soluble Fe, and P. Air drying has been reported by many workers to cause formation of pseudomorphs of sand and silt which became difficult to disperse. This gives some indication of the rehydration properties of allophane.

Surface Area

Aomine and Yoshinaga (1955) reported that ethylene glycol retention was high for their allophane samples; retention by unheated samples was similar to that of montmorillonite, but heated materials gave values higher than those of heated montmorillonite.

Orchiston (1959) indicated that heating of allophane considerably increased the area available to the water molecule at mono-layer coverage. He further stated, from a comparison of the surface areas available to water vapor and nitrogen, that some allophanes may possess the equivalent of internal surface.

Clay contents of soils, containing varying amounts of allophane, were calculated from measurements of surface areas of separated fractions using adsorption of nitrogen, acetic acid, and water-vapor as methods of measurement by Birrell (1966). Values for nitrogen adsorption ranged from 29 to 320 m^2/g of surface area. Since these clays were not pure allophane, the above data should be interpreted with care.

Optical Properties

Allophane is optically isotropic with an index of refraction close to that of glass. Discrete clay units are unobservable in thin sections; however, due to the anisotropic properties of layer silicates, their overall orientation relationships can be observed and interpreted pedogenetically (see Brewer, 1964).

Luna (1969a) reported mainly isotropic clay in thin sections for a Colombian Andosol; however, Luna (1970) indicated that as allophane weathered to a relatively more crystalline state, it also gradually took on some anisotropic properties.

Steen and Fryxell (1965) stated that weathering has had little

differential effect on modal values of the index of refraction of pumice glasses from Mt. Majama and Glacier Park.

Ross and Kerr (1934) observed a variable index of refraction (1.472 - 1.496) for allophane.

Ion Exchange and Sorption

The ion exchange properties of allophane place Andosols in a very unique management position. Ion exchange capacities of allophane are highly pH-dependent.

Aomine and Yoshinaga (1955) reported a CEC (at pH 7.0) range of 23-57 meq/100 g oven-dried clay from three Japanese Andosols; however, Birrell and Gradwell (1956) published data indicating that conventional CEC methods were not necessarily appropriate for allophane.

Wada and Ataka (1958) then shed considerable light on the CEC and AEC pH-dependency of allophane. The CEC and AEC values were determined with NH_4Cl solutions varying in concentration and pH. Two adsorption mechanisms were discerned, based on pH and equilibrium concentration. They found that the higher the pH of the solution, the more cations adsorbed with the opposite true for anions; also that the higher the concentration of NH_4Cl, the greater was the apparent CEC or AEC.

Aomine and Jackson (1959) claimed to be able to use "cation exchange capacity delta value" (ΔCEC = CEC pH 10.5 - CEC pH 3.5) to calculate allophane content of Andosols.

Fieldes and Schofield (1960) reported on two allophanic soil clays which had a net positive charge below pH 5.5 but acquired considerable negative charge between pH 6 and 7. They postulated that in allophane, because of its origin from glasses and disordered feldspars,

octahedral positions were lacking and its characteristic variable charge was attributed to the behavior of specific sites originating from broken bonds of Al in tetrahedral co-ordination. In light of Wada's (1967) observations, octahedral positions were not necessarily "lacking", especially in "imogolite." It could also be that the amount of tetrahedral aluminum was less than that inferred by Fieldes and Schofield.

Houng et al. (1966) published data indicating that the pH-dependent charges of allophane were more likely due to dissociation of surface hydroxyl groups associated with silicon atoms (silanol groups), and that permanent charges were probably due to tetrahedrally co-ordinated aluminum in the alumino-silica network. They further suggested that the amount of exchangeable bases should be expressed in terms of percentage of the permanent charges, since the pH-dependent charges were considered not to take part in the exchange reaction under normal soil conditions.

Aomine and Egashira (1968) reported flocculation of allophane occurred with a relatively small amount of divalent anions such as sulfate as against monovalent anions. Their results indicated that allophane was positively charged at the prevailing pH of Andosols, unlike the usual crystalline soil colloids.

Eschena and Gessa (1969) showed negative charge density of allophanic clays calculated from permanent cation exchange capacity (CECp) as lower than that of bentonite and kaolinite. Heating for 2 hours at 400C reduced pH-dependent exchange capacity (CECv) and specific surface, but had no effect on CECp. Tan (1964) used CECv as a criterion for classifying the Andosols of Indonesia.

Wada (1959) investigated the reaction of phosphate with allophane. At pH 4.0, ammonium phosphate $[(NH_4)_2 HPO_4]$ reacted rather rapidly with allophane to form an insoluble phosphate; while at pH 7.0, the reaction seemed to be retarded. This illustrated the importance of phosphate fixation in moderately acid Andosols.

Allophane-Organic Reactions

Andosols typically have thick dark A horizons which are high in organic matter. Organic matter accumulation takes place rapidly after new additions of volcanic ash and is exceptionally resistant to biological decomposition. A series of Japanese papers in the early and mid 1960's were concerned with the relationship between allophane and decompositionally resistant organic matter of Andosols.

Early papers by Kosaka (1963), Adachi (1963), and Tan (1964) of Indonesia were concerned with humification stages and humic-fulvic acid contents from a soil classification viewpoint. A series of publications then followed on specific allophane-organic reactions.

Aomine and Kobayashi (1964a, 1964b) found that allophane inhibited the activity of protease, α- and β-amylases, and cellulase enzymes. Allophane seemed to adsorb enzymes at both positive and negative charge sites.

Polyphenols were found to undergo rapid oxidative changes in the presence of allophane according to Kyuma and Kawaguchi (1964). Non-biological catalytic oxidation appeared to be responsible for the changes. These polyphenols could be adsorbed by allophane and catalytically oxidized to give dark-colored, highly acidic polymerized products similar to humic substances, regardless of the acid environment and low base status of the soil. Tannin-rich quercus species are often found among the vegetation on Andosols.

Kobo and Fujisawa (1964) claimed that allophane showed preferential adsorption for different types of humic acids. Tokudome and Kanno (1965a, 1965b) reported that in Japan, young Andosols have lower humic/fulvic acid ratios than older Andosols indicating that the concentration of humic acids, the alteration of fulvic acids to humic acids, and the carbon content of the soils increased with development of pedogenetic processes. Based on their analytical data, they claimed that most of the humus was bound with allophane and sesquioxides, especially aluminum. Humic acids were characterized by high carbon contents and high C/H, C/N ratios while fulvic acids had low carbon contents and C/H ratios.

According to Tan (1966), Al and/or Fe will migrate to lower horizons depending on the humic/fulvic ratio. In Latosols, Al appeared to be mobilized due to the large amounts of fulvic acids present while Al and Fe were both mobile in Andosols due to the presence of both fulvic and humic acids.

Pedogenetic Weathering

Under well-drained, moist conditions, the weathering of volcanic ash may lead to formation of many different secondary minerals. Besoain (1969b) claimed that under humid conditions accompanied by good drainage conditions a mineralogical sequence from allophane to kaolinitic type minerals almost invariably occurred with time. The incidence of allophane and/or kaolinite type clay minerals in arid environments is rare.

Fieldes (1955) stated that andesitic volcanic ash developed in time, the following series: Allophane (B, A3, A) ⟹ halloysite/metahalloysite ⟹ kaolinite.

Besoain (1969b) suggested that the inclusion of kaolinite was a

logical but theoretical possibility since even the oldest soils confirmed to have developed from ash had not yet passed the stage of halloysite.

Fieldes (1955) outlined a general structural continuum for the above-mentioned weathering sequence: (a) allophane B in which amorphous silica was discrete and clay particles ultra fine, (b) allophane A in which alumina and silica were randomly combined and particle size was greater, and (c) metahalloysite in which alumina and silica are combined in a kaolin structure.

Hay (1960), on the island of St. Vincent, B.W.I., reported that andesitic ash originally consisting largely of glass and the minerals anorthite, labradorite, hypersthene, augite, and olivine had altered to hydrated halloysite, allophane, and hydrated ferric oxide in 4,000 years.

For Hawaiian Andosols, Swindale and Sherman (1964) indicated that in the early stages glass weathers to yellow, brown, and orange palagonite (Ca, Mg, and K - containing amorphous alumino-silicate) due probably to hydroxylation and physical breakdown. They said that glass contained much strain energy; consequently expansion due to hydroxylation increased the strain, and physical comminution occurred as a strain-relieving mechanism. Some removal of alkali and alkaline-earth cations undoubtedly occurred simultaneously with hydroxylation.

Ohmasa (1964) outlined what he conceived as the weathering sequence of volcanic ash in Japan: (a) leaching caused immediate neutrality of acidic new ash, (b) large amount of bases are released to a great depth and the ash becomes alkaline, (c) freed bases are leached quickly along with Si due to the alkaline or basic conditions,

se both Si-gels and Al-gels occur, (d) Si and Al are weakly combined in the beginning but later allophane gradually forms, and (e) allophane gradually crystallizes to hydrated halloysite and, in some cases, gibbsite.

Fieldes (1966) considered structural randomness in hydrous aluminosilicates as being highly significant in the formation of allophane. He outlined four possible mechanisms of allophane formation in soils: (a) weathering of basic silicate minerals - dissolution of discrete Si - tetrahedra occurs under local alkaline conditions with subsequent reprecipitation with Si and Al ions under more acid pH after leaching of basic cations, (b) weathering of glasses - direct formation from glass, (c) weathering of feldspars - the ability of feldspars to alter to sericite apparently depends on the proportions and ordering of Al and Si in 4 - coordination. Thus in suitably ordered feldspars, single chains with Al - Si order identical with feldspar can detach from (100) and (010) surfaces and polymerize to produce mica sheets. Feldspars in which Al and Si have disordered arrangements such transformations are not possible, so that sericitisation cannot occur and alumino-silicate weathering products of such feldspars appear as allophane. Fieldes claimed that this process occurs during initial weathering of feldspars from New Zealand volcanic ash, and (d) grinding of minerals.

Kanno et al. (1968) claimed that allophanization of glasses proceeds through desilication, hydration, and replacement of Si-O-Si linkages by Si-O-Al linkages.

Mejía et al. (1968) recognized a weathering sequence from allophane to halloysite in a Colombian Andosol, while Luna (1969a) also recognized allophane A and B in Colombia.

Besoain (1969) reported the presence of considerable "imogolite" in some Andosols of Chile. He suggested that many Andosols contain "imogolite" as a dominant species of the clay fraction and that its occurrence is probably related to the development of a more ordered structure than that of allophane.

Definition

Utilizing information presented in this literature review, Van Olphen (1971) reported that members of a recent amorphous aluminosilicate workshop in Japan agreed to the following tentative definition of allophane:

"Allophanes are members of a series of naturally occurring minerals which are hydrous aluminum silicates of widely varying chemical composition, characterized by short range order, by the presence of Si-O-Al bonds, and by a differential thermal analysis curve displaying a low temperature endotherm and a high temperature exotherm with no intermediate endotherm."

MATERIALS AND METHODS

Site Selection

Soil profile sites were selected by investigation of available aerial photographs in Bogotá and an initial land reconnaissance of the Nariño area about one month before actual field work commenced. It was decided, after observing Nariño Andosols occurring widely between 2,000 m and 3,500 m in altitude, that meaningful pedogenetic data could be obtained by profile selection in an altitudinal sequence.

Profile locations in the Departmento of Nariño are shown in Fig. 1. Profiles No. 1-5 were selected at altitudes between 2,000 m and 3,200 m within a 25 km radius of Volcano Galeras (Pasto) in order to allow the assumption of ash-province uniformity. Profile 6, representing the highest altitude investigated at 3,510 m, was near Volcano Cumbal about 80 km southwest of Galeras. Substitution of this site was necessary because thick ash deposits do not occur above 3,500 m on the flanks of Galeras. An assumption was made that ash mineralogy was not overly dissimilar in the Cumbal region due to predominance of andesite throughout the uplands of Nariño. These six profiles were considered to represent approximately the maximum range of weathering severity experienced by loessial pyroclastic deposits in the altiplano of Nariño. Factors supporting this assumption will be discussed in a later section.

Profile 7 was sampled 67 km northeast of Galeras in the vicinity of Volcano Doña Juana at 2,000 m for comparison purposes with profile 1.

Fig. 1.--Departamento of Nariño located in southwestern Colombia. Small inset numbers indicate locations of profiles 1-10.

Profile 8 was sampled in a large valley (Sabana de Guachacal) near profile 6 for the purpose of ascertaining the influence of volcanic activity on alluvio-lacustrine soils within the study area. Profiles 9 and 10, although morphologically similar to Andosols, were found by NaF field test to be low in allophane. Obviously, these soils merited further investigation.

Field Procedures

All soil profiles were sampled from road cuts. Descriptions were made and samples obtained after removal of approximately 50 to 75 cm of soil material parallel to the profile face. Profile descriptions for all sites were made in accordance with criteria described in the Soil Survey Manual (Soil Survey Staff, 1951).

Bulk samples (approximately one-half gallon) were collected from each horizon and placed in plastic bags. Undisturbed core samples, approximately 8 cm in diameter, were collected from selected horizons of most soils for bulk density measurements.

Naturally oriented clods were collected from selected major horizons of profiles 1 through 6 for thin section analysis. These specimens were placed in labelled metal tins with the orientation marked on the containers. Slopes were determined by use of an Abney level.

Physical Methods

Particle Size Distribution

Particle size determination was by a modified hydrometer method adopted from Bouyoucos (1926). Organic matter, when present, was removed prior to analysis using hydrogen peroxide. The dispersing

agent was sodium hexametaphosphate. Particle size differentiation was according to the U. S. Department of Agriculture classification scheme (Soil Survey Staff, 1951).

Bulk Density

This determination was a modification of the core method outlined by Blake (1965). Since coarse skeleton content was virtually non-existent in the Marino Andosols, the core method was considered to be a satisfactory technique for bulk density determination.

Fifteen-Atmosphere Water Content

This determination was made according to the method outlined by the U. S. Salinity Laboratory Staff (1954).

Chemical Methods

pH Determination

A soil-solution ratio of 1:1 in distilled water and, in most cases, 1 N KCl was measured by a Beckman Model G pH meter.

Cation Exchange Capacity

This parameter was determined after the method of Bower et al. (1952) using 1 N ammonium acetate at pH 7.0 as a leaching agent.

Exchangeable Calcium and Magnesium

These elements were determined separately using the EDTA method of Barrows and Simpson (1962). Ten grams of air-dry soil was leached with 100 ml of N NH_4OAc at pH 7.0 as described in Peech et al. (1947).

Exchangeable Potassium

An aliquot of the NH_4OAc leachate used for Ca-Mg determination

was analyzed for potassium using a Coleman Jr. Spectrophotometer at 770 mμ.

Exchangeable Sodium

An aliquot of the NH_4OAc leachate used for Ca-Mg determination was analyzed for sodium using a Coleman Jr. Spectrophotometer at 590 mμ.

Organic Carbon

This was determined by the Walkley and Black (1934) method.

Exchangeable Aluminum

Exchangeable aluminum was determined by the fluoride titration method of Yuan (1959).

Free Iron Oxides

Free Fe_2O_3 was analyzed by a technique reported by Cheng et al. (1953).

Mineralogical Methods

Dispersion and Fractionation of Clay

Portions of the soil samples in plastic bags were removed and allowed to air-dry, while the remainder was maintained at approximately field moisture. This was done because Andosols, upon drying, often form sand and silt pseudomorphs of clay particles (Birrell, 1964). This could decrease tremendously the amount of clay that might be dispersed (Wright, 1964).

Duplicate 5 g samples of soil from each horizon were placed in 100 ml polyethylene centrifuge tubes. Air-dry surface samples were

utilized since the high amounts of organic matter tended to retain sufficient moisture restricting irreversible drying and aggregation. Subsurface horizons were kept at approximately field moisture since in most cases drying was irreversible in the B and C horizons. Organic matter was then oxidized for surface horizons by the method of Kavkulich and Wiens (1970) using sodium hypochlorite solution adjusted to pH 9.5 by 1.0 N HCl immediately prior to use.

Ten milliliters of NaOCl solution (minimum 6% available chlorine) was added to each soil sample in the polyethylene tubes. This was repeated four to five times, heating the suspension in a boiling water bath for 15 minutes during each treatment. The supernatant was decanted after centrifugation. Surface horizons treated in this manner were quite well dispersed after completion of NaOCl oxidation.

Considerable amounts of aluminum oxalate and ferric oxalate complexes in peroxide extracts of soil clays have been reported by Farmer and Mitchell (1963), especially in soils containing a high amount of allophanic colloids. Since Andosols contain large quantities of allophane, which is quite vulnerable to common pretreatments such as organic matter oxidation and free iron oxide removal, it would be advantageous to minimize possible pretreatment effects. Therefore, iron oxides were not removed and NaOCl rather than H_2O_2 was used as an oxidizing agent for organic matter.

Subsurface samples were dispersed with 2% Na_2CO_3. Approximately 5 g of moist soil was placed in 100 ml polyethylene centrifuge tubes. Twenty milliliters of 2% Na_2CO_3 solution was then added to the soil samples and the suspension was stirred for 2 minutes. The less than 2 μ fraction was then separated by centrifuging as described by

Whittig (1965). Subsequently, the less than 2 μ fraction was separated into 2 - 0.2 μ and less than 0.2 μ fractions by centrifugation.

X-Ray Diffraction

Clay suspensions representing the 2 - 0.2 μ and less than 0.2 μ fractions were plated on ceramic tiles after the method of Kinter and Diamond (1956) as modified with the use of a suction apparatus described by Rich (1969). The initial treatment prior to irradiation was saturation by magnesium (1 N $MgCl_2$). The tile with plated sample was subsequently irradiated, glycerol solvated, irradiated, washed with methanol and water, saturated with potassium (1 N KCl), irradiated, heated to 500C for ¼ hours, and then irradiated once more. In some cases, the sample was heated to 100C for 12 hours after KCl saturation and irradiated prior to 500C treatment.

Obtaining and storing the aforementioned oriented clay specimens presented some problems especially for the fine clay ($< 0.2\mu$) samples. There was a tendency for the fine clay to be drawn through the ceramic tiles under vacuum. This was alleviated by concentrating and flocculating the suspension with 1 N $MgCl_2$ prior to applying it to the tile. Minimum water washings, usually equivalent to volume of $MgCl_2$ used were necessary; otherwise, the problem arose again. Cracking and flaking of the fine clay specimens of the tiles, even in a 100% glycerol atmosphere, also created difficulties. This was tempered in most cases by thorough saturation with a 30% glycerol solution drawn through the clay under suction.

Potassium-saturated samples were irradiated immediately after treatment with 1 N KCl. Anticipating the cracking and flaking brought on by dehydration and dehydroxylation of allophane at temperatures

above 100C, K-saturated samples were covered by a blank ceramic tile and then heated to 500C. With a very few exceptions for fine clay and around 20% of the cases for coarse clay (0.2 - 2 μ), it was impossible to mount the tile for irradiation without losing all of the sample. This difficulty was circumvented by either of two methods which seemed to work equally well. Double stick transparent tape was mounted on a glass slide and then pressed onto the dry, loose clay flakes lying on the ceramic tile. The glass slide could then be placed in the X-ray beam path. The second method was somewhat more time consuming. It involved transferring the clay from the tile to an agate mortar and pestle. The sample was then gently ground in a small amount of water until most of the aggregates were completely broken. At this time the suspension was transferred with a dropper to a glass slide and placed in an oven at 100C for about 2 hours. After drying, the clay was irradiated.

X-ray diffractograms were obtained utilizing a General Electric XRD-700 instrument. Radiation was detected with a proportional counter. Mg-saturated specimens were X-rayed from 3 to 32° (2 θ). Mg-saturated-glycerol-solvated, K-saturated, 100C and 500C treated specimens were irradiated from 3 to 15° (2 θ). Instrument conditions and settings were as follows:

Radiation: Copper K alpha.

Filter: Nickel

Potential: 25 KV.

Current: 25 ma.

Goniometer scan speed: 2° (2 θ) per minute.

Strip-chart drive speed: 30 inches per hour.

Pulse ht. selector: E_L = 5V.

Scale expansion: 600.

Zero offset: 20.

Plot: Linear.

Receiving slit: 0.1°.

Divergence slits: 1°.

Counter tube high voltage: 2.25 KV.

Amplifier ratemeter: Time constant - 2.5 seconds, range 2.5 K, amplifier gain - 16 low pps.

Take-off angle: 3°.

Differential Thermal Analysis

Portions of the stored fine clay and coarse clay suspension were transferred to aluminum weighing pans, dried at 40C, and subsequently gently pulverized in an agate mortar and pestle. A 100-mg portion of the dried sample was then transferred to one of the four sample positions in the insert holder of the Deltatherm thermoanalyzer where it was gently tamped into place around a platinum thermocouple following improved packing procedures as outlined by Reneau and Carlisle (1970) wherein the clay sample was "sandwiched" between asbestos which had been fired at 1000C and passed through a hammer-mill fitted with a fine screen. The sample holder containing the four clay samples with alternating reference sample positions was then connected to a transistorized circuit. Determinations were made at 25% sensitivity using a heating rate of 10C per minute from room temperature (approximately 23C) to 950C.

Infrared Spectrometry Analysis

Infrared region absorption by clay minerals was investigated with a Beckman IR-10 spectrophotometer. Magnesium-saturated clays were dried at 40C and gently pulverized using an agate mortar and pestle. A mixture consisting of 1.0 mg of the ground magnesium-saturated clay and approximately 400 mg of spectroscopic-grade KBr was used to form a transparent pellet. The pellet was formed using a Beckman KBr die. Approximately 200 mg of the KBr-clay mixture was placed in a Wig - L - Bug electric mortar and pestle (made by Crescent Dental Mfg. Co., 1839-49 South Pulaski Road, Chicago 23, Ill.) to reduce the particle size and thoroughly disperse the sample in KBr. The optimum grinding time appeared to be approximately 20 seconds. The Beckman KBr die consisted of an anvil and a ram constructed in such a manner that when pressed together by a hydraulic press, the sample is compressed into a disc by the confined space. A partial vacuum was created in this space by a vacuum pump connected to a hose coupling on the die which led to the aforementioned confined space. This tended to remove entrapped moisture and air which otherwise could result in a cloudy to opaque pellet.

After cleaning all parts of the die with acetone, it was assembled and the 200 mg of KBr-clay mixture was transferred from the Wig - L - Bug mortar and pestle to the die. The assembly was then placed in a hydraulic press and the vacuum pump activated. After 1 minute, slight pressure was applied to the ram for 3 minutes. Hydraulic pressure was then increased to a reading of 8,000 psi and maintained for 5 to 10 minutes. The vacuum was then released after which the hydraulic pressure was gradually released.

The pellet was removed with tweezers and placed in a Beckman

infrared sample holder. It was then introduced to the infrared beam for analysis. The scan speed was 15 minutes from 4,000 to 350 cm^{-1}. The instrument was calibrated by scanning a standard polystyrene film from 4,000 to 350 cm^{-1}. A KBr blank and Ward's halloysite No. 12 were scanned as reference samples.

Sodium Fluoride Test for Allophane

Fieldes and Perrott (1966) indicated that large quantities of hydroxyls were released when allophane was treated with NaF. The magnitude of release was great relative to other soil constituents. The aforementioned authors outlined certain modifications of this knowledge which allowed a positive field and laboratory test for allophane.

This procedure was used for field work in Colombia by placing a small portion of soil on phenolphthalein paper and treating it with 1 N NaF. The appearance of red color was accepted as an indication of an appreciable allophane content. In the laboratory, pH values were obtained by suspending 1 g of soil in 50 ml of 1 N NaF solution. The suspension was stirred constantly for two minutes after which a reading was immediately taken on a pH meter. If pH values were greater than 9.4 after two minutes, the sample was assumed to have an allophane content equal to or greater than 60% of the colloidal complex.

Luna (1969b) pointed out, however, that this test has been found to be positive for certain Colombian soils in the presence of appreciable halloysite and gibbsite.

Sand Mineralogy

Sand mineralogy was determined for the 500 - 50 μ fraction sepa-

rated from the soil by mechanical analysis. Light and heavy minerals were separated by density using Bromoform (s. g. 2.9). Heavy minerals were mounted in Canada balsam and were identified with a polarizing microscope. The light minerals were examined in Nitrobenzene (n = 1.552). Both fractions were reported on the basis of species present in 100 transparent grains counted. Opaque minerals were tabulated separately in the case of heavy minerals.

Micromorphology - Thin Section Techniques

Major horizons from profiles no. 1 through no. 6 were selected for micromorphological investigations.

Impregnation

Vertically-oriented undisturbed peds were removed from the metal containers used in the field and placed in small aluminum containers approximately 4 cm in diameter and 8 cm high and allowed to air-dry for a few days. Dry peds remaining in aluminum containers were then placed in a vacuum desiccator. An impregnation solution consisting of a mixture of 50% Laminac resin #4116, 49% monomeric styrene, and 1% Lupersol DDM hardener (Pettry, 1969) was then periodically introduced to each container over a period of 4 to 6 hours under vacuum. Samples were then removed from the vacuum and placed in an initially cold oven and heated slowly to 100C for approximately 12 hours. After cooling, the aluminum container was peeled off and the samples were ready for sectioning.

Preparation of Thin Sections

The initial step was to block out a section 2.5 x 2.0 cm between 0.8 to 1.2 cm thick using a Felker Di-Met, Model 11-R saw with a diamond

blade and water as a coolant. The slab obtained in this manner was then lap-ground on one side using a Von Huene Thin Section Grinder. This was done in three steps, starting with coarse 150-mesh silicon carbide on the rough grinding lap using water as a lubricant. This operation was then followed by lap grinding on the intermediate lap with 320-mesh silicon carbide. Final grinding was done on a 15 cm agate lap with #1200 optical finishing powder. The last two operations used kerosene as a lubricating agent.

The smoothly ground surface was then cemented to a 2.5 x 7.5 cm petrographic slide using an epoxy cementing agent. The excess sample was then removed to a thickness of about 90 μ above the glass slide. This was accomplished using a specially constructed slide holder which allowed a parallel cut to be made with the diamond saw. Further reduction of thickness was obtained by intermediate grind with 320-mesh abrasive on the cast iron lap. This process was continued until birefringent colors of second order blue for highest orientation of quartz and feldspar were obtained. This indicated a thickness of about 60 μ. Final grinding was necessary to reduce the specimen to about 30 μ in thickness. This was done on the agate lap with #1200 aluminum oxide optical finishing powder. At the desired thickness, the highest birefringent colors of quartz and feldspar were light yellow or white. The slide was then thoroughly washed, and a cover glass was mounted over the thin section with epoxy cement (n = 1.58).

Analysis

Thin section slides were described using a petrographic microscope. Photomicrographs were obtained with a 35 mm camera attached to the microscope. Thin section descriptions were made using the terminology of Brewer (1964).

DESCRIPTION OF NARIÑO STUDY AREA

Location

The Departamento of Nariño is located in the extreme southwestern part of Colombia, South America (Fig. 2). Nariño is bounded on the north by the Departamento of Cauca, the Pacific Ocean on the west, the Departamento of Putumayo on the east and Ecuador on the south. It has an area of 32,704 km^2 (Banco de la Republica, 1969) and lies from less than 1° to slightly more than 2° north of the equator.

Physiography

Nariño is characterized by elevations ranging from sea level along its Pacific Ocean shoreline to a maximum of 4,890 m at the snow covered summit of Volcano Cumbal near Tuquerres in the Andean uplands. The terminal ranges of the Andes divide in the northern part of Nariño into three distinct chains called "cordilleras" and extend almost to the Atlantic Ocean (or Caribbean Sea). This junction imparts a very rugged, mountainous character to the eastern part of the departamento. The Andean highlands are constituted by alternating intermontane valleys and ridges. Probably the most striking feature of the uplands is the abundance of volcanoes. Blasco (1969) reported that 23 volcanoes have been identified in Nariño of which 5 are known to be active (Cumbal, Chiles, Galeras, Azufral and Doña Juana).

Intermontane basins of considerable extent occur frequently in

Fig. 2.--Colombia, South America, showing location of the Departamento of Nariño.

the highlands. Typical of these is a large basin near Tuquerres aligned approximately parallel to three active volcanoes (Chiles, Cumbal, and Azufral) near the western periphery of the Andes. The basin floor is approximately 3,000 m in altitude and is occupied by meandering underfit streams. A smaller basin exists east of Volcano Caleras at an altitude of 2,500 m.

The western part of Nariño is comprised of Andean piedmont foothills which merge rather rapidly into the Pacific coastal plain.

Bedrock and Surficial Geology

Luna (1969a) indicated that Andean basement rock composition in Nariño was primarily andesite, basalt, and tuff of the Cenozoic. Varela (1963) concluded that recent eruptive rocks due to volcanic activity of the Cenozoic dominated a major part of Nariño.

Luna (1969a) stated that volcanism studies and pyroclastic material inventories were quite limited in Colombia. He reported that most references were to specific eruptions with insubstantial details on quantity and composition of pyroclastic materials. A maximum age of 7,000 years by C^{14} has been reported for an ash deposit in the Departamento of Tolima.

Empirical observations by the author in the Nariño area revealed that the highlands have been universally affected by aeolian and fluvial pyroclastic deposits; however, the influence of this factor on soil development varied considerably in magnitude. Volcanic ash accumulation and distribution in the Nariño highlands has been manifested as a "patchwork" or discontinuous pattern over the landscape. Several basic factors have probably contributed to this pattern. Due to the strongly

dissected nature of the region, considerable ash has been eroded from the steeper slopes. Differential deposition due to abberant intermontane wind patterns has, undoubtedly, been a supplemental factor. Additionally, it was very difficult to assess the territorial limit of various ash deposits. Wright (1964) indicated that mapping of ash-derived soils is a problem in peripheral areas at the outer territorial confines of ash-mantled landscapes. Figure 3 shows the general distribution of volcanic ash deposits associated with Volcano Galeras in addition to locations of profiles 1-6.

Areas in the Nariño highlands which were covered by thick ash deposits characteristically exhibited smooth, rounded land forms which generally conformed to pre-existing surface configurations.

Nature of the pyroclastic deposits changed considerably from northeast to southwest in the highlands. Deposits in the Pasto-Buesaco region (Fig. 2) were composed of finely comminuted andesitic ash exhibiting little or no stratification. The character of these deposits indicated gradual accretion of ash where eruptions were infrequent and not of great magnitude. The contrasting nature of pyroclastic deposits in the Túquerres - Ipiales region (Fig. 2) was manifested in stratified beds of ash and lapilli. Lapillitic strata were quite often pumiceous in nature.

Thick well-stratified and well-sorted fluviatile pumice beds were observed along the western walls of the previously mentioned Túquerres basin. Similar pumice beds were observed along drainage outlets towards the Pacific lowlands and 1 km north of the Ecuadorian border (Fig. 4).

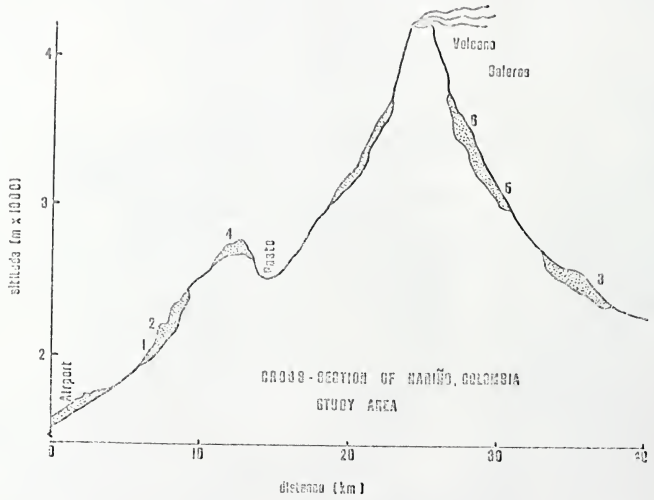

Fig. 3.--Cross-section of Nariño, Colombia study area showing locations of profiles 1-6 relative to Volcano Galeras. Stippled areas show idealized distribution of volcanic ash.

Fig. 4.--Pumice beds 1 km north of Ecuadorian border.

Climate

There is a paucity of climatological data for Departamento Nariño. The few stations that exist have furnished rather inconsistent meteorological information. Blasco reported that the Obonuco station (ICA) at 2,670 m on the flanks of Volcano Galeras registered an average annual precipitation of 700 mm and an average temperature of 13C. At the Botana agricultural station (2,750 m), the average annual rainfall and temperature were 781 mm and 13C, respectively. A station near Consaca (1,400 m) in the subtropical zone had an average annual precipitation of 1,392 mm and temperature of 20C. Tumaco, on the Pacific coast, reported 2,849 mm of rainfall per year and 26C annual temperature.

The complex topography and wide altitudinal range of Nariño impart considerable variety to local climatic conditions. Proximity to the equator, however, dictates an isothermic temperature regime which is closely related to elevation. Luna (1969a) stated that temperature is related to elevation in Colombia by a 6C decrease for each 1,000 m increase in altitude. Espinal and Montenegro (1962) recognized five major temperature zones in Nariño based on the aforementioned thermal gradient (Table 1). These zones ranged from tropical (> 24C) in the Pacific lowlands to sub-alpine (3-9C) in the Andean highlands. Within each thermal region, subdivisions were made on the basis of precipitation differences. Precipitation is maximum along slopes facing the Pacific lowlands and tends to decrease with depth in intermontane valleys. Varela (1963) reported a distinct dry season occurring during July, August, and September in the Pasto-Rio Mayo sector of Nariño.

Table 1. Climate-vegetation relationships in Departamento Nariño, Colombia (Espinal and Montenegro, 1962)

Temperature (C)	Rainfall (mm)	Vegetation	Approximate Altitude (m)
3 - 9	500 - 2,000	g - SA	3,500 +
9 - 12	500 - 1,000	hf - M	3,000 - 3,500
	1,000 - 2,000	vhf - M	
	> 2,000	pf - M	
12 - 18	500 - 1,000	df - LM	2,000 - 3,000
	1,000 - 2,000	hf - LM	
	2,000 - 4,000	vhf - LM	
	> 4,000	pf - LM	
18 - 24	500 - 1,000	df - ST	800 - 2,000
	1,000 - 2,000	hf - ST	
	2,000 - 4,000	vhf - ST	
	> 4,000	pf - ST	
> 24	500 - 1,000	vdf - T	0 - 800
	1,000 - 2,000	df - T	
	2,000 - 4,000	hf - T	
	4,000 - 8,000	vhf - T	
	> 8,000	pf - T	

g = grassland ("paramo")
pf = pluvial forest
vhf = very humid forest
hf = humid forest
df = dry forest
vdf = very dry forest

SA = sub-alpine
M = montane
LM = lower montane
ST = sub-tropical
T = tropical

Plant Ecology

Espinal and Montenegro (1962) using the system of Holdridge (1947) prepared a general, panoramic view of vegetation formations in Colombia. Utilizing aforementioned elevation-temperature-precipitation interrelationships, they identified 23 different formations of which 17 are indigenous to Departamento Nariño (Table 1). The Nariño study area encompassed 5 major vegetation formations ranging from dry sub-tropical forest to sub-alpine grassland. These pertinent formations are discussed below as outlined by Espinal and Montenegro (1962).

Dry Sub-Tropical Forest

This formation is found predominantly in intermontane valleys and is characterized by 18-24C annual temperature and 500 - 1,000 mm annual precipitation. Rainfall deficiency in these valleys is most likely due to orographic effects which produce aberrant local wind patterns. The major part of this formation occurs in mountainous terrain with moderate to very steep slopes. The original vegetation has been almost entirely altered by man. The lone Nariño plant species list published by Espinal and Montenegro (1962) was enumerated in the Guaitara river valley for this formation. They reported that the area was covered with dense clusters of a tree called "coca" (Erythroxylon sp.) associated with:

Croton ferrugineus H.B.K. (mosquero),
Fagara pterota ? (tachuelo),
Calliandra sp. (carbonero),
Acacia farnisiana Willd. (pela),
Lantana canescens H.B.K. (venturosa),
Euphorbia caracasana Boiss (lechero),
Opuntia sp. (tuna),
Cephalocereus sp. (camelon),
Tecoma Fuss. (chirlobirlo),
Bursura tomentosa Tr. and Pl. (tatamaco),
Caesalpiniaceae (tintilla), and
Verbenaceae (pendo).

In Nariño, areas of dry sub-tropical forest are used for the cultivation of coffee, sugar cane, plantain, and in some cases extensive grasslands for cattle production.

Dry Lower Montane Forest

In general this vegetation formation has as climatic limits an annual temperature between 12C to 18C and annual rainfall between 500 mm and 1,000 mm. Dry lower montane forests are generally encountered between altitudes of 2,000 m and 3,000 m in intermontane valleys and basins of the Andes. The primary vegetation of this formation has been completely altered and destroyed by man. Due probably to an ideal climate, indigenous pre-Colombians populated a large part of these areas. In establishing their agricultural systems they initiated the demise of the natural plant communities of this ecosystem. Areas which are left uncultivated are invaded by grasses and small trees or shrubs such as Cordia sp.

Some common species identified in this formation are as follows:

Dodonaea viscosa,
Solanum marginatum,
Euphorbia orbiculata,
Opuntia sp.,
Sparticum junceum,
Phyllanthus salviaefolius H.B.K.,
Baccharis sp.,
Croton sp., and
Prunus capuli.

Large tracts of this formation have been reforested with eucalyptus (Eucalyptus globulus) and pine (Pinus radiata). This vegetation formation has traditionally supported a high population concentration in the Andean highlands. Dry lower montane forest areas are considered to be some of the most productive regions in the country. Within these areas are located large cattle ranches and commercial forests. Inten-

sive production of wheat, corn, potatoes, and tree fruits is encouraged in some areas by irrigation systems.

Humid Lower Montane Forest

This vegetation formation is of limited occurrence in Colombia. The temperature and altitude range in this formation is similar to that of the dry lower montane forest system; however, average annual rainfall is higher ranging between 1,000 mm and 2,000 mm. Climate is generally mild with gentle rains occurring throughout the year. Occasional frosts occur at the higher elevations of this formation. These forest formations occur on undulating to moderately steep mountain slopes and intermontane valleys and basins.

In areas where the population has been established for several centuries the natural vegetation has been considerably altered.

Some common species identified in this formation are as follows:

Quercus sp.,
Cordia,
Cedrela,
Rapanea sp.,
Ficus sp.,
Weinmannia sp.,
Croton,
Phyllanthus, and
Myrica.

In areas where the topography is flat to undulating, crops such as potatoes are grown. More strongly sloping areas have generally been established as pastures composed mostly of kikuyu grass (Pennisetum clandestinum). Pine and eucalyptus reforestation has occurred in many marginal agricultural areas.

Humid Montane Forest

This formation occurs generally between elevations of 3,000 m and

3,500 m in the Andes although locally it may extend in some cases up to 4,000 m. It has been referred to as "sub-paramo" by natives. The Tuquerres basin in Nariño is composed almost entirely of this vegetative formation. Average temperature generally falls between 9C and 12C. Precipitation ranges between 500 mm and 1,000 mm annually. Even though rainfall is relatively low, the climate is quite humid due to low thermal efficiency that is associated with considerable cloud cover and high altitudes. This is reflected in low evapotranspiration rates. Day temperatures are generally quite cool and nights are frequently below 0C with common frost and ice formation.

Humid montane forests occur on varied topography in the Andean highlands. Considerable areas of the formation have been sacrificed to cultivation; however, remnant trees and on occasion complete community remnants have remained intact. A partial species list of a humid montane forest community in the Departmento of Boyaca is presented as follows:

Weinmannia sp.,
Polylepis sp.,
Viburnum sp.,
Befaris sp.,
Senecio sp.,
Vaccinium sp.,
Rubus sp.,
Orthrosanthus sp.,
Buddleia sp.,
Bomarea sp.,
Espeletiva sp., and
Miconia sp.

Population density is not great at this altitude although the soils in this formation are quite fertile and have sustained cultivation for many years. Potatoes, wheat, barley, and vegetables are grown on the flat and undulating areas while the sloping regions are generally utilized for pasture.

Sub-Alpine Grasslands

This formation occupies the highest elevations in the Andes below permanent snowlines. It is not extensive and is of very little agricultural importance. Colombia's sub-alpine ecosystems have been insufficiently studied due to their inaccessability and inhospitable climate. Rainfall may range from 500 mm to 2,000 mm annually with an annual temperature between 3C and 9C. The vegetation is dominated by grasses, especially Festuca and Calamagrostis, interspersed with bushes and shrubs (Fig. 5) such as:

Diplostephium revolutum Blake,
Gynoxys paramuna,
Senecio vaccinioides,
Valeriana arborea,
Miconia buxifolia,
Polylepis boyacensis,
Hypericum sp., and
Espeletia sp.

Fig. 5.--Typical vegetation of sub-alpine grassland near profile 6. Broad leaf plants are Espeletia sp.

RESULTS AND DISCUSSION

Methodology

Organic Matter Oxidation

Lavkulich and Wiens (1970) presented data clearly showing that not only was NaOCl more efficient in oxidizing organic matter but that the content of Si, Mn, Fe, and Al in extracts after treatments was significantly higher for H_2O_2. Comparative data for selected Andosol horizons using H_2O_2 and NaOCl treatments (Table 2) were even more dramatic than those presented by Lavkulich and Wiens. H_2O_2 removed five to ten times the amount of Si and ten to seventy times the amount of Al than that removed by NaOCl. The H_2O_2 treatment was the same as that reported as H_2O_2 - I by Lavkulich and Wiens (1970).

NaOCl would appear to be less destructive of sesquioxides, silica coatings, allophane, and crystalline clay minerals. It can be concluded from these data that NaOCl was a more acceptable reagent than H_2O_2 for rapid routine organic matter destruction in Colombian Andosols prior to mineralogical analyses.

Dispersion of Andosol Clays

It would be advantageous at this point to examine more closely the dispersion properties of soils containing high quantities of allophane. Although the intent of this study was not method oriented, an interesting point has arisen. Historically most soil mineralogy analyses have been performed on air-dry samples. As has been mentioned previously,

Table 2. Fe, Si, and Al amounts in extracts after treatment of certain Andosol horizons by NaOCl or H_2O_2

Profile No.	Horizon	NaOCl			H_2O_2		
		Fe	Si	Al	Fe	Si	Al
		ppm					
3	A12	2	240	0	0.2	902	88
		2	240	10	0	1,001	99
5	A1	5	230	30	36	1,738	1,705
		6	270	30	35	1,914	1,760
5	AC	6	390	30	117	2,500	2,079
		6	360	30	118	2,519	2,211
6	A1	64	330	170	164	4,026	6,105
		73	350	220	116	3,630	5,830

problems have been encountered in Andosol clay dispersion due to irreversible aggregation. It seems that past investigators have been most concerned with breaking-up these aggregates. A myriad of techniques have been attempted with varying degrees of success (or failure). Many of these methods can have harsh effects on allophanic minerals. Dilute hydrochloric acid (see, for example, Birrell and Fieldes, 1952) has been used by many workers. Fieldes (1955) and Fieldes and Taylor (1961) dispersed Andosols, with varying success, by adjusting the pH to 10.5 with NaOH. Kobo and Oba (1965) used a sonic vibration method for disintegrating aggregates to facilitate mechanical analysis of volcanic ash soils. They reported that in most cases the clay was well dispersed by Calgon after sonic treatment but addition of dilute HCl was still necessary for subsoils dominated by allophane.

In most cases mentioned above, dispersion was obtained by somewhat drastic treatments with little consideration for allophane. Ahmad and Prashad (1970) until recently had been impeded in their investigations of Andosols of the West Indies because they found it impossible to disperse these soils even by the aforementioned "conventional" methods. They discovered that zirconium nitrate ($Zr(NO_3)_4 \cdot 5H_2O$) solutions were very efficient soil dispersing agents, especially for Andosols. They postulated that the high ionic charge, small atomic radius, and low ionization potential of Zr apparently resulted in saturation of the exchange sites and some tetrahedral substitution for Al leading to a net positive charge on the exchange complex. Ahmad and Prashad felt that their data were the most reliable so far quoted for these soils. Unfortunately, zirconium nitrate does not lend itself to use as a dispersing agent in mineralogical investigations. Due most likely to its low ionization potential, it forms precipitates with most

of the accessory solutions such as $MgOAc$, $MgCl_2$, and acetone which are used for saturation and washing of the colloidal complex in clay mineralogy studies.

It was observed by the author that seemingly good production of clay (i.e. good dispersion) was obtained from surface horizons using NaOCl and from field moist subsurface horizons using 2% Na_2CO_3. Zirconium nitrate also seemed to provide adequate dispersion so it was decided to verify qualitative observations using zirconium nitrate as the best available standard. Sample dispersion with zirconium nitrate was according to the method utilized by Ahmad and Prashad (1970). Samples were centrifuged, clay decanted, flocculated (according to Whittig, 1965), and weighed. Silt was separated from sand by wet sieving through a 300-mesh screen and each separate was weighed. Data in Table 3 clearly indicate that in most cases there was no striking difference between dispersive quality of zirconium nitrate and either NaOCl or Na_2CO_3. In 50% of the cases zirconium nitrate gave slightly better clay production. Seventy-five percent of the time zirconium nitrate dispersed samples, in which organic matter was removed by H_2O_2, gave slightly better clay production than NaOCl. Three out of the four horizons dispersed with Na_2CO_3 produced better than zirconium nitrate.

So it would appear that for Andosols of the humid subtropical to sub-alpine uplands of southern Colombia the maintenance of field-moist condition assured adequate dispersion. It also seems that even though these soils contain high quantities of allophane the principle of sodium saturation of the exchange complex and resultant development of strong electrical repulsion forces remain valid.

Table 3. Effect of pretreatment and dispersing agent on particle size distribution

Lab. No.	Profile No.	Horizon	OM Removal	Dispersion	Sand	Silt	Clay
					%	%	%
C-1	2	A11	H_2O_2	a	39	29	32
			NaOCl	b	38	28	34
C-2	2	A12	H_2O_2	a	40	30	30
			NaOCl	b	39	34	27
C-3	2	A3	H_2O_2	a	34	39	27
			NaOCl	b	31	46	23
C-4	2	[B]	-	a	37	40	23
			-	c	35	39	26
C-5	2	C	-	a	29	42	29
			-	c	29	40	31
C-15	3	C	-	a	22	40	38
			-	c	24	46	30
C-17	5	AC	H_2O_2	a	39	34	27
			NaOCl	b	33	41	26
C-34	4	C	-	a	25	48	27
			-	c	22	48	30

- Organic matter removal unnecessary.

a Zirconium nitrate.

b Sodium hypochlorite.

c Sodium carbonate.

Morphology

Detailed field descriptions for the 10 soils selected in this investigation are presented in Appendix Table 8. The discussion of morphological and subsequent data will relate initially to profiles 1-6 which were selected in an altitudinal sequence between 2,000 m and 3,510 m. Profiles 7-10 will be treated individually as ancillary sites providing additional pedogenetic information.

All soils were well drained and quite permeable. The altitudinal sequence of profiles 1-6 exhibited definite morphological trends with decreasing temperature. Horizon sequence at low and middle altitudes (2,000 - 3,000 m) was A[B][1] C; however, above 3,000 m the cambic subsurface horizon was absent imparting an AC sequence to these soils. Surface (A) horizon thickness tended to increase with increasing altitude. Surface color was dark grayish-brown (10YR 3/2) in profile 1, but all subsequent surface horizons at greater elevations were black (10YR 2/1). The [B] horizon thickness tended to decrease with elevation and was replaced by an AC transitional horizon in profile 5 (3,120 m). Cambic horizon colors displayed maximum development (7.5YR 4/4) at 2,000 m. The [B] horizon color at 2,150 m (profile 2) was yellowish-brown (10YR 5/8); and with decreasing temperature, both value and chroma of this horizon tended to decrease. The C horizon colors tended to have similar hue and value but slightly lower chroma than the overlying [B] horizon. Structure of A horizons tended to be subangular blocky

---

[1]Brackets [ ] are used to indicate a cambic diagnostic subsurface horizon. Wright (1964) advocated the use of this symbol in describing Andosols.

below 2,500 m and granular above this elevation. Cambic [B] horizon structures were subangular blocky. In a majority of the soils, C horizon structure tended to be massive except at lower altitudes there was a tendency towards the subangular blocky type. Notable was the lack of oriented clay (argillans) on ped surfaces. Organic coatings were commonly noted on individual sand grain surfaces in A horizons of all soils (Figures 6 and 7).

Profile 7 was a shallow Andosol at 2,000 m in elevation. The A horizon was unusually dark (10YR 2/1) for similar soils (i.e. profile 1). Profile 8 was sampled and described in an alluvio-lacustrine region. It appeared to be a young, well drained soil and showed little evidence of profile development. The most striking feature of this profile was a layer of white (10YR 8/1) silt at 131 cm. It is possible that this layer represented relatively unweathered fluvial volcanic ash deposits. There was a pronounced change in depositional history below 152 cm. Profile 9 had a thick (66 cm) black granular to blocky A1 horizon. Colors of the C horizon were redder in hue (5YR and 7.5YR) than was typical for Andosols at comparable depths in the study area. The C2 horizon was probably developed from andesite. Although morphologically similar to Andosols this profile exhibited negative NaF test results for all horizons. Profile 10 was similar to profile 9 but it was more strongly developed. The A horizon thickness was less (39 cm) and not as dark (10YR 3/2). It was the only profile with an argillic horizon. Although aeolian pyroclastic materials have undoubtedly influenced the pedogenesis of this soil it has developed predominantly in andesitic residuum. According to Wright (1964) the thick dark A horizons exhibited by these soils have some connection with primitive weathering

Profile 1

Profile 2

Profile 3

Profile 4

Fig. 6--Color photographs of profiles 1-4 representing altitudinal sequence of 2,000 - 2,739 m.

Profile 5

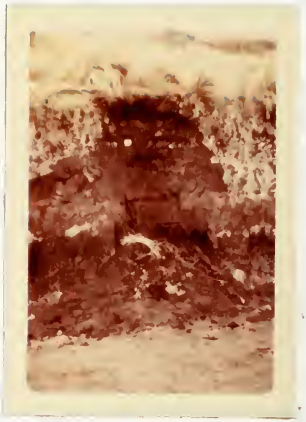

Profile 6

Profile 8

Profile 9

Fig. 7.--Color photographs of profiles 5 and 6 representing altitudinal sequence of 3,120 - 3,510 m and ancillary profiles 8 and 9 at 3,020 and 3,060 m.

products of volcanic glass. The Pachic Andosol A horizons were probably the result of organo-metallic (allophanic) complexes encouraged by occasional uniform depositions of fresh volcanic ash. Increasing thickness of A horizons with altitude was probably due to decreasing biological and/or oxidative decomposition due to decrease in temperature. Proximity to volcanic ash source was most likely an additional thickness-encouraging factor.

Genesis of the [B] horizons was somewhat more difficult to ascertain. The soils are quite permeable but in their natural state do not have well developed ped faces. Due to relatively uniform rainfall the soils appear to remain moist throughout the year. Year-round moist condition is encouraged also by high water retention capacities. These factors tend to discourage desiccation fractures. Lack of layer-lattice silicates whose plate-like morphology expedites orientation on available surfaces is an additional feature contributing to the lack of B horizon development.

Overall development of profiles 1-6 seems to have been highly temperature-dependent. Decreasing potential evapotranspiration with increasing altitude may have discouraged profile development at higher elevations.

Chemical Properties

Soil Reaction

Soil pH measurements in water and 1 N KCl solution are recorded in Table 4 with the exception that neutral salt pH determinations were not made for profiles 9 and 10. In all horizons of profiles 1-8 pH values were higher when measured in water than when measured in 1 N KCl

Table 4. Chemical properties of selected Colombian soils

Horizon	pH 1:1 H_2O	pH 1:1 KCl	Organic Carbon	Ca	Mg	K	Na	Total Bases	CEC	Exch. Al	Base Saturation	Fe_2O_3	pH in 1 N NaF
			%	meq/100 g							%	%	
Profile 1													
A1	5.5	4.6	2.9	7.5	4.9	1.7	0.4	14.4	39.4	0.11	36.7	3.03	9.4
[B]	5.6	4.8	0.6	5.7	4.5	0.4	0.4	10.9	45.5	0.28	24.1	3.35	9.4
C1	6.0	5.3	0.3	7.5	4.5	0.9	1.1	13.9	41.8	0.11	33.2	4.55	9.7
C2	6.0	5.2	0.1	5.2	3.4	0.5	0.3	9.3	23.3	0.11	40.1	1.71	9.7
C3	6.0	5.2	-	-	-	-	-	-	-	-	-	-	-
Profile 2													
A11	5.8	4.5	8.3	5.1	2.6	0.9	0.5	9.0	65.7	1.22	13.7	1.42	11.0
A12	5.8	4.6	6.2	1.1	2.0	0.3	0.2	3.5	51.3	1.21	6.9	1.74	10.9
A3	5.4	4.8	5.8	0.9	1.6	0.3	0.3	3.0	52.6	0.55	5.7	2.26	10.9
[B]	5.3	5.0	1.2	1.9	1.4	0.6	0.3	4.1	53.8	0.30	7.7	3.03	10.6
C	5.7	5.0	1.0	2.0	2.1	0.5	0.4	4.9	52.4	0.29	9.4	3.68	10.3
Profile 3													
A1	5.3	4.7	9.4	0.3	1.0	0.1	0.3	1.7	55.6	0.05	3.1	1.54	11.4
A3	5.7	5.1	5.7	0.3	0.8	0.1	0.3	1.5	63.4	0.28	2.3	2.03	11.2
[B]	5.8	5.3	1.3	0.3	1.5	0.3	0.2	2.3	51.7	0.17	4.3	3.53	10.9
C	5.4	4.8	0.8	0.3	1.4	0.6	0.5	2.8	50.1	0.62	5.6	4.11	10.7

Table 4. Continued.

Horizon	pH 1:1 H_2O	pH 1:1 KCl	Organic Carbon	Ca	Mg	K	Na	Total Bases	CEC	Exch. Al	Base Saturation	Fe_2O_3	pH in 1 N NaF*
			%	meq/100 g							%	%	
Profile 4													
A1	5.6	4.4	6.0	3.4	2.0	1.1	0.1	6.6	34.3	1.82	19.2	2.09	10.1
A3	5.5	4.2	2.3	3.6	2.7	1.3	0.2	7.8	36.8	0.85	21.1	3.31	9.7
[B]	5.7	4.3	1.6	2.7	1.4	0.8	0.2	5.0	35.8	0.35	13.9	3.63	10.2
C	5.8	4.8	1.1	2.5	2.1	0.8	0.3	5.7	35.4	0.27	16.2	4.05	9.9
Profile 5													
A1	5.2	4.6	8.5	3.9	1.6	0.6	0.4	6.4	56.6	1.46	11.4	1.58	11.2
AC	5.3	4.8	4.1	0.4	1.2	0.1	0.1	1.9	53.3	0.82	3.6	2.61	11.2
C1	5.3	4.8	2.9	0.8	1.6	0.7	0.1	3.2	45.1	0.49	7.1	2.81	10.8
C2	5.7	4.7	3.4	1.3	3.8	0.7	0.2	6.0	47.8	0.50	12.6	4.25	10.2
IIC3	6.0	5.3	1.1	0.9	3.3	0.4	0.2	4.8	61.5	0.34	7.8	4.86	10.6
Profile 6													
A1	5.1	4.3	6.9	1.1	2.5	0.3	0.1	3.9	64.8	4.51	6.1	1.32	11.0
As	5.3	4.4	-	-	-	-	-	-	-	-	-	-	-
$IIA1_b$	5.3	4.6	4.1	0.9	0.7	0.1	0.1	1.9	25.1	0.88	7.5	1.64	10.9
$IIC1_b$	5.7	4.7	2.2	1.0	0.4	0.1	0.1	1.6	14.8	0.57	11.0	1.60	10.8
$IIIA1_b$	5.8	4.8	7.5	1.6	1.2	0.1	0.1	2.9	61.9	0.39	4.7	1.98	10.9

Table 4. Continued.

Horizon	pH 1:1 H_2O	pH 1:1 KCl	Organic Carbon	Ca	Mg	K	Na	Total Bases	CEC	Exch. Al	Base Saturation	Fe_2O_3	pH in 1 N NaF
			%	meq/100 g							%	%	
Profile 7													
A1	5.8	4.6	1.9	1.2	1.6	0.3	0.2	3.1	26.6	0.99	11.8	1.35	10.8
A3	5.5	4.2	1.4	2.2	2.8	0.3	0.2	5.4	21.8	1.34	24.7	2.76	7.7
IIC	5.0	4.5	0.4	3.8	4.4	0.4	0.3	8.8	20.7	0.10	42.5	4.75	7.6
Profile 8													
A11	6.6	5.8	3.3	9.5	9.1	4.4	0.2	23.2	28.1	0.05	82.3	1.22	7.5
A12	6.9	5.8	3.1	11.3	7.0	4.9	0.3	23.5	28.8	0.05	81.6	1.47	7.6
A13	6.6	5.1	2.7	11.1	6.8	2.8	0.3	21.0	25.2	0.05	83.3	1.48	7.4
A14	5.7	4.9	2.2	12.7	6.1	2.6	0.5	21.9	32.3	0.05	68.0	2.20	7.4
IIC	-	-	-	-	-	-	-	-	-	-	-	-	7.2
Profile 9													
A11	6.1	-	3.1	10.6	2.9	2.0	0.1	15.6	29.1	-	53.6	2.32	7.8
A12	5.8	-	2.1	10.4	1.9	0.9	0.2	13.4	30.6	0.05	43.8	2.61	-
A3	5.8	-	1.6	9.7	4.4	1.1	0.4	15.6	36.5	0.11	42.7	3.83	7.9
C1	5.9	-	1.3	10.8	2.4	1.4	0.6	15.2	34.9	-0-	43.6	4.08	-
C2	5.9	-	0.8	9.8	3.3	1.8	0.6	15.5	33.8	0.05	45.9	4.29	-

Table 4. Continued.

Horizon	pH 1:1 H_2O	pH 1:1 KCl	Organic Carbon	Ca	Mg	K	Na	Total Bases	CEC	Exch. Al	Base Saturation	Fe_2O_3	pH in* 1 N NaF
			%	meq/100 g							%	%	
							Profile 10						
A11	5.6	-	3.2	8.9	2.1	2.5	0.1	13.5	31.7	0.02	42.6	2.22	-
A12	5.6	-	2.5	7.2	1.3	1.3	0.1	9.8	23.6	0.28	41.5	2.45	-
B1	5.2	-	0.8	5.9	2.3	2.5	0.1	10.7	31.1	0.79	34.4	4.00	-
B2t	4.6	-	0.6	1.7	0.8	0.9	0.2	3.6	37.4	1.43	9.6	4.70	-
C	5.2	-	0.3	5.5	3.7	0.8	0.2	10.2	34.2	0.69	29.8	3.80	-

* pH of 1 gram of soil in 50 ml of 1 N NaF after 2 minutes.

- Not determined.

solution. Carlisle (1982) reported that neutral salt pH values represent active acidity in the soil and therefore would be expected to be lower.

Soil reaction values were remarkably uniform for profiles 1-6 with a range of 5.1 to 6.0 in water and 4.2 to 5.3 in KCl. Even though the magnitude of variability hardly encompassed one pH unit, certain trends were noticeable. The pH values tended to increase with depth in the profile and to decrease with increasing altitude.

Organic Carbon

Organic matter is formed in the biological decomposition of plant and animal residues. Nariño Andosols had unusually high organic carbon contents as shown in Table 4. Organic carbon contents of A1 horizons of profiles 1-6 ranged from a low of 2.9% at 2,000 m to a maximum of 9.4% in profile 3 at 2,440 m. Values tended to decrease with depth and to increase for comparable depths below the A1 horizon with increasing altitude.

Profile 7 exhibited lowest relative organic carbon contents of all profiles investigated. Profiles 8-10 had similar A horizon organic carbon contents;however,for profile 8 these values remained relatively high with depth.

Exchangeable Bases

Exchangeable calcium values generally decreased with depth in the profile and with increasing altitude for comparable depths in profiles 1-6. Trends were more variable for profiles 7-10. Exchangeable Ca increased with depth for profiles 7 and 8; remained relatively constant for profile 9; and decreased with depth to the C horizon for profile 10.

Consistent trends were not displayed by exchangeable Mg distributions

(Table 4) for profiles 1-6. Maximum exchangeable Mg was encountered in profile 1 (2,000 m). Exchangeable Mg increased with depth in profile 7 but decreased with depth in profile 8 where maximum values (6.1 - 9.1 meq/100 g) for all profiles investigated were encountered. Exchangeable Mg values were variable with depth in profiles 9 and 10.

With the exception of profile 3 exchangeable K contents tended to decrease with depth for profiles 1-6. There was a general tendency for exchangeable K to decrease with increasing elevation for these profiles. Maximum exchangeable K contents for all profiles investigated occurred in profiles 8-10.

Exchangeable Na tended to decrease with increasing altitude for profiles 1-6. No noticeable trends were observed within individual profiles. There was some tendency for exchangeable Na to increase with depth in profiles 7-10.

With the exception of profile 3 total exchangeable bases for profiles 1-6 tended to decrease with depth in the profile; although in some cases such as profiles 2 and 5, there was a slight increase in subsurface horizons. Total bases increased with depth in profile 7 and were maximum for all profiles investigated in profile 8. Total exchangeable base contents of profiles 9 and 10 were similar in magnitude to those of profile 1.

Exchangeable Aluminum

Exchangeable aluminum values for profile 1-6 tended to increase with increasing elevation and decrease with profile depth again with the exception of profile 3. Exchangeable Al distribution was erratic with depth in profile 7. Profiles 8 and 9 were quite low in exchangeable Al in comparison to all other profiles investigated. Profile 10

exhibited a maximum exchangeable Al content of 1.43 meq/100 g in the B2t horizon.

Cation Exchange Capacity

Cation exchange capacity values were variable and did not display trends with profile depth or altitude. Profiles 7-10 did have slightly lower CEC values than those exhibited by profiles 1-6. CEC values ranged from a low of 14.9 meq/100 g in a buried C horizon of profile 6 to a maximum of 65.7 meq/100 g in the A1 horizon of profile 2.

Free Iron Oxides

Free iron oxides tended to increase with depth in all profiles and generally decreased with increasing altitude for profiles 1-6. Maximum percent Fe_2O_3 for profile 10 coincided with the B2t horizon.

Sodium Fluoride Test for Allophane

Sodium fluoride reaction values in Table 4 indicate that all horizons of profiles 1-6 were dominated by allophane as evidenced by values greater than pH 9.4. These values ranged from the minimum of pH 9.4 in the A1 and [B]horizons of profile 1 to a maximum of pH 11.4 in the A1 horizon of profile 3.

Genetic Interrelationships of Chemical Properties

The lack of profile development and distribution with depth of most chemical parameters indicated that profiles 1-6 were youthful soils. The A horizons of these soils with their dark colors due to high organic carbon contents provided visible evidence of profile differentiation. Accumulation of organic carbon especially in the surface horizons of profiles 1-6 was most likely encouraged by a high amount

of biologic activity and the presence of highly reactive metallic surfaces in the form of allophane and other amorphous colloids. The relatively low organic carbon content of the A1 horizon of profile 1 was due mainly to the oxidation enhancement of higher temperatures. Organic colloid translocation was noted as evidenced by the relatively high organic carbon contents in lower horizons.

Base saturation and pH values were generally unrelated for profiles 1-7. Interpretation of CEC and base saturation data was confounded by the presence of allophane which has a highly pH-dependent exchange capacity. Cation exchange capacities for these soils were determined with NH_4OAc at pH 7.0 and consequently were high due to the inclusion of a considerable amount of variable charge. Cation exchange capacities determined at lower pH's or at the prevailing field pH of the soil generally give a more realistic picture of the actual charge participating in exchange reactions under natural conditions. The magnitude of permanent charge would be expected to vary according to the degree of tetrahedral substitution of aluminum for silica. The amount and crystallinity of allophane present in addition to the presence of crystalline colloidal species with low pH dependent charges would considerably influence cation exchange capacity measurements at pH 7.0. As would be expected the aforementioned factors vary from horizon to horizon and from soil to soil. Consequently base saturation values have dubious interpretative worth due to a changing cation exchange capacity base. The contribution of organic matter, especially in surface horizons, to confounding interpretation of these data cannot be ignored.

The distribution of free iron oxides with profile depth indicates that Fe has been released from primary minerals and translocated by

percolating water to lower horizons. Cheluviation has most likely been one of the principle mechanisms of iron translocation in addition to reduction and subsequent leaching.

Allophane contents as shown by NaF test pH values were greater at higher altitudes for profiles 1-6. The tendency for these values to decrease with depth in the profile indicates that allophane has taken on a more crystalline character and/or there has been an increase in crystalline phyllosilicates. Either factor or the combination of both implies a decreased capacity to release hydroxyls upon treatment with sodium fluoride solution.

Physical Properties

Particle size distribution data for profiles 1-10 are presented in Table 5. Several horizons in profiles 2, 3, 5, 6, and 7 refused to disperse in sodium hexametaphosphate. The A12 and A3 horizons of profile 2 and the AC horizon of profile 5 were dispersed with NaOCl. The [B] and C horizons of profile 2 and the C horizon of profile 3 were dispersed with Na_2CO_3. Clay distributions with depth for profiles 1-9 indicate no evidence of downward movement and accumulation in lower horizons. A maximum of 48% clay ($< 2\ \mu$) was noted for the B1 horizon of profile 10 which did not coincide with the argillic horizon as determined in the field. Fine clay ($< 0.2\ \mu$) contents are most likely greater in the B2t horizon due to maximum development of clay skins (argillans) in this horizon. Miller (1965) reported that the major portion of argillans in a Canfield silt loam were composed of $< 0.2\ \mu$ clay. This conclusion was confirmed by Calhoun (1968) on similar soils in northeastern Ohio.

Table 5. Physical properties of selected Colombian soils

Horizon	Depth	Particle Size Distribution: Sand 2 - .05 mm	Silt .05 - .002 mm	Clay <.002 mm	15-bar H_2O %	Bulk Density g/cc
	cm		%			
			Profile 1			
A1	0-45	27	39	34	25.0	0.93
[B]	45-73	37	38	25	31.1	0.80
C1	73-121	25	44	31	30.7	0.72
C2	121-151	59	21	20	-	0.90
C3	151+	15	32	53	-	-
			Profile 2			
A11	0-41	45	30	25[1]	29.0	0.44
A12	41-58	39	34	27[1]	26.2	0.71
A3	58-70	31	46	23[1]	29.4	-
[B]	70-96	35	39	26[2]	38.2	0.49
C	96-160	29	40	31[2]	34.7	0.64
			Profile 3			
A11	0-50	*	*	*	33.2	0.44
A12	50-100	*	*	*	29.2	-
[B]	100-120	*	*	*	32.7	0.54
C	120+	27	42	31[2]	33.0	0.64
			Profile 4			
A1	0-68	29	34	37	14.2	0.84
A3	68-88	28	33	39	11.2	-
[B]	88-115	26	41	33	11.7	0.81
C	115+	31	43	26	13.0	0.60
			Profile 5			
A1	0-55	*	*	*	30.9	0.49
AC	55-69	33	41	26[1]	22.5	0.49
C1	69-94	40	30	30	11.9	-
C2	94-139	30	34	36	22.3	0.45
IIC3	139+	*	*	*	-	-

Table 5. Continued

Horizon	Depth	Particle Size Distribution: Sand 2 - .05 mm	Silt .05 - .002 mm	Clay < .002 mm	15-bar H_2O	Bulk Density
	cm		%			g/cc
			Profile 6			
A1	0-38	38	41	21	35.9	0.49
As	38-51	51	35	14	-	-
IIA1b	51-98	60	27	13	10.4	0.66
IIC1b	98-135	*	*	*	-	1.22
IIIA1b	135-190	*	*	*	19.6	0.48
			Profile 7			
A1	0-50	*	*	*	30.0	-
A3	50-67	43	20	37	16.2	-
IIC	67+	25	18	57	11.6	-
			Profile 8			
A11	0-12	51	29	20	9.5	-
A12	12-49	20	50	30	7.4	-
A13	49-67	45	34	21	-	-
A14	67-131	34	38	28	-	-
IIC	131-152	-	-	-	-	-
			Profile 9			
A11	0-27	40	32	28	-	-
A12	27-66	38	30	32	-	-
A3	66-88	48	26	26	-	-
C1	88-105	44	24	32	-	-
C2	105+	36	20	44	-	-
			Profile 10			
A11	0-16	46	32	22	-	-
A12	16-39	42	32	26	-	-
B1	39-50	36	16	48	-	-
B2t	50-85	42	14	44	-	-
C	85-205	48	24	28	-	-

* Sample wouldn't disperse - not determined.

1 Dispersed with NaOCl.

2 Field moist soil dispersed with Na_2CO_3.

Bulk density values for profiles 1-6 varied from a low of 0.44 g/cc for the Ail horizon of profile 2 and the A1 horizon of profile 3 to a maximum of 1.22 g/cc for the IIC1b horizon of profile 6. Bulk densities were characteristically low as expected for soils developed from aeolian pyroclastic materials. The lone exception of the IIC1b horizon mentioned above was due to a high sand content consisting of vitric cinders and other coarse-textured pyroclastic components.

Fifteen-bar water contents were typically high for profiles 1-6 reflecting the volcanic origin of their parent materials. They ranged from a low of 10.4% in the IIC1b horizon of profile 6 to a high of 38.2% in B horizon of profile 2.

Low bulk density values were a reflection of the exceptionally high porosity of Andosols. High 15-bar H_2O contents were a manifestation of the affinity of allophane for water.

Sand Mineralogy

The primary mineral content of the 50 - 500 μ sand fraction represents the original mineralogical nature of the volcanic ash parent material as modified by pedogenetic processes.

Light Minerals

The distribution of light minerals in the 50 - 500 μ fraction is given in Table 6. Quartz was a minor light mineral constituent in all profiles investigated. Feldspar was the dominant species observed generally followed in abundance by volcanic glass. Weathering products represented difficultly identifiable, highly altered minerals which may have been derived from biotite and/or feldspar (Luna, 1970).

Quartz contents generally displayed erratic distribution with

Table 6. Sand (50-500 μ fraction) mineralogy of selected Colombian soils

Horizon	Light minerals in 100 grains						
	Quartz	Feldspar	Volcanic glass	Weathering products	Rock fragments	Biotite	Other minerals
Profile 1							
A1	12	47	5	36	-	-	-
[B]	15	83	-	2	tr	-	-
C1	11	83	tr	6	tr	-	-
C2	7	55	-	18	tr	20	-
C3	8	78	-	10	-	4	-
Profile 2							
A11	19	45	15	21	-	tr	-
A12	5	60	9	22	-	4	-
A3	2	63	11	24	tr	tr	-
[B]	19	60	7	14	-	-	-
C	16	64	2	18	-	-	-
Profile 3							
A11	4	52	22	22	-	-	-
A12	3	66	19	12	-	-	-
[B]	7	80	8	5	-	tr	-
C	4	68	5	23	-	-	-
Profile 4							
A1	2	53	19	26	-	-	-
A3	3	40	16	41	-	-	-
[B]	3	57	12	28	-	-	-
C	10	75	3	10	-	2	-
Profile 5							
A1	tr	57	27	13	-	3	-
AC	3	64	17	12	-	4	-
C1	2	47	22	29	-	-	-
C2	5	45	13	37	-	-	-
IIC3	6	62	8	24	-	-	-

Table 6. Continued

Heavy minerals in 100 transparent grains							
Horn-blende	Oxy-horn-blende	Augite	Hyper-sthene	Zircon	Biotite	Altered	Opaque
			Profile 1				
95	tr	5	tr	-	-	tr	17
100	-	-	tr	tr	-	-	34
96	tr	2	-	-	tr	2	12
100	-	tr	tr	-	tr	-	12
85	-	4	-	tr	9	2	79
			Profile 2				
87	tr	5	8	-	-	-	25
87	-	5	8	-	-	tr	21
89	-	4	7	-	-	-	24
88	2	6	2	-	-	2	11
88	6	tr	4	-	-	2	17
			Profile 3				
86	-	3	8	-	-	3	13
85	-	6	9	tr	-	tr	14
66	2	10	19	tr	-	3	14
47	tr	10	37	-	tr	6	22
			Profile 4				
71	2	7	16	tr	-	4	23
67	2	13	15	-	-	3	15
62	2	18	18	-	tr	tr	23
89	2	4	3	-	4	-	32
			Profile 5				
87	tr	4	9	tr	-	-	12
76	-	8	16	-	-	tr	11
64	-	17	19	tr	-	tr	13
74	2	19	5	-	-	-	10
58	-	18	18	-	2	4	6

Table 6. Continued

Horizon	Light minerals in 100 grains						
	Quartz	Feldspar	Volcanic glass	Weathering products	Rock fragments	Biotite	Other minerals
Profile 6							
A1	3	36	34	27	-	-	-
As	5	32	22	41	-	-	-
IIA1b	11	29	30	28	-	2	-
IIC1b	8	31	35	16	-	5	5
IIIA1b	5	26	42	25	-	-	2
Profile 7							
A1	5	68	16	11	-	tr	-
A3	2	80	8	10	-	tr	-
IIC	17	76	3	4	-	-	-
Profile 8							
A11	9	29	33	16	-	11	2
A12	6	38	33	20	tr	tr	3
A13	7	45	22	19	2	2	3
A14	7	33	39	21	tr	-	-
IIC	tr	25	66	9	tr	-	-
Profile 9							
A11	tr	52	17	31	-	tr	-
A12	-	55	12	28	-	5	-
A3	-	52	11	34	-	3	-
C1	2	41	7	42	-	7	-
C2	-	53	7	40	-	tr	-
Profile 10							
A11	-	79	12	9	-	-	-
A12	-	80	10	10	-	tr	-
B1	tr	77	6	17	-	tr	-
B2t	ND	ND	ND	ND	ND	ND	ND
C	ND	ND	ND	ND	ND	ND	ND
IIB2t	ND	ND	ND	ND	ND	ND	ND

ND Not determined.

tr Trace.

- None present.

Table 6. Continued

Heavy minerals in 100 transparent grains							
Horn-blende	Oxy-horn-blende	Augite	Hyper-sthene	Zircon	Biotite	Altered	Opaque
			Profile 6				
42	-	24	32	-	-	2	8
44	tr	18	32	-	-	6	10
67	-	16	9	-	-	8	9
73	-	10	15	tr	tr	2	16
44	tr	33	23	-	-	-	8
			Profile 7				
87	tr	5	8	tr	4	tr	19
95	tr	3	tr	tr	2	tr	36
93	3	2	2	tr	-	tr	47
			Profile 8				
88	tr	-	7	tr	3	2	7
77	tr	11	3	-	6	3	3
85	-	12	tr	-	-	3	6
81	-	6	8	-	tr	5	7
80	-	9	6	-	-	5	3
			Profile 9				
45	-	21	28	-	-	6	9
53	-	20	27	-	tr	tr	18
33	3	17	33	-	-	12	22
32	4	18	34	-	2	7	11
46	tr	10	40	-	-	-	11
			Profile 10				
96	-	tr	4	-	-	-	11
78	tr	8	12	tr	-	2	10
86	2	5	7	-	2	tr	14
94	2	tr	2	-	2	-	14
97	tr	tr	3	-	-	-	10
85	2	9	-	-	tr	4	54

depth in profiles 1-6. In profile 1, however, this mineral species was concentrated in the surface horizon. There was some tendency for quartz content to decrease with increasing altitude. Quartz content was extremely low to absent in profile 9 and the upper horizons of profile 10.

Potassium feldspars and the plagioclase series were not differentiated but combined and reported as feldspars. Feldspar was present in greatest amounts generally at lower altitudes for profiles 1-6. Feldspar distributions within these profiles were mostly erratic however in profiles 1-4 between 2,600 m and 2,730 m there was some tendency for feldspar to increase with depth. Feldspar content of profile 7 was similar to that of profile 1. The content of this species in profile 8 paralleled that of profile 6. Profile 9 exhibited uniform feldspar distribution with the exception of a discontinuity at the C1 horizon.

Volcanic glass decreased with profile depth and increased with increasing altitude in profiles 1-6. Profile 6 was highest in glass content but did not show trends with depth due to depositional stratification and possibly to reduced weathering intensity at the 3,510 m elevation.

Heavy Minerals

Distribution of heavy minerals in the 50 - 500 μ fraction is shown in Table 6. Hornblende was the dominant individual mineral species for profiles 1-6. The pyroxene group, of which augite and hypersthene were most common species, dominated the A1, As, and IIIAlb horizons of profile 6. Distribution of the heavy mineral suite in profile 6 supports field identification of lithologic discontinuities. These

data suggest that the IIIA1b horizon was developed in materials mineralogically similar to the A1 and A3 horizons. The IIA1b and IIC1b horizons probably represent pyroclastic depositions either from a different source or variation in magma chamber composition from the same source.

Hornblende tended to decrease with profile depth and increasing elevation in profiles 1-6. Profile 9 exhibited lower hornblende contents in contrast to profiles 7, 8, and 10. The pyroxene group dominated all horizons of profile 9 and hypersthene as an individual species was essentially equal in quantity to hornblende in the A3, C1, and C2 horizons.

Zircon, oxyhornblende, and biotite were observed occasionally and only in minor quantities.

Opaque minerals were tabulated separately and were mainly represented by magnetite and iron oxide nodules.

Genetic Relations of Sand Mineral Distributions

Abundance of hornblende, particularly in the heavy mineral fraction, is indicative of parent materials in their initial weathering cycle and of youthful soils developing in these materials. Minor quantities of quartz in the light mineral fraction provide additional evidence for this conclusion. The tendency of hornblende to increase at the expense of hypersthene and augite with decreasing elevation indicates that pedologic weathering has proceeded at a more rapid pace at lower altitudes.

Clay Mineralogy

X-Ray Diffraction

Identification techniques

Clay minerals may be identified through the diffraction of X-rays due to a similarity between interplanar distance (d-spacing) and wavelength. The characteristic d-spacing of a specific clay mineral may be calculated according to Bragg's law ($n\lambda = 2d \sin \theta$) since λ (wavelength) and the angle θ are known. The d-spacing corresponds to the plane perpendicular to the c-axis of layer silicates.

The d-spacing of specific clay minerals will vary predictably according to cation saturation, interlayer liquid (organic molecules) sorbed on clay surfaces and the solution from which the suspended clay was dried (Jackson, 1956).

Hydrated halloysite was identified by a first order spacing of 10.0A which collapsed to 7.41 - 7.20A after heating a Mg-saturated specimen to 100C for 24 hours. Metahalloysite was suggested after Mg-saturation by a 7.25A first order peak. Vermiculite was concluded to be present by the Mg-saturation 14A - 15A spacing and a 10.0A - 10.8A spacing after heating to 500C. Illite was identified by the presistence of a 10A peak for all treatments. Figure 8 demonstrates the technique utilized to identify vermiculite, illite, hydrated halloysite, and metahalloysite. The diffraction pattern for the Mg-saturated coarse clay (0.2 - 2 μ) from horizon A3 of profile 7 exhibits peaks at 14.2A, 9.95A, and 7.25A which can be attributed to vermiculite, illite-hydrated halloysite, and metahalloysite, respectively. Heating of this specimen to 100C for 24 hours revealed diffraction peaks at approximately the same positions. However it can be assumed that the

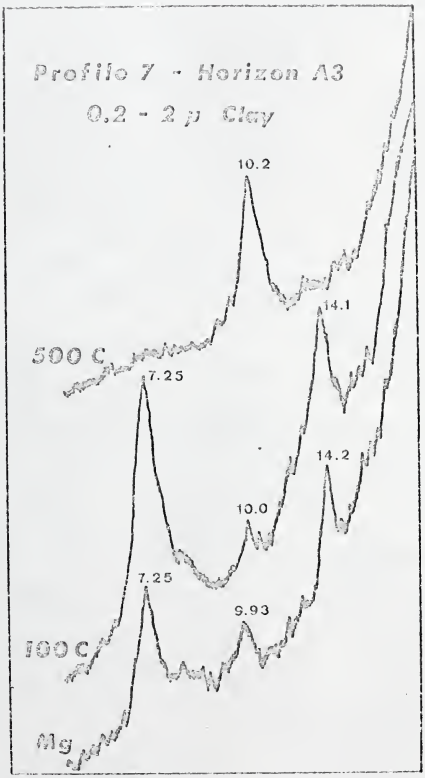

Fig. 8.--X-ray diffraction patterns of Mg-saturated air dry, K-saturated, 100C, and K-saturated 500C treated coarse clay of horizon A3 in profile 7 demonstrating identification of metahalloysite, hydrated halloysite, illite, and vermiculite by changes in d-spacings.

water of hydration has been removed from hydrated halloysite and that it would present a diffraction pattern similar to that of metahalloysite. This can be observed for the 100C diffraction pattern in Figure 8 by the increased intensity of the 7.25A peak and reduced intensity of the 10.0A peak. The small 10.0A peak can be attributed to illite. Further heating to 500C destroyed the halloysite component and caused partial collapse of vermiculite to 10.2A due to destruction of hydroxy-aluminum interlayers. A portion of the 10.2A peak can be assigned to illite which persists at 500C.

Non-crystalline species such as allophane which are amorphous to X-rays cannot be identified due to absence of diffraction maxima. Chlorite and montmorillonite (smectite) were not identified in any of the soils investigated. Peaks in the 7A region were not assigned to kaolinite due to their broadness and 7.2A or greater position. It is often a matter of opinion as to whether components in this region may be identified as metahalloysite or poorly crystallized kaolinite. Obviously a metahalloysite-poorly crystallized kaolinite-crystalline kaolinite continuum exists which complicates assignment of a species name.

Cristobalite and gibbsite were identified by 4.04A and 4.83A spacings, respectively. Spacings of 4.2A and 3.35A were assigned to quartz. Feldspar was identified by diffraction peaks in the 3.10A to 3.25A region.

X-ray diffractograms of fine clay ($< 0.2\ \mu$) and coarse clay ($0.2 - 2\ \mu$) fractions for profiles 1-10 are presented in Figs. 9-18. Recognizable crystalline species from X-ray diffraction patterns are listed in Table 7 and d/n spacings are enumerated in Appendix Table 10 for the above-mentioned clay fractions and profiles.

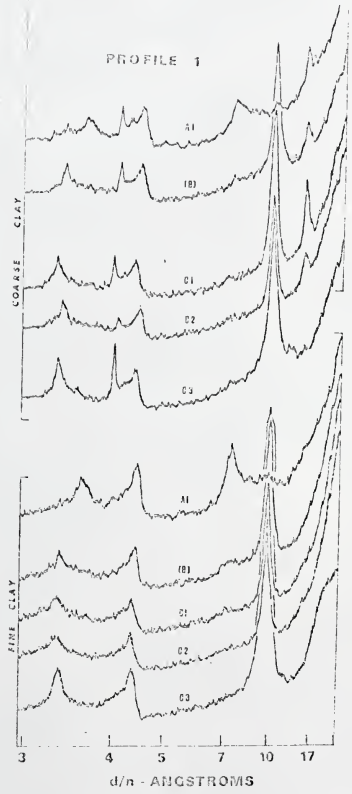

Fig. 9.--X-ray diffraction patterns of Mg-saturated coarse clay (0.2-2μ) and fine clay (< 0.2μ) fractions of profile 1.

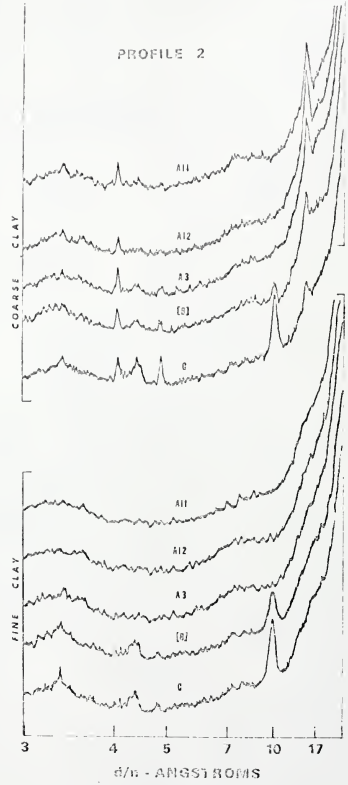

Fig. 10.--X-ray diffraction patterns of Mg-saturated coarse clay (0.2-2μ) and fine clay (< 0.2μ) fractions of profile 2.

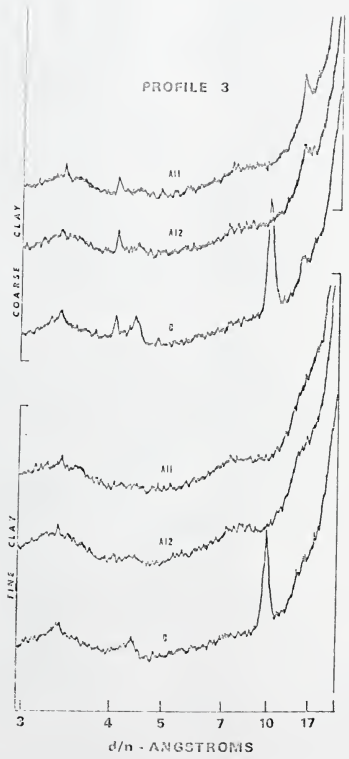

Fig. 11.--X-ray diffraction patterns of Mg-saturated coarse clay (0.2-2μ) and fine clay (< 0.2μ) fractions of profile 3.

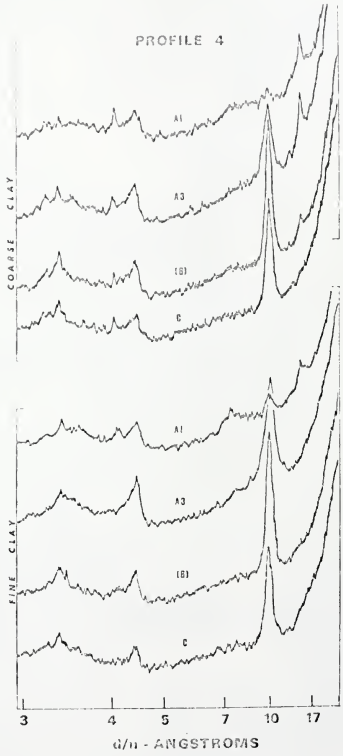

Fig. 12.--X-ray diffraction patterns of Mg-saturated coarse clay (0.2-2μ) and fine clay (< 0.2μ) fractions of profile 4.

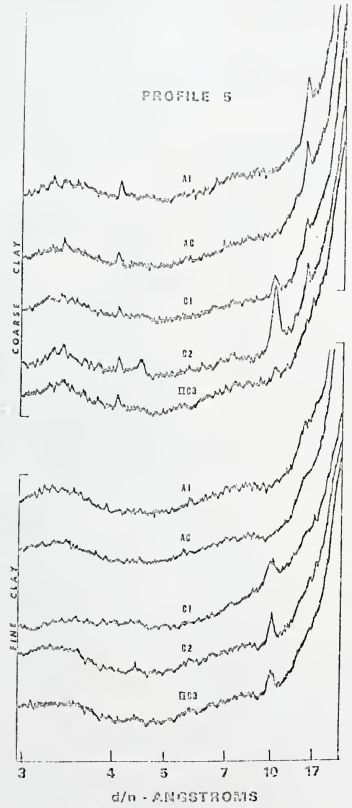

Fig. 13.--X-ray diffraction patterns of Mg-saturated coarse clay (0.2-2μ) and fine clay (< 0.2μ) fractions of profile 5.

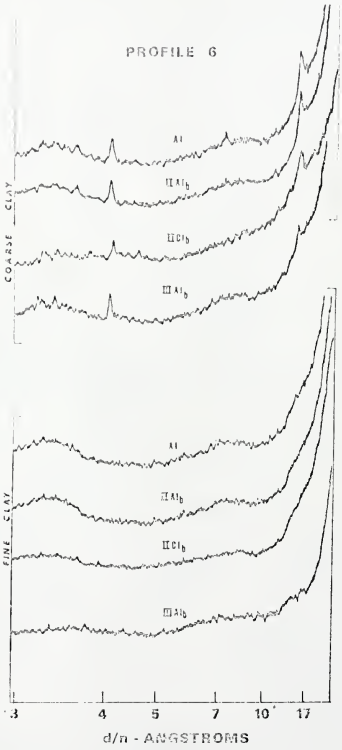

Fig. 14.--X-ray diffraction patterns of Mg-saturated coarse clay (0.2-2μ) and fine clay (< 0.2μ) fractions of profile 6.

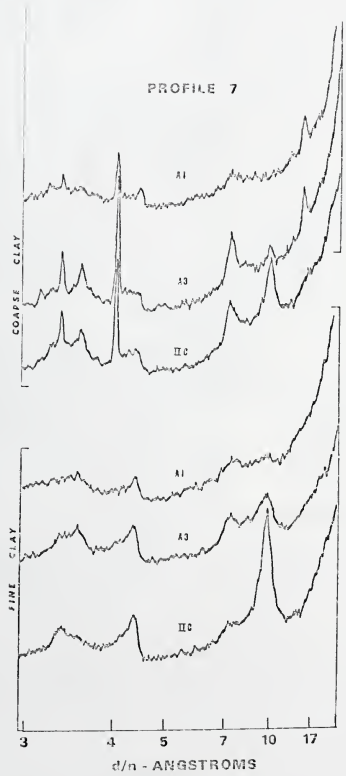

Fig. 15.--X-ray diffraction patterns of Mg-saturated coarse clay (0.2-2μ) and fine clay (< 0.2μ) fractions of profile 7.

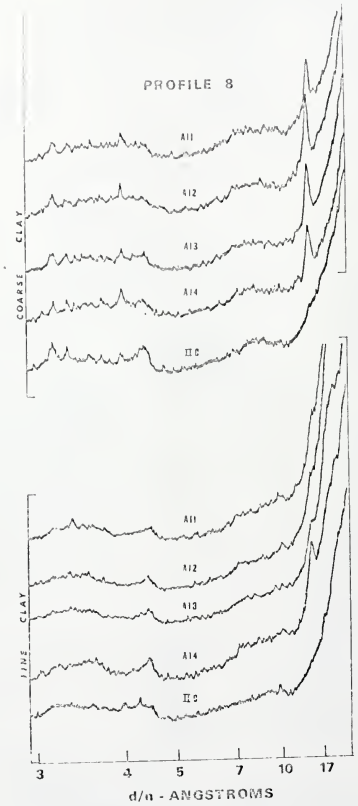

Fig. 16.--X-ray diffraction patterns of Mg-saturated coarse clay (0.2-2μ) and fine clay (< 0.2μ) fractions of profile 8.

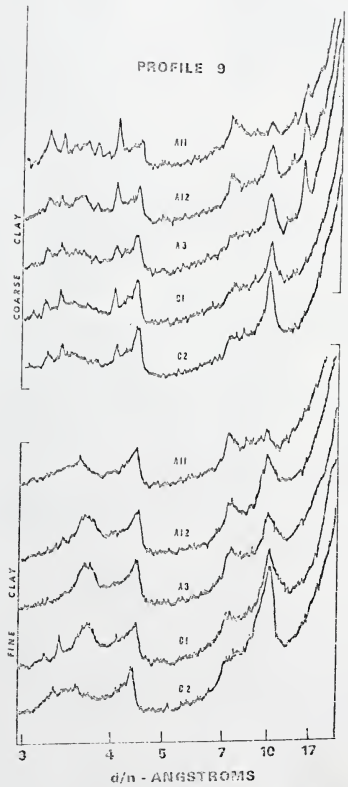

Fig. 17.--X-ray diffraction patterns of Mg-saturated coarse clay (0.2-2μ) and fine clay (< 0.2μ) fractions of profile 9.

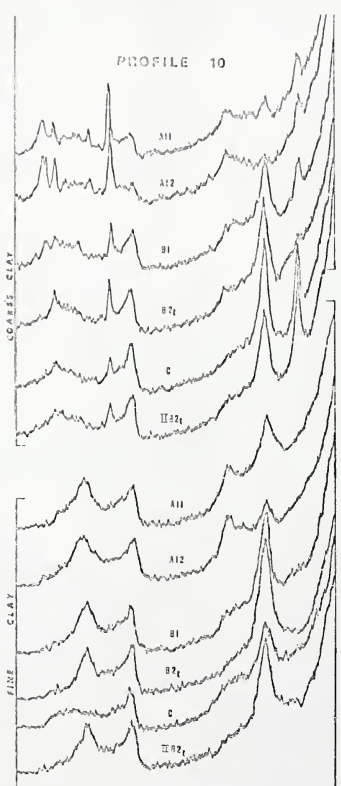

Fig. 18.--X-ray diffraction patterns of Mg-saturated coarse clay (0.2-2μ) and fine clay (<0.2μ) fractions of profile 10.

Table 7. Crystalline minerals recognized from X-ray diffraction patterns of the fine clay (< 0.2 μ) and coarse clay (0.2 - 2 μ) fractions of selected Colombian soils

Profile No.	Horizon	Crystalline Minerals	
		Fine Clay	Coarse Clay
1	A1	$mH_1\ H_2$	$V_1\ mH_2\ H_2\ Cr_3$
	[B]	H_1	$H_1\ V_2\ Cr_3$
	C1	H_1	$H_1\ V_1\ Cr_3$
	C2	H_1	$H_1\ V_2\ Cr_3$
	C3	H_1	$H_1\ Cr_3$
2	A11	Amorphous	$V_1\ Cr_3$
	A12	Amorphous	$V_1\ Cr_3$
	A3	Amorphous	$V_1\ Cr_3\ G_3$
	[B]	$H_1\ G_3$	$V_1\ H_2\ Cr_3\ G_3$
	C	$H_1\ G_3$	$H_1\ V_2\ Cr_3\ G_3$
3	A11	Amorphous	$V_1\ mH_2\ Cr_3$
	A12	Amorphous	$V_1\ Cr_3$
	C	H_1	$H_1\ V_3\ Cr_3$
4	A1	$H_1\ mH_2$	$V_1\ H_2\ Cr_3$
	A3	H_1	$H_1\ V_2\ Cr_3$
	[B]	H_1	$H_1\ V_3\ Cr_3\ F_3$
	C	H_1	$H_1\ Cr_3\ F_3$
5	A1	Amorphous	$V_1\ Cr_3\ F_3$
	AC	Amorphous	$V_1\ Cr_3$
	C1	H_1	$V_1\ H_1\ Cr_3$
	C2	H_1	$H_1\ V_2\ Cr_3\ F_3$
	IIC3	H_1	$H_1\ Cr_3$
6	A1	Amorphous	$V_1\ mH_2\ Cr_3$
	IIA1b	Amorphous	$V_1\ Cr_3$
	IIC1b	Amorphous	$V_1\ Cr_3\ F_3\ Q_3$
	IIIA1b	Amorphous	$V_1\ Cr_3\ F_3\ Q_3$
7	A1	$mH_1\ H_2$	$V_1\ mH_2\ Cr_3\ F_3\ Q_3$
	A3	$H_1\ mH_2$	$V_1\ mH_1\ H_1\ I_2\ Cr_3\ F_3\ Q_3$
	IIC	$H_1\ mH_3$	$H_1\ mH_1\ I_2\ Cr_3\ Q_3$
8	A11	H_1	$V_1\ Cr_3\ F_3\ Q_3$
	A12	$H_1\ V_1$	$V_1\ Cr_3\ F_3\ Q_3$
	A13	$H_1\ V_1$	$V_1\ Cr_3\ F_3\ Q_3$
	A14	$V_1\ H_2$	$V_1\ Cr_3\ F_3\ Q_3$
	IIC	H_1	$V_1\ Cr_3\ F_3\ Q_3$

Table 7. Continued

Profile No.	Horizon	Crystalline Minerals: Fine Clay	Crystalline Minerals: Coarse Clay
9	A11	H_1 mH_1	V_1 mH_1 H_1 I_2 V/I_2 Cr_3 F_3
	A12	H_1 mH_2	V_1 H_1 mH_1 I_2 V/I_2 Cr_3 F_3
	A3	H_1 mH_2	V_1 H_1 mH_2 V/I_3 Cr_3 F_3
	C1	H_1 mH_3	H_1 mH_2 V_2 Cr_3 F_3 Q_3
	C2	H_1 mH_3	H_1 mH_3 Cr_3 F_3 Q_3
10	A11	H_1 mH_2	V_1 H_2 mH_2 Cr_3 F_3 Q_3
	A12	H_1 mH_1	V_1 H_2 mH_2 Cr_3 F_3 Q_3
	B1	H_1 mH_3	V_1 H_1 mH_2 Cr_3 F_3 Q_3
	B2t	H_1 mH_3	H_1 V_2 mH_2 Cr_3 Q_3
	C	H_1 mH_3	H_1 V_1 Cr_3 Q_3
	IIB2t	H_1	V_1 H_1 Cr_3 Q_3
Km 119	B2tb	H_1	H_1 Cr_3 F_3 Q_3

H = Halloysite (hydrated)

mH = Metahalloysite

V = Vermiculite

I = Illite (mica)

Cr = Cristobalite

G = Gibbsite

F = Feldspar

Q = Quartz

Subscript numerals indicate relative intensities with 1 being the highest, 2 intermediate, and 3 the lowest.

Coarse clay mineralogy

Crystallinity and data of profile 1 are shown in Fig. 9 and Table 7, respectively. The coarse clay fraction of profile 1 was composed of varying amounts of vermiculite, metahalloysite, hydrated halloysite, and cristobalite. Peak intensities for vermiculite increased with depth to a maximum in the C1 horizon. A very weak 10A band for hydrated halloysite was noted in the A1 horizon; however, this species dominated the coarse clay fraction in subsequent horizons. Metahalloysite occurred in greatest quantity in the A1 horizon. Cristobalite was present in all horizons.

Profile 2 (Fig. 10 and Table 7) consisted of varying quantities of vermiculite, hydrated halloysite, cristobalite, and gibbsite. The 14A peak of vermiculite gradually decreased in intensity with depth in the profile. A weak 10A peak attributed to hydrated halloysite appeared in the [B] horizon and increased in intensity in the C horizon. The 4.83A peak of gibbsite emerged in the A3 horizon and increased with depth. Cristobalite content remained stable throughout the profile.

Vermiculite, hydrated halloysite, metahalloysite, and cristobalite were identified in the coarse clay fraction of profile 3 (Fig. 11 and Table 7). The 14A peak of vermiculite decreased in intensity and sharpness with decreasing depth. A trace amount of metahalloysite was noted in the A11 horizon. Hydrated halloysite was encountered only in the C horizon. The 4.04A peak of cristobalite was uniformly intense with depth in the profile.

Vermiculite, hydrated halloysite, metahalloysite, cristobalite, and feldspar were noted in profile 4 (Fig. 12 and Table 7). Vermiculite decreased with profile depth and was absent in the C horizon. The 10A

peak of hydrated halloysite increased in intensity with depth to a maximum in the [3] horizon. Cristobalite remained uniform in quantity with depth. Trace amounts of feldspar were noted in the [8] and C horizons.

Hydrated halloysite, metahalloysite, vermiculite, cristobalite, and feldspar were identified in rather small quantities in profile 5 (Fig. 13 and Table 7). Vermiculite displayed a slight tendency to decrease with depth and was absent in the IIC3 horizon. Hydrated halloysite was absent in the A1 and AC horizons. The 10A peak of this species appeared in the C1 and increased in intensity for the C2 and then decreased in the IIC3. Uniform minor quantities of cristobalite were observed in all horizons. Trace amounts of metahalloysite in the C2 and feldspar in the A1 and C2 horizons were identified.

Vermiculite, cristobalite, and small amounts of quartz, metahalloysite, and feldspar were found in profile 6 (Fig. 14 and Table 7). The 14A peak of vermiculite remained rather uniform in intensity with depth to the IIIA1b horizon where there was a slight decrease. Cristobalite content remained stable throughout the profile. A small amount metahalloysite was observed in the A1 horizon. Trace quantities of quartz and feldspar were noted in the IIC1b and IIIA1b horizons.

Profile 7 (Fig. 15 and Table 7) was composed of varying amounts of vermiculite, illite, hydrated halloysite, metahalloysite, cristobalite, feldspar, and quartz. Vermiculite was observed in the A1 and A3 horizons but was absent in the IIC horizon. A very weak 7A region diffraction band in the A1 horizon was assigned to metahalloysite. This peak was well resolved but rather broad in the A3 and IIC horizons. Hydrated halloysite, although absent in the A1 horizon, increased in

intensity with profile depth. Cristobalite, quartz, and feldspar were present in all horizons but in greater quantities in the A3 and IIC horizons.

Vermiculite, cristobalite, feldspar, and quartz were identified in profile 8 (Fig. 16 and Table 7). The 14A peak of vermiculite dominated the first four horizons of this profile but was present only as a slight shoulder in the IIC horizon. Peak intensity remained uniform with depth except for the IIC. Trace quantities of cristobalite, quartz, and feldspar were noted in all horizons.

Profile 9 (Fig. 17 and Table 7) contained varying amounts of vermiculite, illite, hydrated halloysite, metahalloysite, vermiculite-illite intergrade, cristobalite, feldspar, and quartz. Peak intensity and resolution of vermiculite tended to increase with profile depth to the A3 horizon. A faint 14A shoulder was observed in the C1 horizon but was absent in the C2. The 10A peak of halloysite increased in intensity and resolution with increasing depth. A minor portion of this peak was assigned to illite in the A11 and A12 horizons. A poorly resolved band in the 11.6 - 12.6A region was assumed to represent an illite-vermiculite intergrade. Metahalloysite was represented by a broad, weak 7.2A peak in the A11 and A12 horizons. Below this depth metahalloysite presence was indicated by a weak shoulder in the 7.2 - 7.4A region. Cristobalite and feldspar were identified in all horizons; however, quartz was noted only in the C1 and C2 horizons.

Vermiculite, halloysite, metahalloysite, cristobalite, feldspar, and quartz were identified in the coarse clay fraction of profile 10 (Fig. 18 and Table 7). The 14A peak of vermiculite varied in intensity with profile depth. This diffraction peak remained equal in intensity

in the A11, A12, and B1 horizons; occurred as a weak shoulder in the B2t; and was well resolved and more intense in the C and IIB2t horizons. The 10A peak of hydrated halloysite tended to increase in intensity and resolution with profile depth. The presence of metahalloysite was noted by a 7A region shoulder which decreased in intensity with profile depth and subsequently disappeared in the C and IIB2t horizons. Cristobalite was present in greater amounts in the A11 and A12 horizons and then showed some tendency to decrease with depth. Feldspar was noted only in the top three horizons; however, quartz was identified in all horizons.

Fine clay mineralogy

Metahalloysite and hydrated halloysite were identified in the fine clay ($<0.2\ \mu$) fraction of profile 1 (Fig. 9 and Table 7). Metahalloysite was noted by the presence of a broad 7.2 - 7.4A peak in the A1 horizon. Only a trace quantity of hydrated halloysite was observed in the A1 horizon but intense 10A peaks were noted in subsequent horizons especially the C3.

Profile 2 (Fig. 10 and Table 7) was amorphous in the upper three horizons. Hydrated halloysite and small quantities of gibbsite were identified in the [B] and C horizons.

Profile 3 (Fig. 11 and Table 7) was amorphous with the exception of the C horizon where the 10A peak of hydrated halloysite was observed.

The content and distribution of phyllosilicates in profile 4 (Fig. 12 and Table 7) were similar to that of profile 1. Hydrated halloysite and metahalloysite contents were similar in the A1 horizon.

Profile 5 (Fig. 13 and Table 7) was amorphous in the A1 and AC horizons. Small quantities of hydrated halloysite were noted in the lower horizons.

Profile 6 (Fig. 14 and Table 7) was amorphous.

Hydrated halloysite and metahalloysite were identified in the fine clay fraction of profile 7 (Fig. 15 and Table 7). Hydrated halloysite increased with profile depth while the reverse trend occurred for metahalloysite.

Minor quantities of vermiculite and hydrated halloysite were observed in profile 8 (Fig. 16 and Table 7). Vermiculite tended to increase with depth in the A1 horizons but was absent in the IIC horizon.

Profile 9 (Fig. 17 and Table 7) was dominated by varying quantities of hydrated halloysite and metahalloysite. Hydrated halloysite increased with profile depth while the reverse trend occurred for metahalloysite.

Metahalloysite and hydrated halloysite were identified in profile 10 (Fig. 18 and Table 7). Hydrated halloysite generally increased with profile depth to a maximum in the B2t horizon. The 10A peak in the buried argillic horizon (IIB2t) was similar in intensity to that of the B2t. Metahalloysite content reached a maximum in the A11 and A12 horizons and decreased in subsequent horizons.

Distribution of clay minerals

The most striking characteristic noted in data from Figs. 9-18 and Table 7 was the contrasting degree of crystallinity between the fine clay ($\leq 0.2\mu$) and coarse clay ($0.2\text{-}2\mu$) fractions. Invariably, number, intensity, and resolution of diffraction maxima were considerably greater in the coarse clay fraction. The lone exception was the 10A peak of hydrated halloysite which in several cases was equal to or greater in intensity for the fine clay fraction.

In profiles 1-6 coarse clay vermiculite was most prevalent in the

upper horizons. No general trends for this component were displayed with altitude although greatest peak intensities were exhibited in profiles 1 and 2. Coarse clay vermiculite was observed in most horizons of profiles 7-10 and maxima in profile 10, with the exception of C and IIB2t horizon, displayed the same profile trends as profiles 1-6. Fine clay vermiculite was not identified in profiles 1-6;however,this component was observed in profile 8.

Coarse clay hydrated halloysite tended to increase with profile depth and to decrease with increasing elevation in profiles 1-6. An anamolous situation occurred with profile 4 at 2,730 m which was closely allied with profile 1 in content and distribution of coarse clay hydrated halloysite. With the exception of profile 8, which was devoid of coarse clay hydrated halloysite, profile distribution of this constituent for profiles 7-10 was similar to that of profiles 1-6. The distribution of hydrated halloysite in the fine clay fraction of profiles 1-10 was similar to that observed for coarse clay; however, content tended to be slightly greater in the fine clay.

Coarse clay metahalloysite was observed in the A1 horizons of profiles 1 and 3; however, broad weak 7A diffraction bands of dubious interpretation could be noted in other surface horizons of profiles 1-6. Coarse clay metahalloysite was present in greater quantities in profiles 7, 9, and 10 and with the exception of profile 7 it was concentrated in the upper horizons. Fine clay metahalloysite was noted in the A1 horizons of profiles 1 and 4 in the altitudinal sequence of profiles 1-6. This constituent was most prevalent in profiles 7, 9, and 10 but was absent in profile 8. Metahalloysite tended to concentrate in surface horizons and decrease with depth.

Clay mineral genesis

It is necessary to assume, since this is an area of active volcanism, that Andosol profiles 1-6 are accretionary soils which have been under the influence of intermittent additions of fresh volcanic ash. As pointed out previously, profiles 1-5 did not exhibit obvious stratification so it could be assumed, additionally, that particle size and, most likely, mineralogy of ash increments have been uniform. Profile 6 did show obvious stratification; consequently interpretations involving it will be tempered somewhat due to parent material disconformities. The assumption of "accumulative soil" in addition to the high permeability of Andosols dictates that lower horizons will be more severely weathered. It is then logical to conclude that end members of phyllosilicate weathering sequences will occur in the lowest horizons of Andosols.

X-ray diffraction data for the fine clay (< 0.2 μ) fraction of profiles 1-6 indicated a weathering sequence of allophane ---> metahalloysite ---> hydrated halloysite. The degree of completion of this sequence increased with profile depth and with the exception of profile 4 decreased with increasing elevation.

X-ray diffraction data for the coarse clay (0.2 - 2 μ) fraction of profiles 1-6 indicated a weathering sequence similar to that of fine clay. The presence of vermiculite in the coarse clay fraction places Mariño Andosols in a unique position. Vermiculite and/or vermiculite-like clay minerals have been reported in Andosols and mostly interpreted as anamolous occurrences (Besoain, 1969b). According to Jackson (1958) vermiculite formation would occur in Andosols only if mica were present in the parent ash. Data in Table 6 show that insignificant quantities

of biotite occurred in isolated horizons of profiles 1-6. Fieldes (1966) suggested that vermiculite could be formed directly from the "sericitisation" of feldspars. The author observed no sericite formation along plagioclase twins in micromorphological investigations of profiles 1-6. Tercinier and Quantin (1968) reported that in some cases for volcanic ash soils of the humid tropical New Hebrides there was in situ formation of montmorillonite as a transition between allophane and halloysite. Unfortunately they did not suggest a possible mechanism for this sequence. Uchiyama et al. (1968) indicated that for some soils developed on recent volcanic ash near Hokkaido, Japan, montmorillonite was the dominant crystalline species in profiles less than 500 years old. In older soils vermiculite increased and both montmorillonite and vermiculite became increasingly Al interlayered. Kawasaki and Aomine (1966) formulated two alternative 2:1 phyllosilicate formation mechanisms in Andosols: a) Mica → Vermiculite → Montmorillonite → intergrades → Al-chlorite, and b) Pyroxenes → Mg-chlorite → Montmorillonite → intergrades → Al-chlorite.

Data in Appendix Table II clearly show that the 14A d spacing of vermiculite was relatively unaffected by K-saturation. This phenomena is clearly indicative of interlayer Al presence. With the exception of profile 6 there was complete collapse to 10A after 500C heat treatment which negated the presence of chlorite. The incomplete collapse to 10.2 - 10.3A noted in profile 6 could be interpreted as the formation of brucite-like islands in the interlayers of vermiculite. This partially "chloritized" vermiculite could represent a remnant whose formation was encouraged during the base-rich micro-environment which existed shortly after deposition of fresh ash. The abundance of

pyroxenes in the sand (50-500 μ) fraction (Table 6) provide an ample source of Mg and Fe ions for the brucite octahedra.

It is difficult to resolve the presence of a 2:1 phyllosilicate with the structural sophistication of vermiculite in the Andosols of Nariño. It appears that vermiculite pedogenesis has occurred rather rapidly and most likely has formed directly with some modification from a primary mineral source. This can be inferred from its presence only in the coarse clay fraction and its position in the less severely weathered upper horizons. There was no evidence of diagenetic transformation of vermiculite to other 2:1 layered silicates such as illite or montmorillonite. Lack of diagenesis and absence in the fine clay fraction leads to the conclusion that vermiculite in Nariño Andosols is transient or insufficient time has been available for transformation to occur. It is unlikely that the hydrated halloysite increase with profile depth is related to vermiculite degradation.

The author believes that the mechanism of hydrated halloysite formation in Nariño Andosols is similar to that outlined by Fieldes (1955). This involves the gradual rearrangement of random silica tetrahedra and alumina octahedra from allophane into a kaolinite-like framework.

Infrared Analysis

Infrared data are traditionally used to support evidence obtained from other mineralogical analyses. Spectra of the coarse clay (0.2-2 μ) and fine clay (<0.2 μ) fractions for profiles 1-10 are presented in Figs. 19-28. Additional spectra for the coarse and fine clay of a buried argillic horizon (Km 119), a KBr blank, and Ward's halloysite No. 12 are shown in Fig. 29.

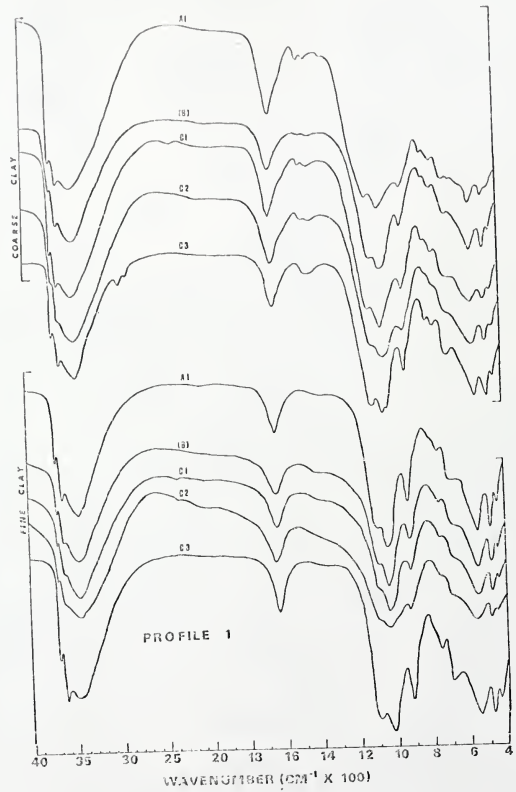

Fig. 19.--Infrared spectra of coarse clay (0.2-2μ) and fine clay ($<0.2\mu$) fractions of profile 1.

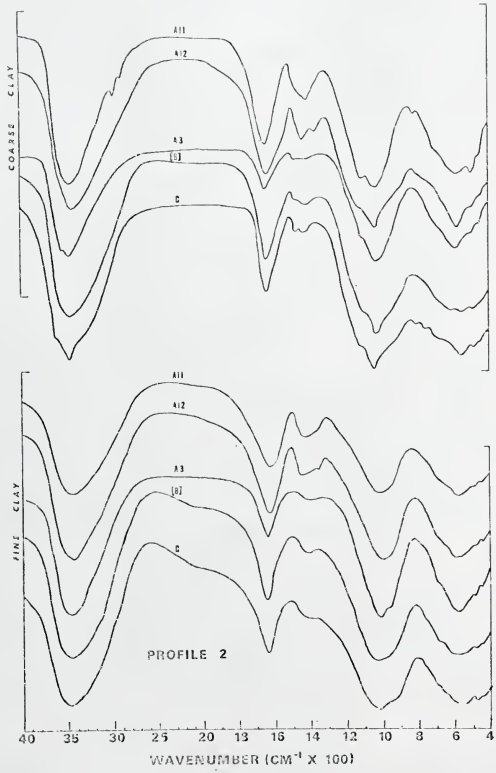

Fig. 20.--Infrared spectra of coarse clay (0.2-2μ) and fine clay (<0.2μ) fractions of profile 2.

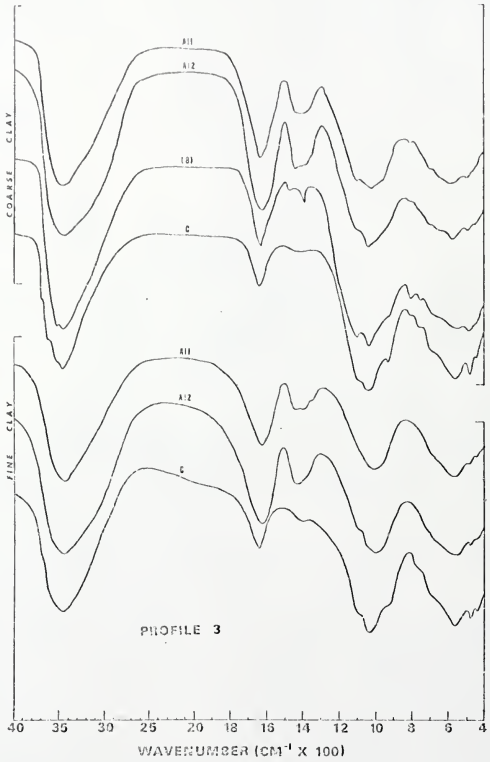

Fig. 21.--Infrared spectra of coarse clay (0.2-2μ) and fine clay (<0.2μ) fractions of profile 3.

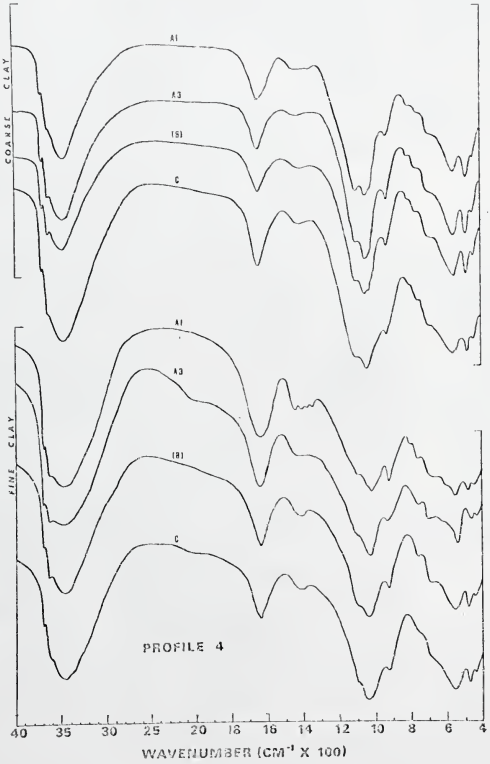

Fig. 22.--Infrared spectra of coarse clay (0.2-2μ) and fine clay ($<0.2\mu$) fractions of profile 4.

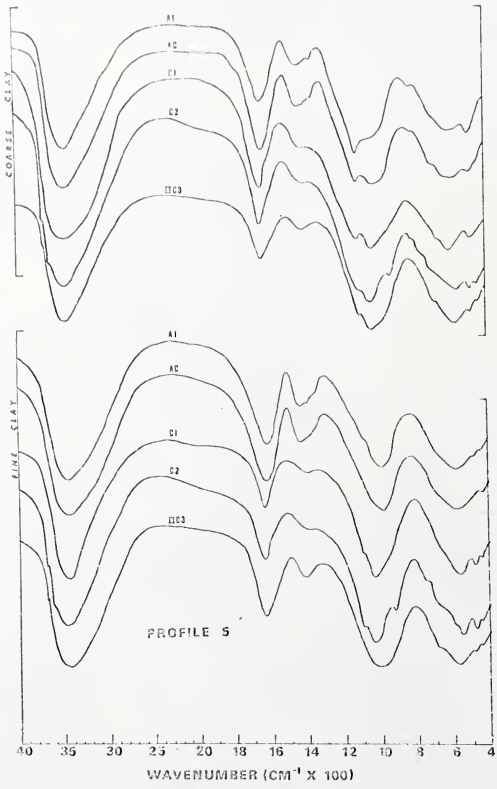

Fig. 23.--Infrared spectra of coarse clay (0.2-2μ) and fine clay (<0.2μ) fractions of profile 5.

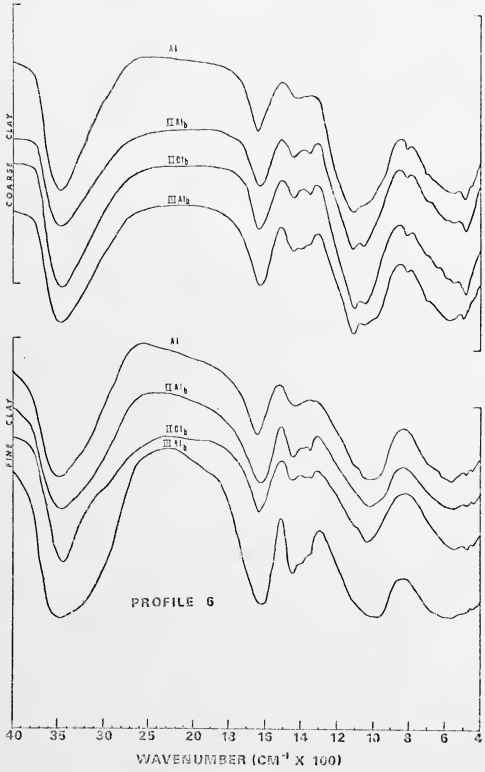

Fig. 24.--Infrared spectra of coarse clay (0.2-2μ) and fine clay (<0.2μ) fractions of profile 6.

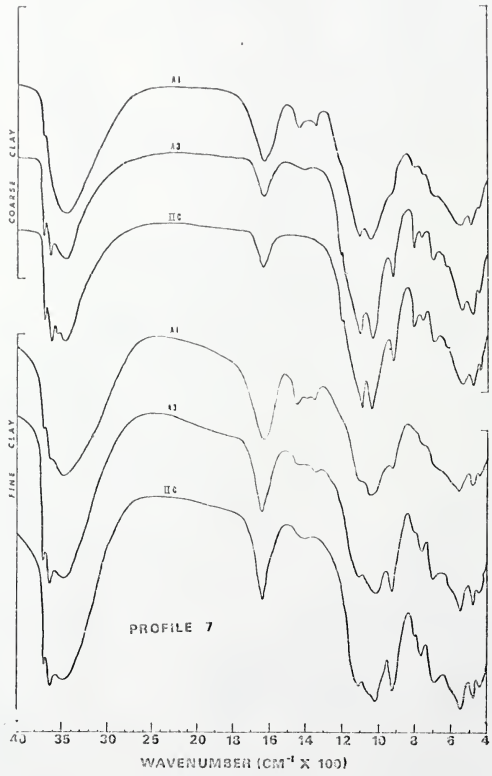

Fig. 25.--Infrared spectra of coarse clay (0.2-2μ) and fine clay (< 0.2μ) fractions of profile 7.

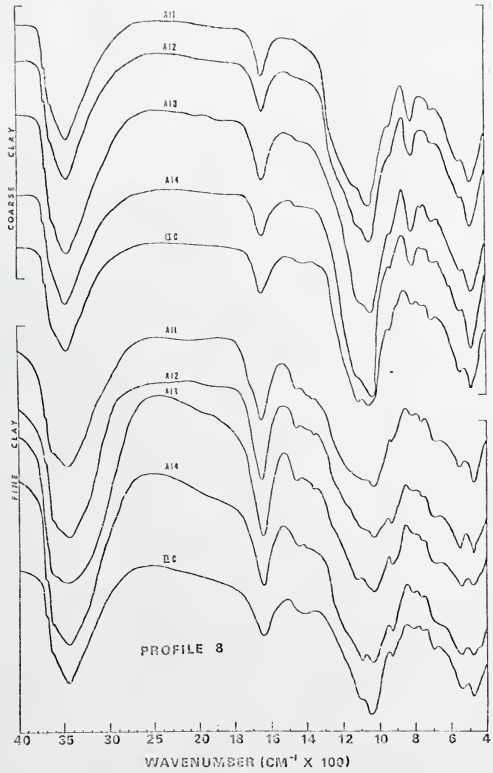

Fig. 26.--Infrared spectra of coarse clay (0.2-2μ) and fine clay (< 0.2μ) fractions of profile 8.

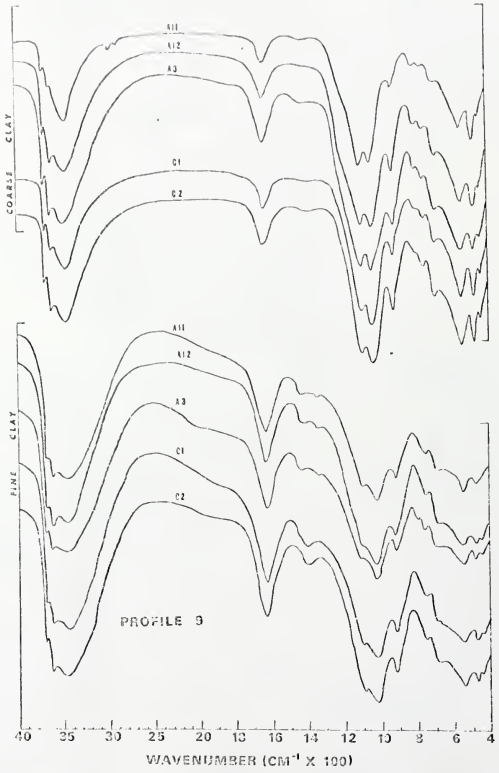

Fig. 27.--Infrared spectra of coarse clay (0.2-2μ) and fine clay (< 0.2μ) fractions of profile 9.

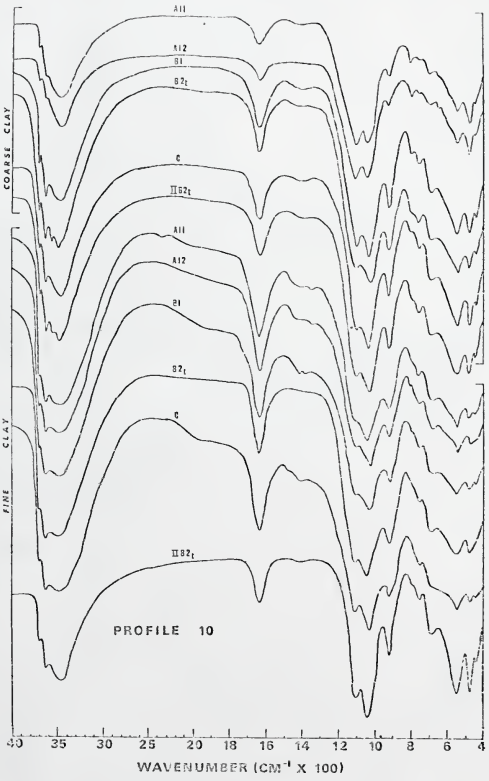

Fig. 28.--Infrared spectra of coarse clay (0.2-2μ) and fine clay (<0.2μ) fractions of profile 10.

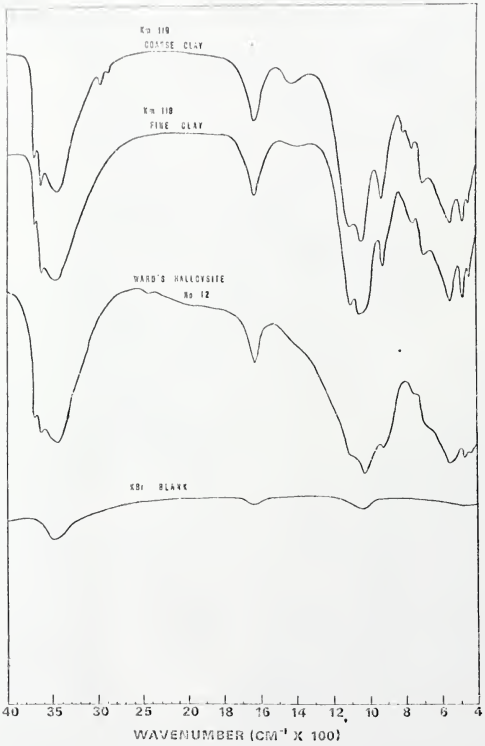

Fig. 29.--Infrared spectra of coarse clay (0.2-2μ) and fine clay (<0.2μ) fractions of km 119 buried argillic horizon; Ward's halloysite No. 12; and KBr blank.

Assignment of absorption maxima

Large absorption bands in the 3,900 cm^{-1} to 2,800 cm^{-1} region were attributed to free O-H stretch at 3,700 cm^{-1}, stretching vibration of octahedral free O-H groups at 3,620 cm^{-1}, and stretching vibration in bonded O-H groups associated with the presence of water on clay surfaces at 3,450 cm^{-1} (Mortensen et al., 1965). The absorption band at 1,630 - 1,640 cm^{-1} was assigned to H-O-H bending (Mortensen et al., 1965). Absorption bands in the 1,400 cm^{-1} region were attributed to ferric silicates (DeMumbrum and Chesters, 1964). Deep absorption peaks observed between 1,250 cm^{-1} and 950 cm^{-1} were assigned to stretching vibration of Si-O while 440 cm^{-1} absorption was due to Si-O bending (Mortensen et al., 1965; Oinuma and Hayashi, 1968). The absorption band between 915 cm^{-1} and 925 cm^{-1} was indicative of X^{+3} -O-H bending which implied dioctahedral layer silicate and/or Al-O-H for kaolin minerals. Absorption maxima in the 450 - 800 cm^{-1} region were assigned to Si-O-X^{+3} vibrations of dioctahedral layer silicates (Oinuma and Hayashi, 1968).

Coarse clay spectra

Coarse clay (0.2 - 2 μ) spectra for profiles 1-10 (Figs. 19-28) displayed deep absorption bands at 3,450 - 3,700 cm^{-1}, 1,630 - 1,640 cm^{-1}, 1,010 - 1,100 cm^{-1} and 500 - 800 cm^{-1}. These absorption maxima indicated the ubiquitous presence of absorbed water, Si-O bonds, X^{+3} -O-H bonds, and X^{+3} -O-Si bonds. The presence of absorption "shoulders" at 3,700 cm^{-1}, 3,620 cm^{-1} and 1,100 cm^{-1} and the band at 910 - 920 cm^{-1} seemed to be correlated with halloysite content as determined by X-ray diffraction. Intensification of the 910 cm^{-1} band and resolution of the 1,100 cm^{-1} "shoulder" to a 1,100 cm^{-1} and 1,040 cm^{-1} doublet could

be indicative of increasing crystallinity of hydrated halloysite. The presence of vermiculite was difficult to ascertain from coarse clay infrared spectra. Data of Oinuma and Hayashi (1968) indicated that absorption maxima of vermiculite would be masked in the presence of halloysite. A weak band at 800 - 810 cm^{-1} was noted in most profiles and was attributed to cristobalite. The well defined doublet at 800 cm^{-1} and 780 cm^{-1} of quartz was not observed in the coarse clay spectra. Although the author believes that the assignment of the 800 cm^{-1} band to cristobalite is corroborated by X-ray diffraction data an interesting point in relation to allophane has surfaced. Fieldes (1955) and Fieldes and Furkert (1966) accepted presence of the 800 cm^{-1} band to be diagnostic of allophane B. Miyauchi and Aomine (1964), however, concluded that strong absorption in the 800 cm^{-1} region was due to cristobalite in the coarse clay fraction of certain Japanese Andosols. This conclusion was substantiated by X-ray diffraction data. In essence Miyauchi and Aomine (1964) questioned the allophane B concept. In light of the Japanese data Fieldes and Furkert (1966) re-examined the soils from which the allophane B concept was derived. They were to some degree vindicated in that quartz and cristobalite contents determined by X-ray analysis of the coarse clay were not sufficient to account for absorption intensity at 800 cm^{-1}. The author suggests that this conclusion is tempered somewhat by the unreliability of quantitative assessment from X-ray diffraction data.

In general it can be observed for the coarse clay fraction, resolution of infrared absorption maxima increased with increasing crystallinity as interpreted from X-ray diffraction analysis.

Fine clay spectra

Fine clay ($<0.2\ \mu$) spectra for profiles 1-10 (Figs. 19-28) exhibit

similar absorption maxima to that of the coarse clay fraction. The basic difference was manifested in generally fewer and less well resolved absorption bands for the fine clay. Of particular interest were the spectra of A11 and A12 horizons of profile 2, A11 horizon of profile 3, AC horizon of profile 5, and IIIA1b horizon of profile 6. Infrared spectra of these soils are similar to those reported for allophane in Japan (Oinuma and Hayashi, 1968) and Colombia (Mejia et al., 1968). Since X-ray diffraction analysis confirmed the absence of quartz and cristobalite in the fine clay, lack of 800 cm^{-1} absorption indicated that the major component of this fraction was allophane A as conceived by Fieldes (1955). Allophane A has been suggested as a precursor to metahalloysite (Fieldes, 1955). Comparison of spectra with Ward's halloysite No. 12 and corroboration with X-ray diffraction data revealed that the assignment of most absorption maxima may be made to halloysite components. As was the case with coarse clay, number and resolution of absorption maxima were closely related to crystallinity.

The fine clay infrared spectrum of a buried argillic horizon (Fig. 29) sampled between Pasto and Ipiales at the Km 119 marker was particularly noteworthy. It was hypothesized at the time of sampling that this soil could represent the ultimate of weathering severity for volcanic ash in the Nariño highlands. Mineralogical parameters suggest that this supposition was valid. X-ray diffraction data (Appendix Table 11) revealed that the crystalline composition of the fine clay was entirely hydrated halloysite. There was a marked similarity between infrared spectra of this sample (Km 119) and that of Ward's halloysite No. 12. Of specific interest was increased resolution of absorption bands at 1,100 cm^{-1}, 920 cm^{-1}, 750 cm^{-1}, 690 cm^{-1}, 545 cm^{-1}, 475 cm^{-1}, and 440 cm^{-1} in comparison to the halloysite standard. This

clearly shows that Km 119 halloysite is of greater crystalline sophistication in respect to Si-O, Al-O-H, and Si-O Al bands of the aluminosilicate framework than Ward's halloysite No. 12. The aforementioned statement can be further projected to include the deepest horizons of profiles 1-6 with the exception of the B3 horizon of profile 1 which is identical in composition and crystallinity to the Km 119 sample.

Differential Thermal Analysis

Clay minerals undergo several reactions upon heating. Reactions at low and intermediate temperatures are generally endothermic in nature due to loss of adsorbed water and crystal-lattice OH^-. High temperature reactions may be endothermic or exothermic resulting from changes in state or crystal structure. Advantage has been taken of the fact that individual clay mineral species react differently at different temperatures through the development of thermal analysis techniques.

Thermal analysis techniques have been especially useful in the detection and characterization of allophane in Andosol clays (Fieldes and Furkert, 1966). These workers reported that the presence of an intense high temperature (900C) exotherm was indicative of allophane A while reduction or absence of this peak was diagnostic of allophane B. Allophane typically displays a strong endotherm between 150-170C.

Unfortunately only a few differential thermograms were obtained in the present investigation due to equipment failure. Thermograms for the coarse clay (0.2 - 2 μ) fraction of four horizons each from profiles 1 and 10 are presented in Fig. 30. The classic asymmetric dehydroxylation endotherm of halloysite near 550C is readily evident in profile 1. The small broad endotherm near 130C was due to adsorbed water. The exotherm between 300-400C was possibly the result of trace quantities

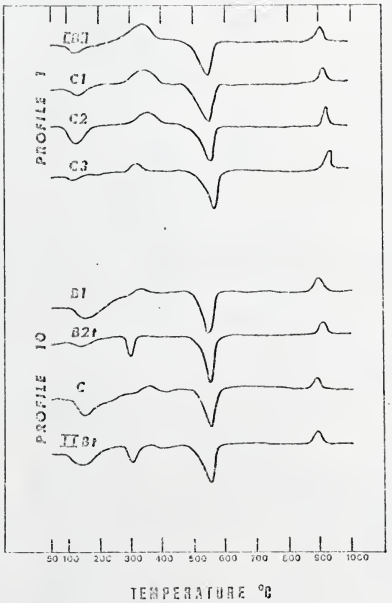

Fig. 30.--Differential thermal patterns of coarse clay (0.2-2μ) fraction of selected horizons from profiles 1 and 10.

of illuvial organic matter. Dehydroxylation endotherm position for halloysite has crystalline implications (Grim, 1968). Endothermic maximum occurred at 545C in horizon [B] and increased with profile depth to 560C in the C3 horizon. This can be interpreted as increasing crystallinity of hydrated halloysite with profile depth. A similar conclusion was derived from X-ray diffraction and infrared patterns of profile 1. Vermiculite presence was not detected in profile 1 by thermal techniques.

Differential thermograms for profile 10 (Fig. 30) were similar to those reported for profile 1 with one major exception: the presence of an endotherm at 320C indicative of gibbsite. An additional benefit of differential thermal analyses was quite evident in this case since gibbsite was not identified in the C and IIB2t horizons by either X-ray diffraction or infrared analysis.

Micromorphology

According to Brewer (1964, p. 402) "fabric and mineral analyses are powerful tools for studying the genesis of soil profiles." At this juncture the investigation herein is concerned with soil fabric or more specifically that portion of soil fabric which is necessarily observed through a petrographic microscope. Brewer (1964, p. 131) defined soil fabric as "the physical constitution of a soil material as expressed by the spatial arrangement of the solid particles and associated voids."

Detailed micromorphological descriptions of major horizons from the altitudinal sequence of profiles 1-6 are presented in Appendix Table II. Selected photomicrographs of thin sections of profile 3 are presented in Figs. 31-38. Profile 3 represented, in general, the median

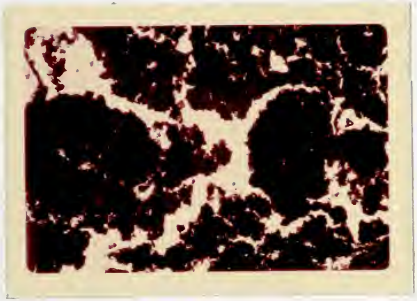

Fig. 31.--Photomicrograph of A11 horizon, profile 3 showing two fecal pellets set against matrix of interconnected ortho-craze planes and orthovughs. Viewed under plain light; magnification approx. 12.5 x.

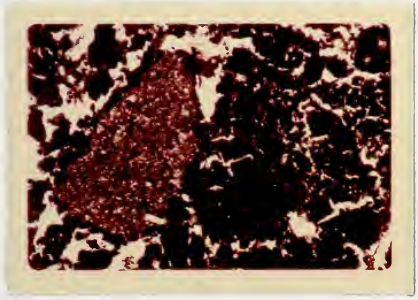

Fig. 32.--Photomicrograph of A11 horizon, profile 3 showing organan on andesite lithorelict and subrounded blocky secondary structural unit set against matrix of interconnected orthovughs. Viewed under plain light; magnification approx. 12.5 x.

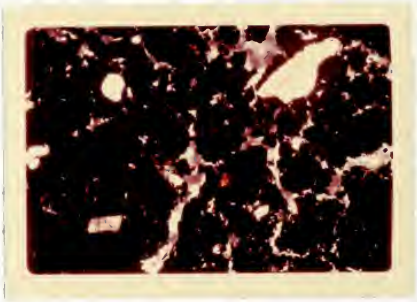

Fig. 33.--Photomicrograph of A11 horizon, profile 3 showing isotic plasmic fabric. Light areas displaying undulose extinction are interconnected orthovughs and planes. Viewed under crossed nicols; magnification approx. 12.5 x.

Fig. 34.--Photomicrograph of A12 horizon, profile 3 showing feldspar grain with weathering fractures perpendicular to twins. Note isotic plasmic fabric. Viewed under crossed nicols; magnification approx. 12.5 x.

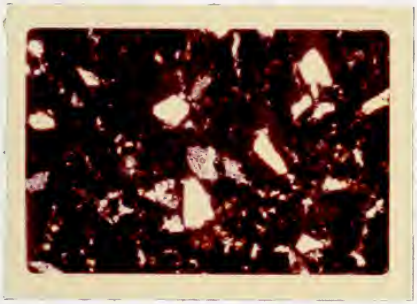

Fig. 35.--Photomicrograph of [illegible] horizon, profile 3 showing weakly silasepic and undulic plasmic fabric. Viewed under crossed nicols; magnification approx. 12.5 x.

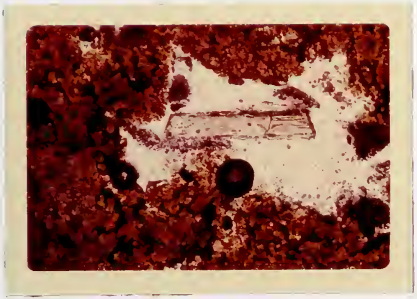

Fig. 36.--Photomicrograph of [illegible] horizon, profile 3 showing hornblende grain with thin, siliceous isotropic border. Hornblende is setting in an orthovugh. Black spherical forms due to entrapped air bubbles during section preparation. Viewed under plain light; magnification approx. 50 x.

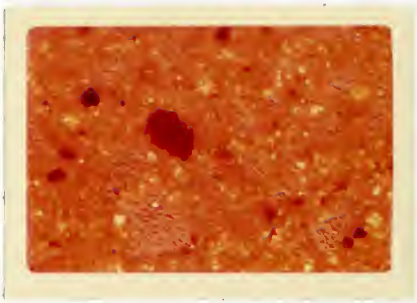

Fig. 37.--Photomicrograph of [B] horizon, profile 3 showing large sesquioxidic (hematitic) nodule and several smaller ones. Viewed under reflected sodium light; magnification approx. 12.5 x.

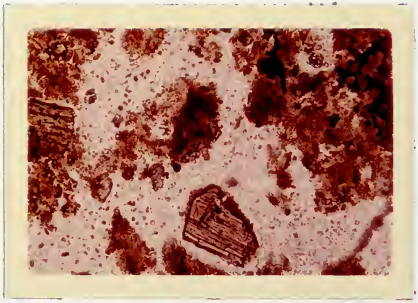

Fig. 38.--Photomicrograph of C horizon, profile 3 showing hornblende grain with thin, discontinuous sesquan (hematan) set against matrix of interconnected orthovughs. Viewed under plain light; magnification approx. 50 x.

of micromorphologic phenomena observed in the above mentioned sequence. Data from Appendix Table II will be discussed as to trends occurring with profile depth and increasing elevation. These data will also be organized according to the following categories as outlined by Brewer (1964): Pedality, voids, cutans, glaebules, fecal pellets, pedotubules, c-matrix, and special features (lithorelicts, mineralogy, etc.).

Descriptive Features

Pedality

In contrast to field descriptions (Appendix Table 8), which generally exhibited rather weak structural units, the A horizons of profiles 1-6 were remarkably pedal when observed in thin section. Surface horizons generally displayed both a primary and secondary level of structure. The primary structural level tended to have poorly formed faces and was generally classified as rounded blocky. Secondary structural units generally had somewhat better formed faces and were noted as subrounded blocky. These forms were noted in field descriptions by a statement such as: "moderate medium subangular blocky breaking into fine medium granular structure." There was some tendency to weak pedality or even spedality in subsurface horizons especially in profiles 1 and 2. There were no major trends in pedality with altitudinal changes.

Voids

Perhaps the most striking micromorphologic feature of profiles 1-6 was the extremely open, porous aspect of their fabric. The A horizons characteristically were composed of strongly interconnecting orthovughs with occasional interconnected ortho-craze planes. Subsurface horizons tended to retain a vughy nature but also took on more planar characteristics as evidenced by interconnected orthocraze planes and ortho-joint

planes. Since void patterns are to some degree dependant upon structural forms it was not surprising to note as before that there were no significant trends with elevation.

Cutans

Cutans are modifications of the soil plasma which occur on natural surfaces (Brewer, 1964). This feature is most commonly thought of as referring to "clay skins" or argillans occurring on faces of structural units and/or mineral grains. Actually cutans can be composed of any component substances able to be modified in the soil material. Cutans occurring in Nariño Andosols were predominantly composed of organic and/or sesquioxidic compounds with a minimal contribution by layer silicates. Cutanic materials in surface horizons were dominated by organic colloids. The indeterminate basic fabric of these organans was indicative of unpreferred orientation with respect to the free grain surfaces. The organans tended to increase in thickness and continuity with increasing elevation. Cutan mineralogy became more sesquioxidic in subsurface horizons. Sesquans were generally rather thin and discontinuous on mineral surfaces. In some cases, especially in the lowest horizons, grain surfaces were completely free of cutans. Cutan composition tended to retain an organic character to greater profile depths at higher elevations.

Glaebules

Glaebules are recognizable units due to constituent concentration or fabric differentiation from enclosing material (Brewer, 1964). Glaebules may be composed of sesquioxides, manganese, carbonates, sulfates, silica, or clay minerals. Nariño Andosols generally contained many glaebules in the form of normal sesquioxidic nodules. The ses-

quioxide content was predominantly hematitic and in a few cases limonitic. Sesquioxidic nodules were particularly abundant at lower elevations. They also tended to increase in amount with profile depth.

Fecal pellets

Fecal pellets were a common feature in the A horizons of profiles 1-6. Frequency of occurrence decreased with profile depth and they were generally not observed in the lower B and C horizons.

Pedotubules

Pedotubules consist of soil material (skeleton grains or skeleton grains plus plasma) that has a tubular external form (Brewer, 1964). Pedotubules were a common occurrence in the A horizons of Mariño Andosols. They were characterized by organic plasma and classified as organic isotubules (orthotubules). Distribution of pedotubules paralleled that of fecal pellets.

S-matrix (basic structure)

By definition s-matrix is the material in which pedological features occur. S-matrix classification is dependent upon plasmic structure with qualifications regarding characteristics of associated voids and skeleton grains. S-matrixes can be further subdivided into elementary and primary structures (fabrics). Elementary fabric deals only with associations of specific pedological features with specific kinds of s-matrixes, while primary fabric deals with all pedological features (Brewer, 1964).

The A horizons of Mariño Andosols, with the exception of Profile 1, generally had isotic plasmic fabrics. The characteristics of associated voids tended to be highly vughy. The basic structure (s-matix) of

Mariño Andosol A horizons, with the exception noted above, were classified as agglomeroplasmic isotic. The elementary fabric of these horizons was modified by such pedologic features as cutans (organans), glaebules (normal sesquioxidic nodules), fecal pellets, and pedotubules (isotubules). Elementary fabric classification of the A horizons could be stated as follows: Cutanic (organans) glaebular (normal sesquioxidic nodules) fecal pedotubulic (organic isotubules) agglomeroplasmic s-matrix. Glaebular modification of elementary fabric tended to decrease with increasing elevation. The A horizon of profile I had a weakly undulic to silasepic plasmic fabric. The associated voids were crazed and fractured. The s-matrix of this horizon was classified as crazed fractured weakly undulic to silasepic. The elementary fabric was classified as cutanic (sesqui-organans) crazed fractured weakly undulic to silasepic s-matrix.

The subsurface (B and C) horizons of Mariño Andosols generally exhibited weakly undulic to silasepic plasmic fabrics at lower altitudes which were replaced by isotic plasmic fabrics at higher elevations. The basic structure of these horizons was classified as agglomeroplasmic weakly undulic to silasepic at lower altitudes and agglomeroplasmic isotic at higher elevations. The elementary fabric of subsurface horizons at lower elevations was generally classified as cutanic (thin discontinuous sesquans) glaebular (normal sesquiosidic nodules) agglomeroplasmic weakly undulic to silasepic s-matrix. On occasion skew and craze planes were superimposed on the agglomeroplasmic fabric especially in the lower B and C horizons.

Special features

The mineralogy of skeleton grains observed in thin section was

similar in content and distribution to data presented in Table 6. Skeleton grains in s-matrixes of all horizons in profiles 1-6 displayed a random distribution pattern without any specific orientation in regard to plasma and voids. According to Brewer (1964) this is the most commonly observed arrangement of skeleton grains in soil materials.

Andesite lithorelicts were commonly observed in Nariño Andosols. This igneous rock was noted to increase in content with increasing elevation and generally to decrease with profile depth. Glass observed in Nariño Andosols generally displayed a bubbly matrix.

Isotropic borders displaying high negative relief in thin section were noted on many mineral grain surfaces. This phenomenon tended to be most conspicuous in surface horizons. The thickness and continuity of these borders tended to increase with increasing altitude.

Genetic Interpretations

Interpretation of void formation is intimately connected with interpretation of the formation of peds. According to Brewer (1964, p. 363) "there can be no doubt that the same processes are responsible for the formation of both peds and interpedal voids."

Because it was necessary to air dry samples prior to impregnation, void size in Nariño Andosols was accentuated as observed in thin section. This was due to a high magnitude of shrinkage experienced upon drying. It is reasonable to assume that ped surfaces represented pre-existing planes of weakness and observed void forms and size existed in a similar manner on a smaller scale in proportion to the degree of shrinkage which occurred upon drying.

Since the Nariño Andosols contained high quantities of weatherable constituents the orthovughs may have been formed in part by differ-

ential weathering of mineral skeleton grains and complete removal of the weathering products by leaching. The interconnected nature of the orthovughs especially in A horizons could be due to a high degree of faunal activity and the profusion of roots. Ortho-skew and ortho-craze planes in subsurface horizons were most likely encouraged by the aforementioned drying process. Lower quantities of organic matter in these horizons probably discouraged formation of smaller structural units. The omnipresence of allophane assuredly has had a major role in the genesis of these voids. This role is difficult to ascertain. Allophanes' hydrophillic nature and magnitude of hydration would be influential in void formation especially during desiccation periods.

Cutans observed in the A horizons were predominantly composed of organic matter. They were most likely formed by illuviation processes. This involved movement of organic material in suspension with subsequent deposition on grain surfaces. Frei (1964) speculated that colloidal silica acted as a complexing and mobilizing agent for organic matter. Organans are probably intimate mixtures of organic matter, allophane, and possibly colloidal silica although presence of the latter two components is difficult to prove. Sesquioxidic cutans generally prevailed in subsurface horizons. The genesis of these sesquans probably involved both illuviation and diffusion processes. Their morphology suggests that they were formed by diffusion of soluble Fe from surrounding matrix and subsequent deposition on free grain surfaces. Allophane and colloidal silica illuviation have probably also been additional factors in sesquan genesis. Although vermiculite was detected in these soils its cutanic contribution was probably negligible since it occurred only in the coarse clay fraction hence has experienced only

minor illuviation. It is also suggested that anisotropic properties of oriented vermiculite were masked by opaque organic matter in A horizons and isotropic sesquioxides in lower horizons. The cutanic contribution of hydrated halloysite especially in the deepest horizons is open to speculation. Sesquan birefringence was not noted even in horizons of exceptionally high halloysite contents. This is not unusual since Cady (1965) indicated that halloysite, because of tubular habit, should not show birefringence even though it could form oriented aggregates.

The normal sesquioxidic nodules observed in Mariño Andosols were probably formed by accretion of iron hydroxides. The tendency of these nodules to increase with profile depth was presumably due to Fe-rich percolating water. The abundance of ferromagnesium minerals provided an adequate source of iron. Higher evapo-transpiration rates at lower altitudes has probably encouraged periodic high water tensions on natural surfaces which facilitated precipitation of iron hydroxides. This factor has also undoubtedly influenced cutan formation at lower elevations.

Presence of abundant fecal pellets and pedotubules in surface horizons of Mariño Andosols was a logical expectation considering the intense faunal activity observed in the field.

Isotic plasmic fabrics encountered in surface horizons of Mariño Andosols were due to domination of the plasma by organic matter. Quantification of allophane contribution to isotropism in these horizons was difficult to enumerate. X-ray diffraction and NaF test data indicate that allophane influence was considerable especially at higher elevations. Interpretation of silasepic to undulic plasmic fabrics especially in the low altitude Andosols is somewhat more complex.

Silasepic plasmic fabrics were due mainly to birefringent contribution by silt size mineral grains dispersed throughout the soil matrix in a random manner. This fabric gave a faint, flecked extinction pattern while rotating the microscope stage under crossed nicols. Brewer (1964) suggested that there was a high correlation between undulic fabric and relatively high proportions of iron oxides. He further stated that the mechanism was not understood, but iron oxides were known to flocculate and stabilize clay minerals. The author suggests that in the case of Nariño Andosols hydrated halloysite has contributed to the formation of undulic plasmic fabrics. Cady (1965) stated that halloysite does have very faint, patternless birefreingence possibly caused by refraction of light at interfaces between particles.

The ubiquitous presence of andesite lithorelicts was indicative of the prevailing bedrock of the Nariño highlands. Predominance of this component in soils of higher altitudes was in all likelihood due to closer proximity of ash source and decreased weathering severity. Isotropic borders on mineral grains were in all probability due to devitrification of volcanic ash and subsequent precipitation of opaline materials on mineral surfaces. Opal forms were variable of which many, morphologically, appeared to be phytogenic. However, many opal grains observed presumably were derived by precipitation from silica-rich soil solutions.

These micromorphological data reveal that fabric parameters such as pedality, voids, cutans, glaebules, fecal pellets, s-matrix, and mineralogical composition are in an organization exclusive of that observed in soils formed from non-volcanic ash parent materials under humid climatic conditions. It is suggested that this specific fabric

type may have a broad geographic distribution encompassing volcanic ash derived soils in other tropical and sub-tropical areas. The term "Andic" is proposed as a modifier for this unique plasmic fabric (Mejía, 1971).

SUMMARY

Ten soil profiles occurring in the Andean highlands of Departamento Nariño, southwestern Colombia, were investigated by use of chemical, physical, mineralogical, and micromorphological techniques in order to elucidate pedogenetic processes in soils derived from volcanic ash and similar parent materials. Six Andosol profiles, developing entirely in andesitic volcanic ash, were selected in an altitudinal sequence from 2,000 m to 3,510 m. These six profiles were assumed to represent near maximum range of weathering severity experienced by aeolian pyroclastic deposits in the altiplano of Nariño, Colombia. Four additional profiles, developing in other parent materials under varying degrees of ash influence, were investigated as ancillary sites to provide additional pedogenetic information. These soils were influenced by climates characterized by an annual rainfall range of 500 - 2,000 mm and an annual isothermal temperature range of 6C to 18C which was closely related to altitude.

The following physical, chemical, and mineralogical determinations were performed on selected horizons from each profile. (a) particle size distribution, (b) bulk density, (c) fifteen atmosphere water content, (d) soil reaction in water and N KCl, (e) exchangeable cations, (f) cation exchange capacity (g) organic carbon, (h) free iron oxides, (i) X-ray diffraction of fine clay ($<0.2\ \mu$) and coarse clay ($0.2\text{-}2\ \mu$), (j) infrared analysis of fine clay and coarse clay, (k) NaF test for allophane, and (l) light and heavy mineral content of sand ($50\text{-}500\ \mu$)

fraction. Differential thermal data were presented only for coarse clay of profiles 1 and 10 due to equipment failure. Thin sections were prepared from selected horizons of Andosol profiles 1-6 (2,000-3,510 m) and described according to the terminology of Brewer (1964).

Although the intent of this study was not method oriented, interesting points arose pertaining to clay mineralogical pretreatments. It was shown that much smaller amounts of Si, Fe, and Al were removed from selected Andosol horizons by using NaOCl (sodium hypochlorite) solution rather than H_2O_2 (hydrogen peroxide) for organic matter oxidation. Sodium hypochlorite appeared to be less destructive of sesquioxides, silica coatings, allophane, and crystalline clay minerals.

Adequate dispersion was obtained for Nariño Andosols after NaOCl treatment of surface soils and using 2% Na_2CO_3 on field moist subsurface samples. This observation was validated using zirconium nitrate as the best available standard. Zirconium nitrate was an efficient soil dispersing agent for Andosols; however, it formed precipitates with most accessory solutions used for saturation and washing of the colloidal complex in clay mineralogical studies.

The altitudinal sequence of profiles 1-6 exhibited definite morphological trends with increasing elevation. Maximum profile development occurred at lower elevations; however, surface horizon thickness tended to increase with increasing altitude. Profile 10, developing mainly in andesite residuum, was the only soil evolving an argillic horizon.

Soil reaction values were remarkably uniform for profiles 1-6 with a range of 5.1 - 5.9 in water and 4.2 - 5.3 in KCl. There was a tendency for pH values to increase with profile depth and to decrease with increasing altitude. Organic carbon contents tended to decrease

with depth and to increase for comparable depths below the A1 horizon with increasing altitude. Exchangeable calcium values generally decreased with profile depth and with increasing altitude for comparable depths. Consistent trends were not displayed by exchangeable Mg distributions. With the exception of profile 3, exchangeable K contents tended to decrease with depth for profiles 1-6. There was a general tendency for exchangeable K to decrease with increasing elevation. Exchangeable Na tended to decrease with increasing altitude; however, no noticeable trends were observed within individual profiles. With the exception of profile 3 total exchangeable bases for profiles 1-6 tended to decrease with depth. Exchangeable aluminum values tended to increase with increasing elevation and decrease with profile depth. Cation exchange capacity values were variable and did not display definite trends with profile depth or altitude. Free iron oxides tended to increase with depth and generally decreased with increasing elevation. Sodium fluoride reaction values indicated that all horizons of profiles 1-6 were dominated by allophane.

Particle size distribution data for profiles 1-6 indicated no evidence of clay illuvation. Bulk densities were characteristically low as expected for soils developed from aeolian pyroclastic materials. Fifteen atmosphere water contents were typically high reflecting the hydrophillic properties of allophane.

Feldspar was the dominant light mineral species generally followed in abundance by volcanic glass. Feldspar was present in greatest amounts generally at lower altitudes. Volcanic glass decreased with profile depth and increased with increasing altitude. Quartz was a minor light mineral constituent in all profiles investigated. There was some tenden-

cy for quartz content to decrease with increasing altitude. Hornblende was the dominant individual heavy mineral species except in profile 6 where the pyroxene group (augite and hypersthene) dominated the heavy mineral fractions of several horizons. Hornblende tended to decrease with profile depth and increasing elevation. The pyroxenes generally tended to increase with increasing elevation and profile depth.

X-ray diffraction and infrared data revealed that more identifiable crystalline components occurred in the coarse clay fraction than in the fine clay. Varying amounts of hydrated halloysite, metahalloysite, vermiculite, cristobalite, gibbsite, feldspar, and quartz were identified in the coarse clay fraction of Andosol profiles 1-6. Additionally illite and vermiculite-illite intergrade were noted in profiles 7 and 9. Varying amounts of hydrated halloysite, metahalloysite, and allophane A were identified in the fine clay fractions of Andosol profiles 1-6. Additionally, gibbsite was observed in the [B] and C horizons of profile 2. The fine clay of surface horizons of profiles 2, 3, and 5 and all of profile 6 were amorphous to X-rays. In both fine clay and coarse clay fractions, hydrated halloysite tended to increase with profile depth and to decrease with increasing elevation. Metahalloysite, when present, tended to be concentrated in surface horizons and decrease with depth. Vermiculite was observed only in the coarse clay fraction of upper horizons of profiles 1-6. No general trends for this component were displayed with altitude although greatest peak intensities were exhibited in profiles 1 and 2. Fine clay vermiculite was observed in accessory profile 8. Infrared data indicated the possible presence of allophane A in the fine clay fraction of surface horizons of profiles 2, 3, 5, and 6.

Differential thermal data indicated increasing crystallinity of coarse clay halloysite with depth in profile 1. Gibbsite was detected by thermal techniques in the coarse clay of profile 10. This component was not identified in profile 10 by X-ray or infrared analyses.

Micromorphological descriptions of selected horizons of profiles 1-6 were presented. Surface horizons of these soils were generally pedal displaying two levels of structure. The primary structural level was classified as rounded blocky while the secondary structural level was classified as subrounded blocky. There was week pedality with a tendency to apedality in subsurface horizons. All horizons were generally composed of interconnecting orthovughs;however,subsurface horizons took on more planar characteristics. There were no major trends in pedality or void patterns with increasing elevation. Cutans were predominantly organic and/or sesquioxidic with minimal contribution by layer silicates. The cutans had no preferred orientation with respect to free grain surfaces. Organans were more prevalent in surface horizons and sesquans prevailed in subsurface horizons. Sesquioxidic nodules were particularly abundant at lower elevations and tended to increase in amount with profile depth. Fecal pellets and pedotubules were common features of A horizons. The A horizons generally had isotic plasmic fabrics while subsurface horizons exhibited weakly undulic and silasepic plasmic fabrics at lower altitudes which were replaced by isotic plasmic fabrics at higher elevations. Andesite lithorelicts were noted to increase in content with increasing elevation and generally to decrease with profile depth. Glass and opal were commonly observed. Isotropic borders displaying high negative relief in thin section were noted on many mineral grain surfaces.

Micromorphological data suggested unique fabric relationships for Colombian Andosols; consequently the term "Andic" was proposed to connote this fabric.

CONCLUSIONS

Based on chemical, physical, mineralogical, and micromorphological data of selected Andosols occurring in the Andean highlands of southern Colombia the following conclusions were made:

1. Sodium hypochlorite is a more acceptable reagent than hydrogen peroxide for rapid routine organic matter oxidation prior to mineralogical analyses.

2. Maintenance of field-moist condition assures adequate dispersion by 2% Na_2CO_3.

3. Particle size data and macro- and micromorphological observations reveal no evidence of clay mineral translocation either within or between horizons.

4. Lack of significant profile development and distribution with depth of most chemical parameters indicates youthful soils.

5. Abundance of weatherable minerals particularly in the heavy mineral fraction is indicative of parent materials in their initial weathering cycle and of soils which have not reached a state of dynamic equilibrium with the factors of soil formation.

6. The tendency of hornblende to increase at the expense of hypersthene and augite with decreasing elevation indicates that pedologic weathering has proceeded more rapidly at lower altitudes.

7. A clay mineral weathering sequence of allophane ⟶ metahalloysite ⟶ hydrated halloysite is postulated. The maturation of this sequence increases with profile depth and decreasing elevation.

8. Vermiculite in the coarse clay fraction of Nariño Andosols is either transient or insufficient time has elapsed for its transformation to other 2:1 phyllosilicates.

9. It is postulated that vermiculite pedogenesis has occurred rather rapidly through direct formation with some modification from a primary mineral source.

10. Cutans observed in the A horizons are composed predominantly of organic matter while those observed in lower horizons are predominantly sesquioxidic.

11. Vermiculite and halloysite cutanic contribution is difficult to ascertain due to opacity of organic matter and iron oxides.

12. Presence of abundant fecal pellets and pedotubules in surface horizons is due to intense faunal activity.

13. Isotic plasmic fabrics encountered in surface horizons are due to domination of the plasma by organic matter; however, mineralogical data indicate that allophane contribution is considerable especially at higher elevation.

14. Silasepic plasmic fabrics are due mainly to birefringent contribution by silt size mineral grains dispersed throughout the soil matrix in a random manner.

15. Undulic plasmic fabrics are related to presence of iron oxides. It is also suggested this plasmic fabric type is related to high quantities of hydrated halloysite.

16. Presence of andesite lithorelicts is indicative of the prevailing bedrock of the Nariño highlands.

17. Isotropic borders on mineral grains are related to the weathering of volcanic glass.

18. Thin section investigations indicate that Mariño Andosols have unique microfabric relationships. The term "Andic Fabric" is proposed.

19. Pedogenesis of Mariño Andosols is closely related to climate.

APPENDIX

Table 3. Detailed field descriptions of selected Colombian soils

Horizon and Depth	Profile Description*
	Profile 1
	Location: North edge of Chachagui, 3 km south of Pasto airport. Classification: Andic Humitropept (Soil Survey Staff, 1970). Physiography: Dissected Andean uplands. Elevation: 2,000 m. Parent material: Andesitic volcanic ash. Slope: 8% convex. Drainage: Well drained. Natural vegetation: Dry subtropical forest. Present vegetation: Grasses, small trees, and shrubs. Approximate annual rainfall: 500 - 1,000 mm. Approximate annual air temperature: 18 C.
A1 0-45 cm	Very dark grayish-brown (10YR 3/2, moist) silt loam; medium weak to moderate subangular blocky structure; friable non-sticky, non-plastic; pedotubules in all stages of development usually with cross sectional size of 6-10 mm; organans not noticeable on sand grains; very few sesquioxidic nodules; abundant roots; clear wavy boundary; pH 6.5.
[B] 45-73 cm	Brown to dark brown (7.5YR 4/4, moist) silt loam; medium weak to moderate subangular blocky structure; friable slightly sticky, slightly plastic; no faunal activity observed at this depth; mineral grains and nodules are clean with no observable cutans; small sesquioxidic nodules are common; frequent roots; diffuse wavy boundary; pH 5.8.
C1 73-121 cm	Yellowish-brown (10YR 5/6, moist) silt loam; medium, weak to moderate subangular blocky structure; friable to firm slightly sticky, slightly plastic; no evidence of faunal activity; some very thin discrete sesquans on mineral grains and nodules; small sesquioxidic nodules are abundant; roots frequent in upper part and occasional in lower part of horizon; gradual wavy boundary; pH 6.0.

Table 8. Continued

Horizon and Depth	Profile Description*
C2 121-151 cm	Light yellowish-brown (10YR 6/4, moist) fine sandy loam; massive; firm slightly sticky, slightly plastic; a few very thin discrete sesquans on mineral grains and nodules; small sesquioxidic nodules are present but not as abundant as in the C1; none to occasional roots; abrupt smooth boundary; pH 6.2.
C3 151 cm +	Dark reddish-brown (5YR 3/4, moist) silty clay loam; massive; firm sticky and plastic; no roots; probably weathered volcanic tuff; pH 6.3.

Remarks: North toward Pasto airport soils are derived mainly from volcanic tuff. About 1 km south of the airport incipient duripan formation can be observed while north of the airport there are well developed duripans - often 2 or 3 in a roadcut. After sampling this profile, closer inspection with two Dutch pedologists of the air photo interpretation team in Bogotá revealed what they interpreted as occasional incipient durinodes in the C2 horizon.

Described and sampled by: Frank Calhoun and Dr. Carlos Luna.

Date: January 22, 1970.

Weather: Sunny and warm (26C).

Profile 2

Location: Pasto-Chachegui between km 24 and 25 markers.
Classification: Typic Dystrandept (Soil Survey Staff, 1970).
Physiography: Smoothly dissected Andean uplands.
Elevation: 2,150 m.
Parent material: Andesitic volcanic ash.
Slope: 32% convex.
Drainage: Well drained.
Natural vegetation: Dry lower montane forest.
Present vegetation: Blackberries, shrubs, and pasture grasses.
Approximate annual rainfall: 500 - 1,000 mm.
Approximate annual air temperature: 17C.

Table 8. Continued

Horizon and Depth	Profile Description*
A11 0-41 cm	Black (10YR 2/1, moist) silt loam; fine, weak subangular blocky structure; friable, non-sticky, non-plastic; faunal activity abundant as evidenced by pedotubules (worm castes); quartz and feldspar grains are thinly coated with organans; occasional sesquioxidic nodules observed with organic cutans; roots are abundant; diffuse irregular boundary; pH 6.0.
A12 41-58 cm	Black (10YR 2/1, moist) silt loam; medium, weak subangular blocky structure breaking into fine weak subangular blocky and granular structure; friable, non-sticky, non-plastic; faunal activity is abundant as evidenced by pedotubules which in some cases have a luster-like matrix; quartz and feldspar grains are thinly coated with organans; occasional sesquioxidic nodules observed with organic cutans; roots are abundant; diffuse irregular boundary; pH 6.0.
A3 58-70 cm	Very dark gray (10YR 3/1, moist) silt loam; weak, fine to medium subangular blocky structure; friable, non-sticky, non-plastic; occasional pedotubules observed; grain and nodule cutans are rather thin but continuous; sesquioxidic nodules are not overly abundant; frequent roots; gradual wavy boundary; pH 5.5.
[B] 70-96 cm	Yellowish-brown (10YR 5/8, moist) silt loam; weak medium subangular blocky structure; friable, non-plastic, non-sticky; no faunal activity observed at this depth; mineral grains and nodules are clean with no observable cutans; many small sesquioxidic nodules observed; few roots; diffuse irregular boundary; pH 5.3.
C 96-160 cm +	Yellowish-brown (10YR 5/6, moist) silt loam; massive breaking to very weak fine and medium subangular blocky structure; firm, non-plastic, slightly sticky; moderately smeary below 120 cm; no faunal activity; no observable cutans; many small sesquioxidic nodules observed; few roots; pH 5.5.

Described and sampled by: Frank Calhoun and Dr. Carlos Luna.

Date: January 22, 1970.

Weather: Sunny and Warm (24 C).

Table 8. Continued

Horizon and Depth	Profile Description*
	Profile 3
	Location: North slope of Eduardo Tufo farm overlooking the town of Narino. Classification: Typic Dystrandept (Soil Survey Staff, 1970). Physiography: Dissected Andean uplands. Elevation: 2,440 m. Parent Material: Andesitic volcanic ash. Slope: 10% convex. Drainage: Well drained. Natural vegetation: Moist lower montane forest. Present vegetation: Grass and eucalyptus. Approximate annual rainfall: 1,000 - 2,000 mm. Approximate annual air temperature: 15 C.
A11 0-50 cm	Black (10YR 2/1, moist) silt loam; very fine to fine, weak granular structure; very friable, non-sticky, non-plastic; moderately smeary; earthworm cavities and pedotubules are abundant; mineral grains have thin weakly adhesive organic coatings; abundant roots; very porous; diffuse wavy boundary; pH 6.0.
A12 50-100 cm	Black (10YR 2/1, moist) silt loam grading to very dark brown (10YR 2/2, moist) in lower part of horizon; weak fine granular structure; friable non-sticky, non-plastic; earthworm cavities and pedotubules are abundant; mineral grains have thin discrete to weakly adhesive coatings; roots abundant to frequent; very porous; clear, irregular boundary; pH 6.0
[B] 100-120 cm	Yellowish-brown (10YR 5/6, moist) silt loam to silty clay loam; weak medium subangular blocky structure; friable, non-sticky, slightly plastic; weakly smeary; very thin discrete sesquans on grains and nodules; roots are frequent; diffuse, wavy lower boundary; pH 5.5.
C 120 + cm	Yellowish-brown (10YR 5/6, moist) fine silt loam; weak, medium subangular blocky structure; friable to firm, non-sticky, slightly plastic; weakly smeary; thin discrete sesquens on a few grains and nodules; occasional roots; pH 5.5.

Described and sampled by: Frank Calhoun, and Dr. Carlos Luna.

Date: January 23, 1970.

Weather: Partly cloudy to rainy (16C).

Table 8. Continued

Horizon and Depth	Profile Description*
	Profile 4
	Location: 4Km 9 marker on east side of Pasto-airport road.
	Classification: Typic Dystrandept (Soil Survey Staff, 1970).
	Physiography: Dissected Andean uplands.
	Elevation: 2,730 m.
	Parent material: Andesitic volcanic ash.
	Slope: 36% convex.
	Drainage: Well drained.
	Natural vegetation: Dry lower montane forest.
	Present vegetation: Grass, ferns, and small shrubs.
	Approximate annual rainfall: 500-1,000 mm.
	Approximate annual air temperature: 14 C.
A1 0-63 cm	Black (10YR 2/1, moist) silt loam; weak fine subangular blocky breaking into weak fine granular structure; friable, non-sticky, non-plastic; very thin discrete organans on sand grains; many earthworm cavities and pedotubules; roots are abundant; diffuse wavy boundary; pH 5.8.
A3 63-88 cm	Very dark grayish-brown (10YR 3/2, moist) silt loam; weak medium subangular blocky breaking into weak fine granular structure; friable, non-sticky, non-plastic; very thin discrete organans on sand grains; earthworm cavities and pedotubules are frequent; roots are frequent; diffuse wavy boundary; pH 5.8.
[B] 88-115 cm	Dark yellowish-brown (10YR 4/4, moist) silt loam; weak, medium subangular blocky structure; friable, non-sticky, non-plastic; pedotubules and worm cavities in upper part of horizon; thin weakly adhesive sesquans on some sand grains; roots are frequent; weakly smeary; diffuse irregular boundary; pH 5.5.
C 115 cm +	Yellowish-brown (10YR 5/6, moist) silt loam; massive friable, non-sticky, non-plastic; thin weakly adhesive sesquans on some sand grains; roots are frequent; weakly smeary; pH 5.5.

Described and sampled by: Frank Calhoun and Dr. Carlos Luna.

Date: January, 28, 1970.

Weather: Cloudy (15 C).

Table 8. Continued

Horizon and Depth	Profile Description*
	Profile 5
	Location: Km 15 marker on east side of Pasto-Ipiales highway. Classification: Typic Dystrandept (Soil Survey Staff, 1970). Physiography: Dissected Andean uplands. Elevation: 3,120 m. Parent material: Andesitic volcanic ash. Slope: 10% convex. Drainage: Well drained. Natural vegetation: Humid montane forest. Present vegetation: Kikuyu grass. Approximate annual rainfall: 500-1,000 mm. Approximate annual air temperature: 11 C.
A1 0-55 cm	Black (10YR 2/1, moist) silt loam; moderate medium subangular blocky breaking into fine weak granular structure; friable, non-sticky, non-plastic; earthworm cavities and pedotubules are abundant; sand grains and nodules have thin weakly adhesive organans; roots are abundant; diffuse wavy boundary; pH 5.8.
AC 55-69 cm	Very dark brown (10YR 2/2, moist) silt loam in the upper part grading to dark brown (10YR 3/3, moist) in the lower part of the horizon; weak medium subangular blocky structure; friable, non-sticky, non-plastic; earthworm cavities and pedotubules are common; sand grains and nodules have thin weakly adhesive sesqui-organans; roots are frequent; diffuse wavy boundary; pH 5.5.
C1 69-94 cm	Dark yellowish-brown (10YR 3/4, moist) silt loam; weak medium subangular blocky structure; friable, non-sticky, non-plastic; occasional earthworm cavities and pedotubules; thin weakly adhesive sesqui-organans on sand grains; roots occasional to frequent; diffuse wavy boundary, pH 5.5.
C2 94-139 cm	Dark brown (10YR 3/3, moist) silt loam; very weak medium to coarse subangular blocky structure; friable, non-sticky, non-plastic; weakly smeary; thin weakly adhesive sesqui-organans on sand grains; roots occasional to frequent; diffuse wavy boundary; pH 5.5.

Table 8. Continued

Horizon and Depth	Profile Description*
IIC 3 139 cm +	Yellowish-brown (10YR 5/6, moist) silt loam; very weak medium subangular blocky structure; friable to firm, slightly sticky, slightly plastic; weakly smeary; thin weakly adhesive sesquans on some sand grains; roots occasional; pH 5.7.

Remarks: The IIC 3 horizon probably represents a major break in ash deposition. Dark colors in C1 and C2 may be due to organic staining.

Described and sampled by: Frank Calhoun and Dr. Carlos Luna.

Date: January 24, 1971.

Weather: Partly cloudy (15 C).

Profile 6

Location: "Paramo de Cumbal." Near a large lake which lies between outlying mountains and volcano Cumbal. About 10-12 km west of the village of Cumbal.
Classification: Dystric Cryandept (Soil Survey Staff, 1970).
Physiography: Smoothly dissected Andean uplands.
Elevation: 3,510 m.

Parent material: Andesitic volcanic ash and some pumice.
Slope: 5% convex.
Drainage: Well drained.
Natural vegetation: Subalpine grassland (paramo).
Present vegetation: Relatively undisturbed paramo with small shrubs, bunch grasses and most prominently espeletia sp. ("frailejon").
Approximate annual rainfall: 500-2,000 mm.
Approximate annual air temperature: 6 C.

01 5-0 cm	Sphagnum-like mat with grass roots.

Table 8. Continued

Horizon and Depth	Profile Description*
A1 0-38 cm	Black (10YR 2/1, moist) mucky silt loam; moderate medium granular structure; friable to firm, non-sticky, non-plastic; abundant earthworm cavities and pedotubules; thick weakly adhesive organans on sand grain surfaces; roots abundant; diffuse wavy boundary; pH 5.8.
As 38-51 cm	Gravelly stone line filled with A1 material, very porous.
IIA1b 51-98 cm	Black (10YR 2/1, moist) silt loam; massive; friable, non-sticky, non-plastic; thin to thick weakly adhesive organans on sand grain surfaces; roots frequent; diffuse wavy boundary; pH 6.0.
IIC1b 98-135 cm	Very dark grayish-brown (10YR 3/2, moist) sandy loam; massive; abundant light gray (10YR 7/1) pumiceous sand grains dispersed throughout the horizon; friable, non-sticky, non-plastic; sand grains are relatively free of coatings; roots are rare; diffuse wavy boundary; pH 6.8.
IIIA1b 135-190 cm	Black (10YR 2/1, moist) silt loam; massive; firm non-sticky, non-plastic; occasional light gray (10YR 7/1) pumiceous sand grains present; thin weakly adhesive organans on some sand grains; roots rare to absent; clear smooth boundary; pH 6.0.

Remarks: This is part of an extensive area of paramo extending from volcano Chiles to and past volcano Cumbal. At about 4,000 m, Cumbal and Chiles are quite often snow covered. Cumbal is the tallest volcano in southern Colombia at 4,890 m.

Described and sampled by: Frank Calhoun and Dr. Carlos Luna.

Date: January 25, 1971.

Weather: Partly cloudy (7 C).

Profile 7

Location: "El Pedregal" - 67 km northeast of Pasto, near Buesaco on road to Papayan.

Classification: Oxic Dystrandept (Soil Survey Staff, 1970).

Physiography: Dissected Andean uplands.

Table 8. Continued

Horizon and Depth	Profile Description*
	Elevation: 2,000 m. Parent material: Andesitic volcanic ash. Slope: 22% convex. Drainage: Well drained. Natural vegetation: Dry lower montane forest. Present vegetation: Grass and small trees. Approximate annual rainfall: 500-1,000 mm. Approximate annual air temperature: 18 C.
A1 0-50 cm	Black (10YR 2/1, moist) silt loam; weak medium granular structure; friable, non-sticky, non-plastic; thin discrete organans on some sand grains; earthworm cavities and pedotubules are abundant; diffuse wavy boundary; pH 5.6.
A3 50-67 cm	Very dark brown (10YR 2/2, moist) fine silt loam; weak medium to coarse subangular blocky structure; friable to firm, slightly sticky, slightly plastic; roots are frequent; diffuse wavy boundary; pH 5.5.
IIC 67 cm +	Dark reddish-brown (5YR 3/4, moist) silty clay loam; massive; firm.

Described and sampled by: Frank Calhoun and Dr. Carlos Luna.

Date: January 29, 1970.

Weather: Sunny (24 C).

Profile 8

Location: "La Siberia" - near town of Guachacal.
Classification: Typic Eutrandept?(Soil Survey Staff, 1970).
Physiography: Wide intermontane valley - "Sabana de Guachacal."
Elevation: 3,020 m.
Parent material: Ash-influenced alluvio-lacustrine deposits.
Slope: 0%.
Drainage: Well drained.
Natural vegetation: Humid montane forest.
Present vegetation: Small crops and pasture grasses.
Approximate annual rainfall: 500-1,000 mm.
Approximate annual air temperature: 12 C.

Table 8. Continued

Horizon and Depth	Profile Description*
A11 0-12 cm	Very dark gray (10YR 3/1, dry) sandy loam; weak fine granular structure; friable, non-plastic, non-sticky; thin weakly adhesive organans on sand grains; roots are abundant; gradual wavy boundary; pH 6.0.
A12 12-49 cm	Very dark gray (10YR 3/1, dry) fine sandy loam with pockets of light gray (10YR 7/1, dry) silt loam near center of horizon; weak fine granular structure; slightly hard when dry; firm, slightly plastic, slightly sticky, a few earthworm cavities; roots are abundant; diffuse irregular boundary; pH 6.0.
A13 49-67 cm	Dark grayish-brown (10YR 4/2, dry) fine sandy loam; massive except in upper part where there is weak fine granular structure; slightly hard when dry, firm when moist, slightly sticky, slightly plastic; a few earthworm cavities; roots are frequent; diffuse irregular boundary; pH 5.8.
A14 67-131 cm	Very dark gray (10YR 3/1, dry) silt loam; strong medium granular structure; slightly hard when dry; friable when moist, plastic, slightly sticky; occasional roots; abrupt smooth boundary; pH 5.5.
IIC1 131-152 cm	White (10YR 8/1, dry) silt; massive; very hard when dry, very firm when moist, slightly sticky, plastic; some iron segregation in the form of strong brown (7.5YR 5/6, dry) stains; abrupt smooth boundary; pH 5.8.
IIIA1b 152-159 cm	Very dark grayish-brown (10YR 3/2, dry) silt loam; moderate medium subangular blocky structure; firm slightly sticky, slightly plastic; some of IIC1 material admixed; clean smooth boundary.
IVC1b 159-165 cm	Dark gray (10YR 4/ , dry) loamy sand; structureless.
165-174 cm	Very dark gray (10YR 3/1, dry) silt loam.
174-179 cm	Light-colored sand.
179-188 cm	Admixture of dark sand and silt loam.
188-195 cm	White (10YR 8/1, dry) silt.

Table 8. Continued

Horizon and Depth	Profile Description*
195-206 cm	Light-colored sand.
206-211 cm	Black (10YR 2/1, dry) silt loam.
211-217 cm	Light-colored sand.
217-223 cm	Black (10YR 2/1, dry) silt loam.

Remarks: No evidence of allophane by NaF test. This is a large valley which appears to have a similar geomorpho-genesis to the "Sabana de Bogota." This site was sampled for the purpose of investigating the influence of local volcanic activity on lacustrine and alluvio-lacustrine soils. This profile has had a marked change in depositional history above and below 131 cm.

Described and sampled by: Frank Calhoun and Dr. Carlos Luna.

Date: January 27, 1971.

Weather: Sunny (15 C).

Profile No. 9

Location: Obonuco substation (ICA); flanks of volcano Galeras, overlooking the city of Pasto.
Classification: Typic Humitropept ? (Soil Survey Staff, 1970).
Physiography: Slope of semi-active volcano in Andean uplands.
Elevation: 3,060 m.
Parent material: Andesite and andesitic volcanic ash.
Slope: 22% convex.
Drainage: Well drained.
Natural vegetation: Humid montane forest.
Present vegetation: Grass.
Approximate annual rainfall: 500-1,000 mm.
Approximate annual air temperature: 11 C.

A11 0-27 cm	Black (10YR 2/1, moist) silt loam; strong medium granular structure; friable, non-sticky, slightly plastic; feunal activity evidenced by earthworm cavities and excreta; fungal hyphae on some ped surfaces; thin weakly adhesive organans on sand grain surfaces; roots are profuse; diffuse wavy boundary; pH 6.0.

Table 8. Continued

Horizon and Depth	Profile Description*
A12 27-66 cm	Black (10YR 2/1, moist) silt loam; weak medium subangular blocky structure breaking into strong medium granular structure; earthworm cavities and excreta are abundant; friable, non-sticky, slightly plastic; thin weakly adhesive organans on sand grains; roots are abundant; gradual wavy boundary; pH 5.8.
A3 66-88 cm	Very dark grayish-brown (10YR 3/2, moist) silt loam; weak medium subangular blocky breaking into weak fine and medium granular structure; friable, non-sticky, slightly plastic; few earthworm cavities at this depth; thin organans on sand grain surfaces; incipient placic horizon which is black (10YR 2/1, moist) at 83-88 cm sampled separately; roots are abundant; clear to gradual smooth boundary; pH 5.8.
C1 88-105 cm	Dark reddish-brown (5YR 3/4, moist) silt loam; weak medium subangular blocky breaking into weak fine granular structure; firm, non-sticky, slightly plastic; roots are common; diffuse irregular boundary; pH 5.8.
C2 105 cm +	Dark brown to brown (7.5 YR 4/4, moist) clay loam; moderate coarse subangular blocky structure with black (10YR 2/1, moist) ferromaganiferous stains covering about 20% of ped surfaces; very firm sticky, plastic; roots are rare; abundant weathered andesite cobbles up to 6 x 9 cm in size; pH 6.0.

Remarks: All horizons give a negative NaF test for allophanic colloids. This upland profile was selected to investigate mineralogy of soils morphologically similar to Andosols but apparently contain smaller quantities of allophane.

Described and sampled by: Frank Calhoun, Dr. V. W. Carlisle, and Dr. Carlos Luna.

Date: June 24, 1970.

Weather: Cloudy and cool.

Table 8. Continued

Horizon and Depth	Profile description*
	Profile 10
	Location: Km 26 marker on north side of Yacuanquer - Sandona road. Classification: Tropudalf ? (Soil Survey Staff, 1970). Physiography: Dissected Andean uplands. Elevation: 2,630 m. Parent material: Andesite and andesitic volcanic ash. Slope: 2% convex. Drainage: Moderately well drained. Natural vegetation: Dry lower montane forest. Present vegetation: Kikuyu grass and barley. Approximate annual rainfall: 500-1,000 mm. Approximate annual air temperature: 16 C.
A11 0-16 cm	Very dark grayish-brown (10YR 3/2, moist) silt loam; strong medium granular structure; friable, non-sticky, slightly plastic; few earthworm cavities; profuse roots; diffuse wavy boundary; pH 5.8.
A12 16-39 cm	Very dark grayish-brown (10YR 3/2, moist) silt loam; moderate fine subangular blocky structure; friable, non-sticky, slightly plastic; profuse roots; few earthworm cavities; diffuse wavy boundary; pH 5.8.
B1 39-50 cm	Dark brown (10YR 3/3, moist) fine silt loam; moderate medium subangular blocky structure; thin discontinuous, somewhat degraded yellowish-brown (10YR 5/4, moist) ferriargillans on 50% of ped surfaces; firm, slightly sticky, slightly plastic; roots are abundant; diffuse wavy boundary; pH 5.3.
B2t 50-85 cm	Dark yellowish-brown (10YR 3/4, moist) silty clay loam; strong medium subangular blocky structure with thin continuous yellowish-brown (10YR 5/4, moist) ferriargillans on ped surfaces; firm; sticky and plastic; roots are abundant along ped surfaces; clear irregular boundary; pH 4.9.
C 85-205 cm	Dark yellowish-brown (10YR 4/4, moist) silt loam; weak medium to coarse subangular blocky structure with occasional thin discontinuous yellowish-brown (10YR 5/4, moist) ferriargillans on vertical ped surfaces; firm to friable, non-sticky, slightly plastic; roots occur only in B2t tongues; pH 5.4.

Table 8. Continued

Horizon and Depth	Profile Description*
Remarks:	A IIB2tb horizon was sampled below the C-horizon of this profile. It was yellowish-brown (10YR 5/6, moist) clay loam; massive; very firm, sticky and plastic, NaF test results were negative for all horizons of this profile.
Described and sampled by:	Frank Calhoun, Dr. V. W. Carlisle, and Dr. Carlos Luna.
Date:	June 28, 1970.
Weather:	Sunny and mild.

* pH determinations were made with a Hellige-Truog (Colorimetric) kit.

Table 9. The d/n spacing of crystalline minerals recognized from X-ray diffraction patterns of the fine clay (<0.2μ) fraction of selected Colombian soils

Horizon	Treatments				
	Mg saturation[1]	Mg saturation and glycerol solvation[2]	K saturation[2]	Heated (100C)[2]	Heated (500C)[2]
	A spacing				
			Profile 1		
A1	10.0, 7.25, 4.38, 3.56	10.2, 7.25	10.0, 7.25	7.20	NA
[B]	10.0, 4.37, 3.32	10.2	10.0	7.41	NA
C1	10.0, 4.33, 3.30	10.1	10.0	7.25	NA
C2	10.0, 4.39, 3.32	10.1	10.0	7.37	NA
C3	9.71, 4.35, 3.35	10.9	10.0	7.25	NA
			Profile 2		
A11	No peaks	NA	NA	NA	NA
A12	No peaks	NA	NA	NA	NA
A3	No peaks	NA	NA	NA	NA
[B]	10.0	10.2	10.0	7.41	NA
C	10.0, 7.25, 4.49, 3.34	10.4, 7.25	10.0	7.37	NA
			Profile 3		
A11	No peaks	NA	NA	NA	NA
A12	No peaks	NA	NA	NA	NA
C	14.0, 10.0, 4.37, 3.37	14.2, 10.2	14.2, 10.0	13.8, 7.31	No peaks

Table 9. Continued

Horizon	Treatments				
	Mg saturation[1]	Mg saturation and glycerol solvation[2]	K saturation[2]	Heated (300C)[2]	Heated (500C)[2]
	A spacing				
			Profile 4		
A1	10.0, 7.25, 4.41, 3.36	10.3, 7.37	10.0, 7.25	7.37	NA
A3	10.1, 4.41, 3.36	10.2	10.1	7.25	NA
[B]	10.0, 4.39, 3.42, 3.36	10.1	10.0	7.25	NA
C	10.0, 4.39, 3.40	10.2	10.0	7.25	NA
			Profile 5		
A1	15.0-14.0	15.0-14.0	14.5-14.0	NA	No peaks
AC	15.0-14.0	15.0-14.0	14.3-14.0	NA	No peaks
C1	10.2	10.3	10.0	7.49-7.25	NA
C2	10.0, 4.35	10.3	10.0	7.37	NA
IIC3	10.0	10.2	10.0	7.55-7.25	NA
			Profile 6		
A1	No peaks	NA	NA	NA	NA
IIA1b	No peaks	NA	NA	NA	NA
IIC1b	No peaks	NA	NA	NA	NA
IIIA1b	No peaks	NA	NA	NA	NA

Table 9. Continued

Horizon	Treatments				
	Mg saturation[1]	Mg saturation and glycerol solvation[2]	K saturation[2]	Heated (100C)[2]	Heated (500C)[2]
	A spacing				
		Profile 7			
A1	10.0, 7.31, 4.37, 3.53	10.3, 7.25	10.0, 7.25	7.49-7.25	NA
A3	10.0, 7.31, 4.37, 3.53	10.1, 7.31	10.0, 7.25	7.31	NA
IIC	10.0, 7.19, 4.37, 3.36	10.2, 7.31	10.0, 7.31	7.31	NA
		Profile 8			
A11	15.1, 10.0, 4.46, 3.36	15.2, 10.3	14.6, 10.0	7.56-7.25	No peaks
A12	15.0, 10.2, 4.44	15.3, 10.3	14.8, 10.0	7.56-7.25	No peaks
A13	14.3, 10.1, 4.42	14.7, 10.3	14.1, 10.0	No peaks	No peaks
A14	14.3, 10.3, 4.44	14.4, 10.3	14.0, 10.0	13.9, 7.43	10.0
IIC	17.9, 10.0, 4.27	18.8, 10.2	17.0, 10.0	16.8	12.6-10.4
		Profile 9			
A11	9.95, 7.18, 4.41, 3.57	10.5, 7.24	10.0, 7.25	7.25	NA
A12	10.2, 7.43, 4.42, 3.75-3.60	10.8, 7.43	10.0, 7.37	7.37	NA
A3	10.2, 7.37, 4.40, 3.75-3.60	10.7, 7.43	10.0, 7.37	7.25	NA
C1	10.2, 7.37, 4.44, 4.17, 3.67, 3.36	10.8, 7.37	10.0, 7.31	7.37	NA
C2	10.0, 7.31, 4.33, 3.53, 3.29	10.6, 7.43	10.0, 7.25	7.31	NA

Table 9. Continued

Horizon	Treatments				
	Mg saturation[1]	Mg saturation and glycerol solvation[2]	K saturation[2]	Heated (100C)[2]	Heated (500C)[2]
	A spacing				
	Profile 10				
A11	10.0, 7.37, 4.40, 3.65	10.8, 7.43	10.0, 7.37	7.37	NA
A12	10.2, 7.43, 4.44, 3.60-3.70	10.8, 7.43	10.0, 7.43	7.43	NA
B1	10.0, 4.37, 3.72	10.8	10.0	7.37	NA
B2t	10.0, 4.40, 3.70	10.8	10.0	7.37	NA
C	10.0, 4.35, 3.70-3.60	10.6	10.0	7.37	NA
IIB2t	10.0, 4.37, 3.70	10.6	10.0	7.37	NA
	Km 119 Pasto-Ipiales				
B2tb	10.1, 4.41, 3.71	10.8	10.0	7.37	NA

NA Not applicable - 100C heat treatment made only when 10A peak present; 500 C heat treatment made only when 10A peak persisted after 100C treatment and/or 14A peak present.

1 3-32° two theta.

2 3-15° two theta.

Table 10. The d/n spacing of crystalline minerals recognized from X-ray diffraction patterns of the coarse clay (0.2-2μ) fraction of selected Colombian soils

Horizon	Treatments				
	Mg saturation[1]	Mg saturation and glycerol solvation[2]	K saturation[2]	Heated (100C)[2]	Heated (500C)[2]
	A spacing				
Profile 1					
A1	14.2, 10.0, 7.25, 4.39, 4.04, 3.56, 3.34	15.1, 10.2, 7.31	14.1, 10.1, 7.25	14.1-13.8, 7.25	10.0
[B]	14.2, 10.0, 4.37, 4.02, 3.33	15.2, 10.4	14.0, 10.2	13.9, 7.31	10.0
C1	14.2, 9.82, 4.29, 3.95, 3.26	14.5, 10.0	13.2, 10.0	13.1, 7.37	10.0
C2	14.2, 9.87, 4.39, 4.02, 3.32	14.2, 10.2	14.0, 10.0	14.2-13.8, 7.37	10.0
C3	9.93, 4.33, 3.97, 3.28	10.2	10.0	10.0, 7.43	10.0
Profile 2					
A11	14.2, 4.04, 3.35	14.5	14.0	NA[2]	10.0
A12	14.2, 4.06, 3.36	14.3	14.2	NA	10.0
A3	14.3, 4.83, 4.04, 3.34	14.5	14.3	NA	10.0
[B]	14.2, 10.0, 4.83, 4.37, 4.02, 3.35	14.7, 10.0	14.2, 10.0	13.2, 7.49	10.0
C	14.2, 10.0, 4.84, 4.35, 4.04, 3.34	14.3, 10.2	14.2, 10.0	13.8, 7.37	10.0

Table 10. Continued

Horizon	Treatments				
	Mg saturation[1]	Mg saturation and glycerol solvation[2]	K saturation[2]	Heated (100C)[2]	Heated (500C)[2]
	A spacing				
			Profile 3		
A11	14.2, 7.25, 4.06, 3.36	14.3, 7.25	14.2, 7.25	NA	10.0
A12	14.5, 4.06, 3.34	14.3	14.0	NA	10.0
C	14.3, 9.93, 4.37, 4.04 3.34, 3.24	14.3, 10.0	14.1, 10.0	13.9, 7.55	10.0
			Profile 4		
A1	14.2, 9.82, 4.39, 4.06, 3.34	14.2, 10.1	14.2, 10.0	14.2, 13.2, 7.25	10.0
A3	14.2, 9.98, 4.39, 4.02, 3.32, 3.20	14.2, 10.0	14.1, 10.0	14.0, 7.31	10.0
[B]	14.2, 10.0, 4.39, 4.04, 3.34, 3.22	14.2, 10.0	14.0, 10.0	14.0, 7.31	10.0
C	10.0, 4.44, 4.04, 3.34	10.0	10.0	7.43	NA
			Profile 5		
A1	14.3, 4.00, 3.23	14.5	14.0	NA	10.0
AC	14.2, 4.02, 3.34	14.5	14.0	NA	10.0
C1	14.2, 10.0, 4.04. 3.32	14.2, 10.0	14.0, 10.0	13.9, 7.55	10.0
C2	14.2, 10.0, 7.25, 4.41, 4.04, 3.36, 3.26	14.5, 10.1	14.2, 10.0	14.0, 7.43	10.0
IIC3	10.0, 4.04, 3.34	10.3	10.1	7.43	NA

Table 10. Continued

Horizon	Treatments				
	Mg saturation[1]	Mg saturation and glycerol solvation[2]	K saturation[2]	Heated (100C)[2]	Heated (500C)[2]
	A spacing				
			Profile 6		
A1	14.2, 7.20, 4.04, 3.56	14.7, 7.25	14.2, 7.20	NA	10.6
IIA1b	14.4, 4.08, 3.39	15.0	14.0	NA	10.2
IIC1b	14.5, 4.53, 4.09, 3.36, 3.24	15.2	14.2	NA	10.8
IIIA1b	14.2, 4.04, 3.34, 3.20	15.1	14.0	NA	no peaks
			Profile 7		
A1	14.2, 7.25, 4.44, 4.04, 3.34, 3.21	14.5, 7.25	14.2, 7.25	NA	10.1
A3	14.2, 9.93, 7.25, 4.44, 4.04, 3.56, 3.34, 3.14	14.7, 10.2, 7.31	13.8, 10.0, 7.25	14.1, 10.0, 7.25	10.2
IIC	10.0, 7.21, 4.37, 4.27, 4.04, 3.56, 3.34	10.2, 7.21	10.0, 7.21	10.0, 7.25	10.0
			Profile 8		
A11	14.2, 4.04, 3.60, 3.36, 3.20	15.2	14.0	NA	10.0
A12	14.2, 4.04, 3.20	15.0	14.0	NA	10.0
A13	14.2, 4.04, 3.34, 3.19	15.2	14.0	NA	10.0
A14	14.2, 4.02, 3.73, 3.33, 3.20	15.0	14.0	NA	10.0
IIC	14.2, 4.06, 3.37, 3.22	15.0	13.8	NA	no peaks

Table 10. Continued

Horizon	Treatments				
	Mg saturation[1]	Mg saturation and glycerol solvation[2]	K saturation[2]	Heated (100C)[2]	Heated (500C)[2]
	A spacing				
			Profile 9		
A11	14.5, 12.4, 10.0, 7.13, 4.41, 4.04, 3.74, 3.62 3.34, 3.20	15.2, 10.0, 7.25	13.8, 10.1, 7.25	14.2, 10.0, 7.25	10.0
A12	14.4, 12.4, 10.0, 7.25-7.13, 4.39, 4.02, 3.59-3.52, 3.32, 3.19	15.0, 12.5, 10.4, 7.31	13.9, 12.2, 10.0, 7.25	14.2, 10.0, 7.31	10.0
A3	14.2, 12.6-11.6, 9.82, 7.31, 4.37, 4.02, 3.32, 3.18	15.2, 13.0-11.8, 10.4, 7.35	14.2, 12.8, 10.0, 7.24	14.2, 7.28	10.0
C1	14.3, 10.0, 7.37, 4.37, 4.00, 3.32, 3.16	14.8, 10.5, 7.37	14.2, 10.0, 7.31	14.0, 7.27	10.0
C2	9.82, 7.43-7.25, 4.39, 4.04, 3.20	10.4, 7.43-7.25	10.0	10.1, 7.31	10.0
			Profile 10		
A11	14.2, 10.0, 7.49-7.19, 4.37, 4.00, 3.74, 3.32, 3.10	15.2, 10.4, 7.25	13.0, 10.0, 7.25	13.0, 7.25	10.0
A12	14.5, 10.0, 7.25, 4.41, 4.04, 3.75, 3.34, 3.23	15.2, 10.2, 7.25	14.0, 10.0, 7.25	14.0, 7.31	10.0
B1	14.7, 10.0, 7.59-7.25, 4.41, 4.05, 3.60, 3.34, 3.24	15.1, 10.3, 7.52	13.9, 10.0, 7.45	13.9, 7.25	10.0

Table 10. Continued

Horizon	Treatments				
	Mg saturation[1]	Mg saturation and glycerol solvation[2]	K saturation[2]	Heated (100C)[2]	Heated (500C)[2]
	A spacing				
B2t	14.6, 9.82, 7.25, 4.39, 4.02, 3.34	14.9, 10.3, 7.25	14.0, 10.0, 7.25	13.9, 7.25	10.0
C	14.2, 9.95, 4.40, 4.04, 3.33	15.0, 10.1	13.0, 10.0	13.0, 7.25	10.0
IIB2t	14.2, 9.85, 4.41, 4.04, 3.42, 3.34	14.5, 10.0	13.6, 10.0	13.6, 7.25	10.0
		Km 119 Pasto-Ipiales			
B2tb	10.0, 4.41, 4.04, 3.35, 3.22	10.0	10.0	10.0, 7.25	10.0

NA Not applicable - 100C heat treatment made only when 10A peak present; 500 C heat treatment made only when 10A peak persisted after 100C treatment and/or 14A peak present.

[1] 3-32° two theta.

[2] 3-15° two theta.

Table II. Micromorphology of selected Colombian Andosols

Horizon and Depth	Profile Description
	Profile 1
A1 0-45 cm	Two levels of pedality were noted in the A1 horizon. Secondary structural level was composed of peds with a polysphedral basic form while primary peds were both polysphedral and spheral. Secondary units exhibited low sphericity and roundness while primary peds displayed medium sphericity and roundness. Secondary peds were partially accomodated while primary units were mostly unaccomodated. Both levels of structure were characterized by random packing and vertical inclination. The specific form name at the secondary level was subrounded blocky while at the primary level it was rounded blocky. Macrovoids were abundant while meso- and microvoids were common in occurrence. The majority of the voids were irregular in conformation while a few macro- and mesovoids were curved. Most of the larger macrovoids were transpedal with the remainder interpedal. Meso- and microvoids were interpedal with a few intrapedal microvoids. The majority of the macrovoids were classified as ortho- craze planes including a few meta- craze planes. Meso- and microvoids were classified mainly as ortho-skew planes with a very few small orthovughs. A few cutans were observed on free grain surfaces. Boundary sharpness was rather diffuse with an indeterminate basic fabric. The cutans were slightly separated and discrete. Mineralogical nature was assumed to be a complex of amorphous alumino-silicates, sesquioxides and organic matter. Thus they were classified as complex amorpho-sesqui-organans. Glaebules were not common in this horizon. They were characterized by an undifferentiated internal fabric and mineralogically were both hematitic and limonitic. They had rather sharp boundaries and were weakly to moderately adhesive with spherical shapes. These glaebules were classified as normal sesquioxidic nodules. A large, slightly eroded fecal pellet was observed which had an associated neoorganan. A few other features with rounded forms and grossly concentric internal fabric were interpreted as single fecal pellets. No pedotubules were observed in this horizon. The plasmic fabric of this horizon was classified as weakly undulic to weakly silasepic. Due to the

Table 11. Continued

Horizon and Depth	Profile Description
	planar nature of this horizon, the s-matrix was classified as crazed and fractured weakly silasepic. The lithorelict content of this horizon was very low. Occasional small rhyolite and andesite lithorelicts with thin, oxidized peripherics and interiors were observed. Magnetite was common, however glassy, magmatic borders were not observed on mineral grains. Occasional opal phytoliths and glass shards were observed at 400X magnification. Some feldspars were noted with corroded edges. Hornblende was the dominant heavy mineral.
[B] 45-73 cm	A single level of structure was noted in this horizon. Basic form was generally spheral with isolated areas of polysphedral forms. Spheral units generally displayed high sphericity and medium roundness. Peds were partially accomodated to unaccomodated, randomly packed with a vertical inclination. Specific name for this structure was noted as rounded blocky. Few macrovoids were noted in this horizon while meso- and microvoids were common to abundant. Macrovoids were irregular in conformation while meso- and microvoids were irregular and curved. All voids were interpedal. Macrovoids were classified as ortho-craze planes while meso- and microvoids took the form of both ortho-craze planes and orthovughs. Meso- and micro-ortho-craze planes and orthovughs were moderately interconnected. A few cutans were observed on some free grain surfaces. Boundary sharpness was rather diffuse and basic fabric was indeterminate. Cutans were slightly separated and discrete. Mineralogical nature of cutans was assumed to be a combination of amorphous aluminosilicates and sesquioxides. Cutans were classified as complex amorpho-sesquans. Glaebules were numerous in the form of nodules. Their internal fabric was undifferentiated and sesquioxidic in nature (>95% hematitic). They had rather diffuse to rather sharp boundaries and were moderately adhesive with spherical shapes. They were classified as normal sesquioxidic nodules. Many nodules had central quartz or feldspar grains. No fecal pellets or pedotubules were observed at this depth.

Table 11. Continued

Horizon and Depth	Profile Description
	The plasmic fabric of this horizon was classified as weakly undulic to silasepic. The s-matrix was classified as glaebular moderately agglomeroplasmic weakly undulic to silasepic. The lithorelict content of this horizon was low. Occasional fine-grain andesitic lithorelicts with oxidized peripherics were observed. A few very small, corroded sialic (granitic) lithorelicts were noted. Magnetite was common along with hornblende and feldspars. The edges of some feldspars were corroded. No magmatic (glassy) borders were observed on mineral grains. Occasional glass and opal phytoliths were observed.
C1 73-121 cm	Two levels of structure were noted in this horizon. Secondary structural level was composed of peds with a polysphedral basic form while primary peds were spheral. Secondary peds displayed low sphericity and low to medium roundness while primary units had medium sphericity and roundness. Secondary peds were partially accomodated while primary peds were unaccomodated. Both levels of pedality were characterized by random packing and vertical inclination. Specific form names were subrounded and rounded blocky for secondary and primary peds, respectively. Meso- and microvoids were abundant while macrovoids were common in occurrence. Most macrovoid walls were curved and a few were irregular. Meso- and microvoid walls were mostly irregular while a few were curved. Macrovoids were mostly transpedal while meso- and microvoids were interpedal. Macrovoids were classified as ortho-skew planes. Meso- and microvoids were noted as interconnected orthovughs and some ortho-craze planes. Cutans were confined mostly to free grain surfaces with only a few observed on nodules. They were characterized by rather diffuse boundaries with an indeterminate basic fabric. The cutans were slightly separated and discrete to weakly adhesive. Mineralogical nature was assumed to be a combination of amorphous alumino-silicates and sesquioxides. Cutans were classified as complex amorpho-sesquans (hematans). Glaebules were numerous in the form of nodules. Internal fabric was undifferentiated and sesquioxidic (>95% hematitic) in nature. They had rather sharp to diffuse boundaries and were moderately to strongly

Table 11. Continued

Horizon and Depth	Profile Description
	adhesive with generally spherical shapes. They were classified as normal sesquioxidic (hematitic) nodules. No fecal pellets or pedotubules were observed. The plasmic fabric of this horizon was classified silasepic. The s-matrix was noted as glaebular agglomeroplasmic silasepic. The lithorelict content was very low. A few andesitic and granite lithorelicts were noted. Magnetite content was low and feldspars displayed corroded peripheries. Glass and opal phytoliths were uncommon and magmatic borders were absent on mineral grains.
C2 121-151 cm	This horizon was apedal (structureless or massive). Mesovoids accounted for approximately 70% of the total void space while microvoids occupied the remainder. The voids, classified as orthobughs, were irregular in conformation and intrapedal in arrangement. Free grain and imbedded cutans were observed at this depth. Boundary sharpness of cutans was diffuse with indeterminate basic fabric. Cutans were slightly separated and discrete to weakly adhesive. They were classified as sesquans and appeared to be very weakly developed simple sesquans. Some glaebules were observed in the form of normal sesquioxidic (hematitic) nodules. The nodules had an undifferentiated internal fabric. They were moderately to strongly adhesive with rather diffuse to diffuse boundaries and spherical shapes. Fecal pellets and pedotubules were not observed. The plasmic fabric was classified as silasepic. The s-matrix was classified as glaebular vughy silasepic. Rhyolitic, andesitic, and granitic lithorelicts were observed. Magnetite, hornblende, and feldspars were abundant. Biotite was also observed at this depth. Glassy borders on mineral grains were not noted. Opal phytoliths were common but glass content was low. This horizon was considerably more skeletal than overlying horizons. Feldspars had a generally fresh aspect.
	Profile 2
A11 0-41 cm	Both secondary and primary levels of pedality were noted. Secondary structural level was composed of

Table 11. Continued

Horizon and Depth	Profile and Description

polysphedral forms while the primary level consisted of both spheroidal and polyspheral forms. Secondary peds displayed high sphericity and medium roundness. Secondary peds were partially accomodated to accomodated while primary peds were partially accomedated to unaccomodated. Both levels of pedality had vertical inclination with random packing. Specific form names were rounded blocky for primary peds and subrounded blocky for secondary peds.

Meso- and microvoids were abundant while macrovoids were common. Void walls in general were irregular however a few were curved. Voids generally displayed an interpedal arrangement. The voids were classified as strongly interconnected orthovughs however a few compound packing voids were noted.

Both free grain and imbedded grain cutans were observed. Cutans had rather diffuse to rather sharp boundaries with an indeterminate basic fabric. They were slightly separated and weakly adhesive to discrete. Mineralogical nature was assumed to be a combination of organic matter and amorphous alumino-silicates. Cutans were classified as complex amorpho-organans.

Two classes of glaebules were observed, both with an undifferentiated internal fabric. One group was essentially organo-sesquioxidic (limonitic) in nature. These glaebules had sharp boundaries and were discrete. They had irregular rounded shapes and were classified as normal organo-sesquioxidic nodules. A second group was sesquioxidic (limonitic) with diffuse to rather sharp boundaries. They were weakly to moderately adhesive. These glaebules had spherical shapes and were classified as normal sesquioxidic nodules.

Both single and welded fecal pellets were observed. A few discrete, elliptical organic isotubules (up to 5 x 9 mm) were observed.

The plasmic fabric of this horizon was classified as isotic. Due to the strongly interconnected vughy nature of this horizon the s-matrix was classified as agglomeroplasmic isotic.

Andesite lithorelicts were common along with a few rhyolites. The majority of lithorelicts were fresh in aspect. Lithorelicts accounted for 10-20% of the sand fraction. Opal phytoliths were commonly observed. Magnetite was common along with feldspars and hornblende. Glassy borders were noted on several mineral grains.

Table 11. Continued

Horizon and Depth	Profile Description
	Lithorelicts and mineral grains were fresh in aspect showing little evidence of weathering.
A12 41-58 cm	Secondary structural level of this horizon was composed of peds with a polysphedral basic form while primary peds were spheral. Secondary peds had medium sphericity and roundness. Polysphedral forms were partially accomodated while spheral forms were unaccomodated. Both levels of pedality were characterized by random packing and vertical inclination. Macrovoids were common in occurrence while meso- and microvoids were abundant. Voids were irregular in conformation and interpedal in arrangement. They were classified as strongly interconnected orthovughs. Free grain, nodule and lithorelict cutans were noted. Boundary sharpness was rather diffuse with an indeterminate basic fabric. They were slightly separated and weakly adhesive to discrete. Mineralogical nature was assumed to be a combination of organic matter and amorphous alumino-silicates consequently they were classified as complex amorphe-organans. Glaebules were common in occurrence. Internal fabric was undifferentiated and sesquioxidic (limonitic and hematitic) in nature. They had rather sharp boundaries and were weakly adhesive to discrete with spherical shapes. Many of the glaebules had a quartz grain nucleus. Glaebules were classified as normal sesquioxidic (hematitic, limonitic) nodules. A few single fecal pellets were observed. Welded fecal pellets were observed with difficulty. A few discrete, eiliptical organic pedotubules (up to 4 x 8 mm) were noted. The plasmic fabric was classified as isotic. Due to the strongly interconnected vughy nature of this horizon the s-matrix was classified as agglomeroplasmic isotic. Andesite lithorelicts were common in occurrence along with those of a pumiceous, glassy nature. More highly birefringent granitic lithorelicts were also observed. Mafic minerals with glassy borders were common. Opal and glass were noted.
A3 58-79 cm	The pedality at this depth was based on spheral forms which were classified as rounded blocky.

Table II. Continued

Horizon and Depth	Profile Description
	Macro- and mesovoids were abundant and microvoids were common in occurrence. Voids were irregular in conformation and generally interpedal in arrangement. The voids were classified as strongly interconnected orthovughs however a few spherical orthochambers up to 2.5 - 3 cm. in diameter were noted. Thin, continuous grain and nodule cutans were observed. Boundary sharpness was diffuse with an indeterminate basic fabric. Cutans were weakly separated and moderately adhesive. Mineralogical nature appeared to be a complex of amorphous aluminosilicates, sesquioxides, and organic matter. These cutans could be classified as amorpho-sesqui-organans. Numerous glaebules were observed with an undifferentiated internal fabric and sesquioxidic mineralogy. They displayed sharp boundaries and were moderately adhesive. Spherical to ellipsoidal shapes were noted with diameter range 0.5 - 1.5 mm. A few glaebules were observed with compound internal fabrics (limonitic and organic) while most were hematitic. Glaebules in general were classified as normal sesquioxidic (hematitic) nodules. A few single fecal pellets were observed. Several pedotubules were noted in the form of discrete circular to mammilated isotubules. Diameter ranged up to 5 mm. The plasma composition of the isotubules had an organic-sesquioxidic appearance. Numerous, very fine meta-skew and meta-craze planes along with a few sesquioxidic nodules were observed as part of the isotubule fabric. Due to the isotic plasmic fabric and strongly interconnected highly vughy character of associated voids the s-matrix was classified as agglomeroplasmic glaebular pedotubulic isotic. Andesite and pumicecus, glassy lithorelicts were common in occurrence. Opal was commonly observed along with glassy borders around mafic minerals. Feldspars dominated the light-mineral fraction while hornblende was dominant in the heavy minerals. Magnetite was commonly observed.
[B] 70-96 cm	Weakly developed polysphedral forms were noted at this depth which were classified as subrounded peds. Their arrangement was characterized by partial accomodation, random packing, and vertical inclination.

Table II. Continued

Horizon and Depth	Profile Description
	Macrovoids were common and meso- and microvoids were abundant. All voids displayed irregular conformation. Macrovoids were generally interpedal while meso- and microvoids were intrapedal. Voids were classified as strongly interconnected orthovughs. Cutans were not observed at this depth. Glaebules were observed with an undifferentiated internal fabric and sesquioxidic mineralogical composition. Sharp to rather sharp boundaries were noted in most cases. They were discrete to moderately adhesive and spheroidal to ellipsoidal in shape. Glaebules were classified as normal sesquioxidic (hematitic) nodules. Fecal pellets and pedotubules were not observed. Plasmic fabric was mainly isotic with occasional weakly silasepic domains. The s-matrix was classified as agglomeroplasmic mainly isotic, partially silasepic. Andesite lithorelicts were common in occurrence along with those of a pumiceous, glassy nature. Glassy borders were noted around a few heavy and light minerals. Feldspars and hornblende dominated the light and heavy mineral fractions, respectively. Opal and magnetite was commonly observed.
C 96-160+ cm	Structural forms in this horizon were confined to weakly developed polysphedral forms while in many cases there was a strong tendency to apedality. The polysphedral units displayed low sphericity and roundness. The peds were partially accomodated with normal and random packing and vertical inclination. The specific form name was subrounded blocky. Macrovoids were common while micro- and mesovoids were abundant. Voids were irregular in conformation and were generally interpedal. Voids were classified as strongly interconnected orthovughs and ortho-craze planes. Cutans were not observed in this horizon. Glaebules were observed with undifferentiated internal fabric and sesquioxidic mineralogical composition. They had rather sharp boundaries and were moderately adhesive with spheroidal to ellipsoidal shapes. Glaebules were classified as normal sesquioxidic (hematitic and limonitic) nodules. Fecal pellets and pedotubules were not observed. Plasmic fabric was weakly undulic with some areas tending to silasepic. The s-matrix was classified as agglomeroplasmic planed weakly undulic to silasepic.

Table II. Continued

Horizon and Depth	Profile Description
	Lithorelict content was very low with occasional andesite lithorelicts noted. Glass was not observed while opal was common in occurrence. Glassy borders around mineral grains were not noted. Feldspars and hornblende were the dominant minerals observed. Magnetite was common.
	Profile 3
All 0-50 cm	Two levels of pedality were noted in this horizon. Secondary structural level was composed of peds with a polysphedral basic form while primary peds were spheral. Secondary units exhibited medium sphericity and low roundness while primary peds displayed high sphericity and medium roundness. Secondary peds were partially accomodated while primary peds were unaccomodated. Both structural levels were characterized by random packing and vertical inclination. The specific form name at the secondary level was subrounded blocky while at the primary level it was rounded blocky. Macro- and mesovoids were abundant while microvoids were common in occurrence. The majority of the voids were irregular in conformation while a few macrovoids had curved walls. Many macrovoids were transpedal but most were interpedal. Meso- and microvoids were interpedal. Voids were classified as interconnected orthovughs. Some macrovoids were classified as orthocraze planes. Free grain, nodule, and lithorelict cutans were noted. Boundary sharpness was rather diffuse to rather sharp with an indeterminate basic fabric. They were slightly separated and weakly adhesive to discrete. Mineralogical nature was assumed to be a complex of amorphous alumino-silicates, sesquioxides, and organic matter. The cutans were classified as complex amorpho-sesqui-organans. A few glaebules were observed with an undifferentiated internal fabric. They had rather sharp boundaries and were weakly adhesive with spheroidal shapes. Mineralogical nature was sesquioxidic (hamatitic and limonitic). Glaebules were classified as normal sesquioxidic nodules. Single fecal pellets were mostly observed with occasional welded specimens noted. A discrete, elliptical (9 mm x 5 mm) organic isotubule was noted.

Table 11. Continued

Horizon and Depth	Profile Description
	Plasmic fabric was isotic. Due to the strongly interconnected highly vughy nature of the associated voids the s-matrix was classified as agglomeroplasmic isotic. Andesitic lithorelicts were commonly observed however a few granitic specimens were also noted. A few andesites had oxidized peripheries while others appeared quite fresh. Some feldspars were noted with glassy (bubbly) interiors and glassy borders. Opal was commonly encountered and a few glass shards were noted.
A12 50-100 cm	Two levels of pedality were observed. Both levels were composed of peds displaying polysphedral basic forms. Secondary units had medium sphericity and roundness while primary peds displayed high sphericity and low roundness. Both structural levels were partially accomodated, with normal and offset packing and vertical inclination. Macro- and mesovoids were abundant while microvoids were few to common in occurrence. The majority of the voids were irregular in conformation while a few macrovoids had curved walls. Some macrovoids were transpedal however most were interpedal. Meso- and microvoids were interpedal in arrangement. Voids were classified as strongly interconnected orthovughs while some macrovoids were classified as ortho-craze planes. Free grain, nodule, and lithorelict cutans were observed. Boundaries were rather sharp and basic fabric was indeterminate. Cutans were slightly separated and weakly adhesive to discrete. Mineralogical nature was assumed to be a complex of amorphous alumino-silicates, sesquioxides, and organic matter. Cutans were classified as complex amorpho-sesquiorganans. Some glaebules were noted with undifferentiated internal fabric. Glaebules were mostly hematitic with a few limonitic in nature. They had rather sharp to rather diffuse boundaries and were discrete to weakly adhesive. The glaebules were classified as normal sesquioxidic (hematitic) nodules. A few welded and single fecal pellets were observed however no pedotubules were noted. Plasmic fabric was classified as isotic. The strongly interconnected highly vughy nature of the

Table 11. Continued

Horizon and Depth	Profile Description
	associated voids suggested a classification of agglomeroplasmic isotic for the s-matrix. Andesite lithorelicts were quite small in size but common in occurrence. Lithorelicts displayed various stages of peripheral oxidation. A large feldspar grain was noted with weathering zones perpendicular to twins. A few feldspar grains were noted with thin isotropic borders. Glass and opal were common to abundant in this horizon.
[B] 100-120 cm	Two levels of pedality were observed in this horizon. Secondary structural level was composed of peds with a polyhedral basic form while primary peds were spheral. Secondary units displayed high sphericity and low roundness. Secondary peds were accomodated while primary units were unaccomodated. Secondary units exhibited normal packing while primary peds were random but both units had vertical inclinations. The secondary level of pedality was classified as blocky while the primary level was classified as rounded blocky. Macro- and mesovoids were abundant while microvoids were very few in occurrence. The majority of the voids were irregular. Some macrovoids had curved walls and some were transpedal but most were interpadal. Meso- and microvoids were predominantly interpedal while a few microvoids were intrapedal. Voids were classified as strongly interconnected orthovughs while some macrovoids were classified as ortho-joint and ortho-craze planes. Free grain, nodule, and lithorelict cutans were noted at this depth. Boundaries were diffuse and basic fabric was indeterminate. Cutans were slightly separated and discrete. The mineralogical nature of the cutanic material was predominantly sesquioxidic. The cutans were thin and discontinuous. They probably contained some allophane and organic matter in addition to iron oxides. Cutans were classified as complex amorpho-sesquans (hematans). Two classes of glaebules were identified both with undifferentiated fabric. Both classes had sharp to rather sharp boundaries and were spherical in shape. Glaebules classified as normal sesquioxidic (hematitic) nodules were more numerous and were weakly to moderately adhesive. Discrete to weakly adhesive normal sesqui-manganiferous nodules were less common in occurrence.

Table 11. Continued

Horizon and Depth	Profile Description
	No fecal pellets were observed. A circular (3 mm diameter) weakly adhesive organo-sesquioxidic isotubule was identified. The plasmic fabric was classified as very weakly silasepic to undulic. The strongly interconnected highly vughy character of associated voids suggested an s-matrix classification of glaebular agglomeroplasmic weakly silasepic to undulic. Lithorelict content was low with those occurring quite small in size and tending to be more sialic in composition. Occasional glass shards were noted along with many opal phytoliths. Thin isotropic borders were observed on some mafic minerals and magnetite.
C 120 cm +	Two levels of pedality were identified at this depth. Secondary units were composed of peds with a polyhedral basic form while primary peds were polysphedral. Secondary peds exhibited medium sphericity and low roundness while primary units displayed high sphericity and medium roundness. Secondary peds were accomodated and had offset and bi-offset packing while primary units were partially accomodated with random packing. Both structural levels had vertical inclination. The secondary level of pedality was classified as blocky while the primary level was classified subrounded blocky. Macro- and mesovoids were abundant while microvoids were common in occurrence. The majority of the voids were irregular in conformation while some macrovoids had curved walls. Many macrovoids were transpedal however most were interpedal while meso- and microvoids were interpedal. Voids were classified as strongly interconnected orthovughs however some macrovoids were classified as ortho-joint and ortho-craze planes. Free grain and lithorelict cutans were observed. Cutans had diffuse boundaries and indeterminate basic fabric. They were slightly separated and discrete. cutans were very thin and discontinuous. Some surfaces were completely clean. The mineralogical nature of the cutans was sesquioxidic (hematitic) with probable inclusions of allophane. Cutans were classified as amorpho-sesquans (hematans). Glaebules were common but not abundant. They had rather sharp to rather diffuse boundaries and were discrete to weakly adhesive with spherical shapes.

Table 11. Continued

Horizon and Depth	Profile Description
	Mineralogical nature of the glaebular material was sesquioxidic (hematitic). Glaebules were classified as normal sesquioxidic nodules. Neither fecal pellets or pedotubules were observed in the C horizon. Plasmic fabric was classified as very weakly silasepic to undulic. Due to the strongly interconnected, highly vughy nature of associated voids the s-matrix was classified as agglomeroplasmic weakly silasepic to undulic. Lithorelict content was low with sialic and simatic species equally abundant. Those that occurred were small in size and some had thin oxidized peripheries. Occasional glass shards were noted along with several opal phytoliths. Thin isotropic borders were observed on some mineral grains.
	Profile 4
A1 0-68 cm	Two levels of pedality were observed. Both structural levels were polysphedral and were partially accomodated with normal packing and vertical inclination. Secondary units were characterized by low sphericity and roundness while primary units had medium sphericity and roundness. Both levels of pedality were classified as subrounded blocky. Macro- and mesovoids were abundant while microvoids were few in occurrence. Voids were generally irregular in conformation while many macrovoids had curved and bi-curved walls. Many macrovoids were transpedal however most were interpedal while meso- and microvoids were interpedal. Voids were classified as predominantly ortho-craze planes with some strongly interconnected orthovughs. Free grain, nodule, and lithorelict cutans were commonly observed with very diffuse boundaries and indeterminate basic fabric. They were slightly separated and weakly adhesive to discrete. The mineralogical nature of the cutanic material was predominantly organic with probable inclusions of sesquioxides and allophane. Cutans were classified as amorpho-organans. A few glaebules were observed with undifferentiated internal fabric. The mineralogical nature of the glaebular material was sesquioxidic. The glaebules had

Table II. Continued

Horizon and Depth	Profile Description
	rather sharp boundaries and were discrete to weakly adhesive with spherical shapes. They were classified as normal-sesquioxidic nodules. A few single fecal pellets were observed. Pedotubules with generally elliptical shapes (up to 7 x 4 mm), and organic plasma were noted. Pedotubules were weakly adhesive and classified as ortho-isotubules. The plasmic fabric was isotic and associated voids were characterized as crazed, highly vughy. The s-matrix was classified as agglomeroplasmic isotic. Andesite lithorelicts were common with variable feldspar content presenting a variety of groundmass textures. Occasional to common glass shards were identified but pumiceous character was not noted. Opal phytoliths were commonly observed at high magnifications. A few feldspars were noted with bubbly zones in their matrix and thin isotropic borders. Hornblende, magnetite and feldspar were the most commonly observed mineral species.
A3 68-88 cm	Two levels of pedality were identified in this horizon. Secondary units were composed of peds with a polysphedral basic form while primary peds were spheral. Secondary peds exhibited low sphericity and roundness. Primary units were unaccomodated while secondary units were partially accomodated. Both structural levels displayed ramdom packing and vertical inclination. The secondary level of pedality was classified as subrounded blocky while the primary level was designated as rounded blocky. Macro- and mesovoids were abundant while microvoids were few in occurrence. The majority of the voids were irregular in conformation while some macrovoids had curved walls. Voids were interpedal in arrangement however a few macrovoids were transpedal. Voids were classified as strongly interconnected orthovughs with a few macrovoids occurring as ortho-craze planes. Free grain and lithorelict cutans were identified at this depth. Cutans had very diffuse boundaries and indeterminate basic fabric. They were slightly separated and weakly adhesive to discrete. The mineralogical nature of the cutanic material was predominantly organic with probably inclusions of allophane and sesquioxides. Cutans were classified as amorpho-organans. A few glaebules were observed with undifferentiated internal fabric. The mineralogical nature of the

Table 11. Continued

Horizon and Depth	Profile Description
	glaebular material was sesquioxidic (hematitic). Glaebules had rather sharp boundaries and were weakly adhesive and spherical in shape. They were classified as normal sesquioxidic (hematitic) nodules. Some single fecal pellets were observed. Pedotubules with generally elliptical (up to 2 x 5 mm) shapes and organic-sesquioxidic plasma were identified. Pedotubules were weakly adhesive and classified as ortho-isotubules. The plasmic fabric was isotic. The s-matrix was classified as agglomerplasmic isotic. Andesite litharelicts were common along with glass and opal phytoliths. A few feldspars were noted with bubbly zones in their matrix and thin isotropic peripheries. Hornblende, magnetite, and feldspars were the most commonly observed mineral species.
[B] 88-115 cm	Two structural levels were noted in this horizon. Secondary peds were composed of polysphedral forms while primary level units were spheral in basic form. Secondary units displayed low sphericity and medium roundness while primary peds had high sphericity and medium roundness. Primary units were unaccomodated while secondary peds were partially accomodated. Both levels of structure exhibited random packing and vertical inclination. The secondary level of pedality was classified as subrounded blocky while the primary level was designated rounded blocky. Macro- and mesovoids were abundant while microvoids were few in occurrence. Most of the voids were irregular in conformation however some macrovoids had curved walls. Voids were interpedal in arrangement while a few macrovoids were transpedal. The voids were classified as strongly interconnected orthovughs and ortho-craze planes. The fabric of this horizon had a general broken fractured appearance. Free grain, nodule, and litharelict cutans were noted in this horizon. Cutans had very diffuse boundaries and indeterminate basic fabric. They were slightly separated and weakly adhesive to discrete. The mineralogical nature of the cutanic material was sesquioxidic with probable inclusions of allophane. The cutanic material was sesquioxidic with probable inclusions of allophane. The cutans were classified as complex amorpho-sesquans. Glaebules were commonly observed with undifferentiated internal fabric. The mineralogical nature of the

Table 11. Continued

Horizon and Depth	Profile Description
	glaebular material was sesquioxidic (hematitic). Glaebules had sharp to rather sharp boundaries and were discrete with spherical and occasionally irregular shapes. They were classified as normal sesquioxidic (hematitic) nodules. Some single fecal pellets were observed. A circular (3 mm diameter), sesquioxidic, moderately adhesive ortho-isotubule was identified. The plasmic fabric was undulic. The s-matrix was classified as glaebular agglomeroplasmic undulic. Andesite lithorelicts were common along with glass shards and opal phytoliths. A few feldspars and magnetite were noted with thin isotropic borders. Hornblende, magnetite, and feldspars were the most commonly identified mineral species.
C 115 cm +	Two levels of pedality were identified at this depth. Secondary structural level was composed of peds with a polysphedral basic form while primary peds were spheral. Secondary peds displayed low sphericity and medium roundness while primary units had high sphericity and medium roundness. Primary peds were unaccomodated while secondary units were partially accomodated. Both levels exhibited random packing and vertical inclination. Macro- and mesovoids were abundant while microvoids were few in occurrence. Meso- and microvoids were irregular in conformation while many macrovoids had curved walls. Voids were interpedal in arrangement however some macrovoids were transpedal. Voids were classified as strongly interconnected orthovughs and ortho-craze planes. This horizon was more planar than the overlying [B] horizon. Free grain, nodule, and lithorelict cutans were noted in this horizon. Cutans had very diffuse boundaries and indeterminate basic fabrics. They were slightly separated and discrete. The mineralogical nature of the cutanic material was predominantly sesquioxidic with probable inclusion of allophane. The cutans were very thin and discontinuous on affected surfaces. They were classified as complex amorpho-sesquans. Glaebules were commonly observed with undifferentiated internal fabric. The mineralogical nature of the glaebular material was sesquioxidic (hematitic). Glaebules had sharp boundaries and were weakly adhesive

Table II. Continued

Horizon and Depth	Profile Description
	to discrete. They were mostly spherical and, in some cases, irregular in shape. The glaebules were classified as normal sesquioxidic (hematitic) nodules. Neither fecal pellets or pedotubules were observed at this depth in the profile. The plasmic fabric was classified as undulic. Associated voids had a highly vughy and crazed character. The s-matrix was classified as glaebular agglomeroplasmic undulic. Andesite lithorelicts were not as common as in overlying horizons. Glass shards were rare but opal phytoliths were common. A few feldspars and magnetite were identified with thin isotropic borders. Hornblende, magnetie, and feldspars were the most commonly identified mineral species.
	Profile 5
A1 0-55 cm	Two levels of pedality were identified. Both structural levels were polysphedral with random packing and vertical inclination. Secondary peds displayed medium sphericity and low roundness while primary units had high sphericity and low roundness. Primary peds were accomodated while secondary units were partially accomodated. Both levels of pedality were classified as subrounded blocky. Macro- and mesovoids were abundant while microvoids were few in occurrence. Voids were generally irregular however many macrovoids had curved walls. Many macrovoids were transpedal however most were interpedal while meso- and microvoids were interpedal. Voids were classified as strongly interconnected orthovughs with some macrovoids classified as ortho-craze planes. Occasional single meta-channals were noted. Free grain, nodule, and lithorelict cutans were commonly observed with very diffuse boundaries and indeterminate basic fabric. They were slightly separated and weakly adhesive to discrete. The mineralogical nature of the cutanic material was predominantly organic with probable inclusions of sesquioxides and allophane. Cutans were classified as complex amorphoorganans. A few glaebules were observed with undifferentiated internal fabric. The mineralogical nature of the glaebular material was sesquioxidic (hematitic).

Table 11. Continued

Horizon and Depth	Profile Description
	Glaebules had rather sharp boundaries and were discrete to moderately adhesive with spherical to irregular shapes. They were classified as normal sesquioxidic (hematitic) nodules. A few single fecal pellets were observed. Pedotubules with generally elliptical shapes (up to 5 x 7 mm) and organic plasma were noted. They were weakly adhesive and classified as ortho-isctubules. The plasmic fabric was isotic and associated voids were strongly interconnected highly vughy and crazed. The s-matrix was classified as agglomeroplasmic isotic. Andesite lithorelicts were quite small and numerous. Some lithorelicts were permeated with oxidized iron. Isotropic borders were common but thin on mineral grains. Glass and opal were frequently observed. Feldspars and hornblende were most commonly noted mineral species.
AC 55-69 cm	A single level of pedality was observed at this depth. Structural units were polysphedral in basic form with high sphericity and low roundness. The peds were partially accomodated with random packing and vertical inclination. Macro- and mesovoids were abundant while microvoids were few in occurrence. Voids were generally irregular however a few macrovoids had curved walls. The largest of the macrovoids were transpedal while most were interpedal. Meso- and microvoids were interpedal. The voids were classified as strongly interconnected orthovughs with a few macrovoids occurring as ortho-craze planes. Free grain, nodule, and lithorelict cutans were commonly noted with very diffuse boundaries and indeterminate basic fabric. They were slightly separated and weakly adhesive to discrete. Cutans were thin and discontinuous on grain surfaces. The mineralogical nature of the cutanic material was predominantly organic with probable inclusions of sesquioxides and allophane. They were classified as complex amorpho-sesqui-organans. A few glaebules were observed with undifferentiated internal fabric. The mineralogical nature of the glaebular material was sesquioxidic (hematitic). Glaebules had rather sharp boundaries and were discrete to weakly adhesive with spherical to irregular shapes.

Table II. Continued

Horizon and Depth	Profile Description
	They were classified as normal sesquioxidic (hematitic) nodules. A few single fecal pellets were identified. Pedotubules with generally elliptical shapes (up to 3 x 5 mm) and organic plasma were noted. They were weakly adhesive and classified as ortho-isotubules. Plasmic fabric was isotic and associated voids were highly vughy and crazed. The s-matrix was classified as agglomeroplasmic isotic. Numerous andesite lithorelicts along with a few rhyolitic in nature were observed. Isotropic peripheries were common and in some cases relatively thick on many mineral surfaces. Glass and opal were frequently observed. Feldspars and hornblende were the most commonly observed mineral species.
C2 94-139 cm	Two levels of pedality were observed at this depth. Secondary structural level was composed of peds with a polysphedral basic form while primary peds were spheral. Secondary peds displayed medium sphericity and low roundness while primary units had high sphericity and medium roundness. Both structural levels exhibited random packing and vertical inclination. Secondary forms were partially accomodated but primary units were unaccomodated. The former was subrounded blocky while the latter was rounded blocky. Macro- and mesovoids were abundant while very few microvoids were observed. The largest of the macrovoids were transpedal while most were interpedal. Meso- and microvoids were interpedal. Voids were irregular in conformation. They were classified as strongly interconnected orthovughs. Free grain and lithorelict cutans were commonly observed with very diffuse boundaries and indeterminate basic fabric. They were slightly separated to weakly adhesive. The cutans were very thin and discontinuous; the majority of grain surfaces were unaffected. The mineralogical nature of the cutanic material was predominantly sesquioxidic with inclusions of organic materials and allophane. They were classified as complex amorpho-organo-sesquans. A few glaebules were observed with undifferentiated internal fabric. The mineralogical nature of the glaebular material was sesquioxidic (hematitic). They had rather sharp boundaries and were weakly to moderately adhesive with spherical and occasionally

Table II. Continued

Horizon and Depth	Profile Description
	irregular shapes. The glaebules were classified as normal sesquioxidic (hematitic) nodules. Neither fecal pellets or pedotubules were observed. The plasmic fabric was isotic. The character of associated voids was highly vughy. S-matrix classification was agglomeroplasmic isotic. Andesite and occasional rhyolite lithorelicts were observed at this depth. Thick isotropic boundaries were common on many mineral grain surfaces. Glass was occasionally observed along with frequent opal phytoliths. Feldspars and hornblende were the most commonly observed mineral species.
IIC3 139 cm +	Two structural levels were noted in the IIC3 horizon. Both levels were composed of peds with a polysphedral basic form. Both structural units displayed random packing with vertical inclination and were partially accomodated. Secondary units exhibited low sphericity and roundness while primary peds had high sphericity and low roundness. The specific form name in both cases was subrounded blocky. Macro- and mesovoids were abundant while microvoids were common in occurrence. Voids were generally irregular in conformation however many macrovoids had curved walls. The largest macrovoids were transpedal; however, most were interpedal. Meso- and microvoids were interpedal. Voids were classified as strongly interconnected orthovughs and ortho-craze planes. This horizon was highly planar with a general vertical inclination of planes. Free grain and lithorelict cutans were occasionally observed with very diffuse boundaries and indeterminate basic fabric. They were slightly separated and weakly adhesive to discrete. The cutans were very thin and discontinuous; the majority of grain surfaces were unaffected. The mineralogical nature of the cutanic material was predominantly sesquioxidic with inclusions of allophane. They were classified as complex amorphosesquans. Glaebules were frequently observed with undifferentiated internal fabric. They had rather sharp boundaries and were discrete to moderately adhesive with spherical to occasionally irregular shapes. The mineralogical nature of the glaebular material was sesquioxidic (hematitic). Glaebules were classified as normal sesquioxidic (hematitic) nodules.

Table II. Continue.

Horizon and Depth	Profile Description
	Neither fecal pellets or pedotubules were observed. The plasmic fabric was isotic with occasional very weak domains of undulic and silasepic. The character of associated voids was highly vughy and crazed. The s-matrix was classified as glaebular agglomeroplasmic isotic. Andesite and occasional rhyolite lithorelicts were noted. Isotropic borders were not evident on mineral surfaces. Glass was not common however opal was frequently observed. Feldspar and hornblende were the most frequently encountered mineral species.
	Profile 6
A1 0-38 cm	Two levels of pedality were identified. Secondary structural level was polysphedral while primary peds were spheral. Secondary peds displayed low sphericity and roundness while primary units exhibited high sphericity and low to medium roundness. Both structural levels had random packing with vertical inclination. The secondary units were partially accomodated while primary units were unaccomodated. The former was classified as subrounded blocky while the latter was rounded blocky. Macro- and mesovoids were abundant while few microvoids were identified. Voids were generally irregular in conformation while a few macrovoids had curved walls. Macrovoids were generally interpedal however a few were noted with transpedal arrangement. Meso- and microvoids were interpedal. Voids were classified as strongly interconnected orthovughs with occasional ortho-craze planes. Free grain lithorelict cutans were commonly observed with very diffuse boundaries and indeterminate basic fabric. They were slightly separated and discrete. The cutans were very thin and discontinuous. Their mineralogical nature was predominantly organic with probable inclusions of sesquioxides and allophane. Cutans were classified as complex amorpho-organans. A few glaebules were noted with undifferentiated internal fabric. Their mineralogical nature was sesquioxidic (hematitic). They had rather sharp boundaries and were weakly adhesive with generally spherical shapes. Glaebules were classified as normal sesquioxidic (hematitic) nodules.

Table II. Continued

Horizon and Depth	Profile Description
	Both welded and single fecal pellets were observed. Pedotubules were noted in the form of moderately adhesive, elliptical (up to 3 x 5 mm) ortho-isotubules. They were characterized also by organic plasma composition. The plasmic fabric was isotic and associated voids were characterized by a highly vughy nature. The s-matrix was classified agglomeroplasmic isotic. Andesite was the dominant lithorelict identified. Some feldspars were noted with bubbly matrix. Glass and opal phytoliths were frequently encountered. Isotropic borders were a common occurrence on most mineral grains. Pyroxenes appeared to be in greater abundance than hornblende. Feldspars dominated the light mineral fraction.
IIAlb 51-98 cm	A single level of pedality was noted in this horizon. Peds had a polysphedral basic form with high sphericity and medium to low roundness. They were partially accomodated with random packing and vertical inclination. The peds were classified as subrounded blocky. Macro- and mesovoids were abundant however microvoids were not observed. They were irregular in conformation and interpedal in arrangement. Voids were classified as strongly interconnected orthovughs. Free grain, nodule, and lithorelict cutans were commonly encountered with very diffuse boundaries and indeterminate basic fabric. They were slightly separated and discrete. The mineralogical nature of the cutanic material was predominantly organic with probable inclusions of allophane. Cutans were classified as complex amorpho-organans. Occasional glaebules were observed with undifferentiated internal fabric. They had rather sharp boundaries and were weakly adhesive with spherical shapes. Their mineralogical nature was sesquioxidic (hematitic). Glaebules were classified as normal sesquioxidic (hematitic) nodules. A few single and welded pellets were observed however no pedotubules were identified. Plasmic fabric was isotic and associated voids were highly vughy. The s-matrix was classified agglomeroplasmic isotic. Numerous fresh andesite and a few rhyolite lithorelicts were noted. Glass and opal phytoliths were

Table II. Continued

Horizon and Depth	Profile Description
	frequently encountered. Most mineral species including magnetite had thick isotropic boundaries. Hornblende and feldspars were dominant mineral species.
IIC1b 98-135 cm	This horizon was classed as apedal. Voids occurred as mostly macro- and mesovoids. They were irregular in conformation and intrapedal in arrangement. The voids were classified as interconnected orthovughs. Free grain and lithorelict cutans were commonly noted with very diffuse boundaries and indeterminate basic fabric. They were slightly separated and discrete. Their mineralogical nature was mostly organic with considerable inclusions of allophane and other amorphous components. The cutans were classified as complex amorpho-organans. A few glaebules were observed with undifferentiated internal fabric. They had rather diffuse boundaries and were moderately to strongly adhesive with irregular shapes. Glaebules were classified as diffuse sesquioxidic nodules. No fecal pellets or pedotubules were identified. Plasmic fabric was isotic and associated voids were highly vughy. The s-matrix was classified agglomero-plasmic isotic. Andesite was the dominant lithorelict identified. Isotropic borders were a common occurrence on the majority of mineral grains. Glass and opal were abundant. Hornblende and feldspars were dominant mineral species.
IIIA1b 135-190 cm	Both levels of pedality had polysphedral basic forms. They were partially accomodated with random packing and vertical inclination. Secondary units had low sphericity and low to medium roundness while primary peds had high sphericity and medium roundness. Both structural levels were designated as subrounded blocky. Macro- and mesovoids were abundant while microvoids were few in occurrence. Voids were irregular in conformation with the exception that some macrovoids had curved walls A few of the macrovoids were trans-pedal but most were interpedal. Voids were classified as strongly interconnected orthovughs with some ortho-craze planes.

Table 11. Continued

Horizon and Depth	Profile Description
	Free grain and lithorelict surfaces were affected by cutans. The cutans had very diffuse boundaries and indeterminate basic fabric. They were slightly separated, discrete, thin, and discontinuous. The mineralogical nature of the cutanic material was predominantly organic with probable inclusions of sesquioxides and allophane. They were classified as complex amorpho-organans. Two classes of glaebules were identified, both with undifferentiated internal fabric. The less commonly encountered glaebules class had spherical shapes and were rather sharp and weakly adhesive. Their mineralogical nature was organo-sesquioxidic. They were classified as normal organo-sesquioxidic nodules. The most abundant group had irregular shapes and were rather diffuse and moderately adhesive. Their mineralogical composition was sesquioxidic (hematitic). These glaebules were classified as diffuse sesquioxidic (hematitic) nodules. Both welded and single fecal pellets were observed. Pedotubules were noted in the form of moderately adhesive, circular (2mm diameter) ortho-isotubules. Plasmic fabric was isotic and associated voids were highly vughy. The s-matrix was classified agglomeroplastic isotic. Andesite lithorelicts were numerous and often permeated and covered with oxidized iron. Glass and opal were frequently encountered. Isotropic borders were common on mineral grain surfaces. Magnetite was permeated with oxidized iron. Mineral grains and lithorelicts appeared to be more highly weathered than overlying horizons.

LITERATURE CITED

Adachi, T. 1963. On the humus compositions of volcanic ash soils in Kashima, Ibaragi Pref. (Part I). Jour. Sci. Soil Manure 34:278-290.

Ahmad, N. and S. Prashad. 1970. Dispersion, mechanical composition and fractionation of West Indian volcanic yellow earth soils (andepts). Jour. of Soil Sci. 21:63-71.

Anonymous. 1964. Summary and technical discussion. World Soil Resources Report, FAO 14:139-142.

Aomine, S. and K. Egashira. 1968. Flocculation of allophanic clays by electrolytes. Soil Sci. Pl. Nutr. 14:94-98.

Aomine, S. and M. L. Jackson. 1959. Allophane determination in Ando soils by cation exchange capacity delta value. Soil Sci. Soc. Amer. Proc. 23:210-214.

Aomine, S. and Y. Kobayashi. 1964a. Effect of allophane on the activity of some enzymes. Trans. 8th Intern. Cong. Soil Sci. III:697-703.

Aomine, S. and Y. Kobayashi. 1964b. Effects of allophane on the enzymatic activity of a Protease. Soil Sci. Pl. Nutr. 10:28-32.

Aomine, S. and N. Miyauchi. 1965. Imogolite of imogo-layers in Kyushu. Soil Sci. Pl. Nutr. 11:28-35.

Aomine, S. and N. Yoshinaga. 1955. Clay minerals of some well-drained volcanic ash soils in Japan. Soil Sci. 79:349-358.

Banco de la Republica. 1959. Atlas de Economia Colombiana. Aspecto Fisico y Geografico. Ed. B. Republica, Bogotá, Colombia.

Barrows, H. L. and E. C. Simpson. 1962. An EDTA method for direct routine determination of calcium and magnesium in soils and plant tissue. Soil Sci. Soc. Amer. Proc. 26:443-445.

Besoain, E. 1969a. Imogolite in volcanic soils of Chile. Geoderma 2:151-169.

Besoain, E. 1969b. Clay mineralogy of volcanic ash soils. Panel on Volcanic Ash Soils in Latin America. IAIAS, Turrialba, Costa Rica. p.1. 1 - p.1. 16.

Birrell, K. S. 1964. Some properties of volcanic ash soils. World Soil Resources Report. FAO 14:74-81.

Birrell, K. S. 1956. Determination of clay contents in soils containing allophane. N. Z. Jour. Agr. Res. 9:554-564.

Birrell, K. S. and M. Fieldes. 1952. Allophane in volcanic ash soils. Jour. Soil Sci. 3:156-166.

Birrell, K. S. and M. W. Gradwell. 1956. Ion-exchange phenomena in some soils containing amorphous mineral constituents. Jour. Soil Sci. 7:130-147.

Blake, G. R. 1965. Bulk density. In C. A. Black (ed.) Methods of Soil Analysis. Part I. Amer. Soc. Agron., Madison, Wisc. p. 375-377.

Blasco, L. M. 1969. Chemical characteristics of the volcanic ash soils of Nariño, Colombia. Panel on Volcanic Ash Soils in Latin America. IAIAS, Turrialba, Costa Rica. B. 8.1 - B. 8.9.

Bouyoucos, G. J. 1926. Estimation of the colloidal material in soils. Science 64:362.

Bower, C., R. F. Reitemeier and M. Fireman. 1952. Exchangeable cation analysis of saline and alkali soils. Soil Sci. 73:251-261.

Brewer, R. 1964. Fabric and Mineral Analysis of Soils. John Wiley and Sons, Inc., New York.

Cady, J. G. 1965. Petrographic microscope techniques. In C. A. Black (ed.) Methods of Soil Analysis. Part I. Amer. Soc. Agron., Madison, Wisc. p. 604-631.

Calhoun, F. G. 1968. A weathering characterization of two northeastern Ohio Aquic Fragiudalfs. M. Sc. Thesis, The Ohio State University. Columbus.

Campbell, A. S., B. D. Mitchell and J. M. Bracewell. 1968. Effects of particle size, pH and organic matter on the thermal analysis of allophane. (Note) Clay Min. Bull. 7:451-454.

Carlisle, V. W. 1962. The genetic relation of finer-textured horizons in some northeast Florida soils. Ph.D. Dissertation, University of Florida, Gainesville.

Cheng, K. L., R. H. Bray and T. Kurtz. 1953. Determination of total iron in soils by disodium dihydrogen ethylendiamine-tetracetate titration. Analytical Chemistry 25:347.

DeMumbrum, L. E. and G. Chesters. 1964. Isolation and characterization of some soil allophane. Soil Sci. Soc. Amer. Proc. 28:355-359.

Kechena, T. and C. Gessa. 1969. Variable charge exchange capacity of some allophanic materials. Agrochimica 13:11-17.

Espinal, S. and E. Montenegro. 1962. Formaciones vegetales de Colombia. Departamento Agrologico, Instituto Geografico "Agustin Codazzi." Bogotá, Colombia.

Farmer, V. C. and B. D. Mitchell. 1963. Occurrence of oxalates in soil clays following peroxide treatment. Soil Sci. 96:221-229.

Fieldes, M. 1955. Clay mineralogy of New Zealand soils. Part II: Allophane and related mineral colloids. N. Z. Jour. Sci. Tech. Bull. 37:336-350.

Fieldes, M. 1966. The nature of allophane in soils. Part I. Significance of structural randomness in pedogenesis. N. Z. Jour. Sci. 9:599-607.

Fieldes, M. and F. R. Furkert. 1966. Nature of allophane in soils. Part II. Differences in composition. N. Z. Jour. Sci. 9:608-622.

Fieldes, M. and K. W. Perrott. 1966. The nature of allophane in soils. Part III. Rapid field and laboratory test for allophane. N. Z. Jour. Sci. 9:623-629.

Fieldes, M. and R. K. Schofield. 1960. Mechanisms of ion adsorption by inorganic soil colloids. N. Z. Jour. Sci. 3:563-579.

Fieldes, M. and N. H. Taylor. 1961. Clay mineralogy of New Zealand soils. V. Mineral colloids and genetic classification. N. Z. Jour. Sci. 4:686-700.

Flach, K. 1964. Genesis and morphology of ash-derived soils in the United States of America. World Soil Resources Report. FAO 14:61-70.

Flach, K. 1969. The use of the 7th approximation for the classification of soils from volcanic ash. Panel on Volcanic Ash Soils in Latin America. IAIAS, Turrialba, Costa Rica. A.7.1 - A.7.18.

Frei, E. 1964. Micromorphology of some tropical mountain soils. In A. Jongerius (ed.) Soil Micromorphology. Elsevier Publ. Co., Amsterdam, Holland.

Frink, C. R. 1964. The effect of wash solvents on cation exchange capacity measurements. Soil Sci. Soc. Amer. Proc. 28:506-511.

Gradwell, M. W. and K. S. Birrell. 1954. Physical properties of certain volcanic clays. N. Z. Jour. Sci. Tech. Bull. 36:108-122.

Grim, R. E. 1968. Clay Mineralogy. McGraw-Hill, Inc., New York.

Hay, R. L. 1960. Rate of clay formation and mineral alteration in a 4,000 year-old volcanic ash soil on St. Vincent, B.W.I. Amer. Jour. of Sci. 258:354-368.

Holdridge, L. R. 1947. Determination of world plant formation from simple climatic data. Science 105:367-368.

Moung, K. H., S. Ushirs and G. D. Sherman. 1966. On the exchange properties of allophanic clays. Pacific Sci. 20:507-514.

Jackson, M. L. 1956. Soil chemical analysis - Advanced course. Pub. by the author, Dept. of Soils, Univ. of Wisc., Madison.

Jackson, M. L. 1958. Frequency distribution of clay minerals in major great soil groups as related to the factors of soil formation. Proc. 6th Nt. Clay Cong., Pergamon Press, New York. pp. 133-143.

Kanno, I., Y. Onikura and T. Higashi. 1968. Weathering and clay mineralogical characteristics of volcanic ashes and pumices in Japan. Trans. 9th Intern. Cong. of Soil Sci. III:111-122.

Kawasaki, H. and S. Aomine. 1966. So called IHA clay minerals in some ando soils. Soil Sci. Pl. Nutr. 2:144-150.

Kinter, E. B. and S. Diamond. 1956. A new method for preparation and treatment of oriented-aggregate speciments of soil clays for X-ray diffraction analysis. Soil Sci. 81:111-120.

Kobo, K. and T. Fujisawa. 1964. Studies on clay-humus complex (Part 4). Preferential adsorption of humic acid by clay. Jour. Sci. Soil and Manure 35:40-46.

Kobo, K. and Y. Oba. 1965. Dispersion of clay fraction of volcanic ash soil by sonic treatment. Jour. Sci. Soil and Manure 36:207-210.

Kosaka, J. 1963. Division of the process of humification in upland soils and its application to soil classification. Soil Sci. Pl. Nutr. 9:14-18.

Kosaka, J., C. Honda and A. Iseki. 1962. Transformation of humus in upland soils, Japan. Soil Sci. Pl. Nutr. 8:23-28.

Kyuma, K. and K. Kawaguchi. 1964. Oxidative changes of polyphenols as influenced by allophane. Soil Sci. Soc. Amer. 28:371-374.

Lai, Sung-Ho and L. D. Swindale. 1969. Chemical properties of allophane from Hawaiian and Japanese soils. Soil Sci. Soc. Amer. Proc. 33:804-808.

Lavkulich, L. M. and J. H. Wiens. 1970. Comparison of organic matter destruction by hydrogen peroxide and sodium hypochlorite and its effects on selected mineral constituents. Soil Sci. Soc. Amer. Proc. 34:755-758.

Luna, C. 1969a. Genetic aspects of Colombian Andosols. Panel on Volcanic Ash Soils in Latin America. IAIAS, Turrialba, Costa Rica. A.3.1 - A.3.12.

Luna, C. 1969b. A pedological study of the soils of Antioquia, Columbia, South America with particular reference to Andosols. Ph.D. Dissertation. University of Utrecht, Holland.

Luna, C. 1970. Personal communication.

Mejía, C. L. 1971. Personal communication.

Mejía, G., J. Kohnke and J. L. White. 1968. Clay mineralogy of certain soils of Colombia. Soil Sci. Soc. Amer. Proc. 32:665-670.

Miller, F. P. 1965. Physical, chemical and mineralogical properties related to the micromorphology of the Canfield silt loam - a fragiudalf. Ph.D. Dissertation, The Ohio State University, Columbus.

Miyauchi, N. and S. Aomine. 1964. Does "allophane B" exist in Japanese volcanic ash soils? Soil Sci. Pl. Nutr. 10:199-203.

Miyauchi, N. and S. Aomine. 1966. Effects of exchangeable cations on the high temperature exothermic peak of alophane. Soil Sci. Pl. Nutr. 12:13-17.

Miyazawa, K. 1962. Distribution of clay minerals in the horizons of humified allophanic soils. I. Jour. Sci. Soil and Manure 33:317-321.

Mortensen, J. L., D. M. Anderson and J. L. White. 1965. Infrared spectrometry. In C. A. Black (ed.) Methods of Soil Analysis, Part II. Amer. Soc. Agron., Madison, Wisc. p. 743-770.

Müller, L., F. Balerdi, R. Diaz-Romeu and H. W. Fassbender. 1968. Estudio del fosforo en suelos de America Central. I. Ubicacion, caracteristicas fisicas y quimicas de los suelos estudiados. Turrialba 18:319-332.

Ohmasa, M. 1964. Genesis and morphology of volcanic ash soils. World Soil Resources Report, FAO 14:56-60.

Oinuma, K. and H. Hayashi. 1968. Infrafred spectra of clay minerals. Jour. Tokyo Univ. 9:57-98.

Orchiston, H. D. 1959. Adsorption of water vapor: 7. Allophane and some clay minerals at 25 degrees C. Soil Sci. 88:159-163.

Peach, M., L. T. Alexander, L. A. Dean and J. F. Reed. 1947. Methods of soil analysis for soil fertility investigations. USDA circular No. 757:11.

Pettry, D. E. 1969. Personal communication.

Perreau, R. B. and V. W. Carlisle. 1970. Clay mineral differential thermograms as affected by fired asbestos. Soil and Crop Sci. Soc. Fla. Proc., Vol. 30 (in press).

Rich, C. I. 1969. Suction apparatus for mounting clay specimens on ceramic tile for X-ray diffraction. Soil Sci. Soc. Amer. Proc. 33: 815-816.

Ross, C. S. and P. F. Kerr. 1934. Halloysite and allophane. U. S. Geol. Surv. Prof. Paper 185-G:135-148.

Russell, J. D., W. J. McHardy and A. R. Fraser. 1969. Imogolite: A unique alumino-silicate. Clay Min. Bull. 8:87-99.

Saunders, W. M. H. 1959. Effect of phosphate top dressing on a soil from andesitic volcanic ash. II. Effect on distribution of phosphorous and related chemical properties. N. Z. Jour. Agric. Res. 2:445-462.

Schalsa, E. B., C. Gonzalez, I. Vergara, G. Galindo and A. Schatz. 1965. Effect of drying on volcanic ash soils in Chile. Soil Sci. Soc. Amer. Proc. 29:481-482.

Soil Survey Staff. 1951. Soil Survey Manual. USDA Handbook No. 18. Gov't. Printing Office, Washington, D. C.

Soil Survey Staff. 1970. Soil Taxonomy (selected chapters from the unedited text). Soil Conservation Service, U. S. Department of Agriculture, Washington, D. C.

Steen, V. C. and R. Fryxell. 1965. Mazama and Glacier Peak pumice glass: Uniformity of refractive index after weathering. Science 150: 878-880.

Swindale, L. D. 1969. The properties of volcanic ash soils. Panel on Volcanic Ash Soils in Latin America. IAIAS, Turrialba, Costa Rica. B. 10.1 - B. 10.9.

Swindale, L. D. and G. D. Sherman. 1964. Hawaiian soils from volcanic ash. World Soil Resources Report, FAO 14:36-49.

Tan, K. H. 1964. The Andosols in Indonesia. World Soil Resources Report, FAO 14:30-35.

Tan, K. H. 1966. On the pedogenetic role of organic matter in volcanic ash soils under tropical conditions. Soil Sci. Pl. Nutr. 12:80-84.

Tercinier, G. and P. Quantin. 1968. Effect of the weathering of recent volcanic ash and pumice on the type, properties and fertility of soils in the Hebrides. Cah. Pedol. ORSTOM 6:203-224.

Tokudome, S. and I. Kanno. 1965a. Nature of the humus of humic allophane soils in Japan. Part I. Humic acids (Ch) fulvic acids (Cf) ratios. Soil Sci. Pl. Nutr. 11:1-8.

Tokudome, S. and I. Kanno. 1965b. Nature of the humus of humic allophane soils in Japan. Part II. Some physicochemical properties of humic and fulvic acids. Soil Sci. Pl. Nutr. 11:9-15.

Uchiyama, N., J. Masui and S. Shoji. 1968. Crystalline clay minerals of the soils derived from recent volcanic ashes in Hokkaido, Japan. I. Mineralogical composition of clay fractions. Soil Sci. Pl. Nutr. 14:125-132.

U. S. Salinity Laboratory Staff. 1954. Diagnosis and improvement of saline and alkali soils. USDA Handbook No. 60. Gov't Printing Office, Washington, D. C.

Van Olphen, H. 1971. Amorphous clay materials. Science 171:91-92.

Varela, J. 1963. Estudio general de suelos del sector Pasto-Rio Mayo. Instituo Geografico "Agustin Codazzi," Bogota, Colombia.

Wada, K. 1959. Reaction of phosphate with allophane and halloysite. Soil Sci.87:325-330.

Wada, K. 1966. Deuterium exchange of hydroxyl groups in allophane. Soil Sci. Pl. Nutr. 12:176-182.

Wada, K. 1967. A structural scheme of soil allophane. Amer. Miner. 52:690-708.

Wada, K. and H. Ataka. 1958. The ion uptake mechanism of allophane. Soil and Plant Food. 4:12-18.

Walkley, A. and I. A. Black. 1934. An examination of the Degtjareff method for determining soil organic matter and a proposed modification of the chromic acid titration method. Soil Sci. 37:29-38.

Whittig, L. D. 1965. X-ray diffraction techniques for mineral identification and mineralogical composition. In C. A. Black (ed.) Methods of Soil Analysis. Part I. Amer. Soc. Agron . Madison, Wisc. p. 676-681.

Wright, A. C. A. 1964. The "Andosols" or "Humic Allophane" soils of South America. World Soil Resources Report, FAO 14:9-22.

Yamazaki, F., T. Yawata and S. Sudo. 1963. Physical properties of Kanto Loam. Trans. Agric. Engng. Soc. Japan 7:1-13.

Yoshinaga, N. and S. Aomine. 1962a. Allophane in some Ando soils. Soil Sci. Pl. Nutr. 8:6-13.

Yoshinaga, N. and S. Aomine. 1962b. Imogolite in some Ando soils. Soil Sci. Pl. Nutr. 8:22-29.

Youngberg, C. T. and C. T. Dyrness. 1964. Some physical and chemical properties of pumice soils in Oregon. Soil Sci. 97:391-399.

Yuan, T. L. 1959. Determination of exchangeable hydrogen in soils by titration method. Soil Sci. 88:164-167.

BIOGRAPHICAL SKETCH

Frank Gilbert Calhoun, Jr., was born in South Charleston, West Virginia, on March 13, 1939. He received his elementary education in the Montgomery, West Virginia, school system. His family moved to Berlin Heights, Ohio, in 1952 where he completed his secondary education at Berlin Heights High School. Upon graduation in 1957 he entered the United States Army Reserve and served on active duty until January, 1958. He then entered the Ohio State University where in December, 1962, he received the degree Bachelor of Science in Agriculture. From 1963 to 1965 he divided his time between graduate studies at the Ohio State University and employment as a Conservationist with the Ohio Department of Natural Resources, Division of Lands and Soil. During this time period he contributed to surveys of Stark and Lorain counties in Ohio.

In June, 1965, he was employed as a Divisional Superintendent by the Firestone Plantations Company, Liberia, West Africa. Upon completion of a two-year contract in June, 1967, the author traveled extensively throughout Africa and Greece. He then re-entered the Graduate School of the Ohio State University and in August, 1968, received the degree Master of Science in Agriculture with a major in Soils.

He entered the Graduate School of the University of Florida in 1968, as a NDEA Title IV Fellow, during which time he has pursued his work toward the degree of Doctor of Philosophy.

Frank Gilbert Calhoun, Jr. is married to the former Nancy Helen

Platou. They have a daughter, Heather Suzanne. He is a member of the American Society of Agronomy and the Soil Science Society of America. He is also a member of Gamma Sigma Delta agricultural honor fraternity and Sigma Xi research honorary society.

I certify that I have read this study and that in my opinion it conforms to acceptable standards of scholarly presentation and is fully adequate, in scope and quality, as a dissertation for the degree of Doctor of Philosophy.

Dr. Elizabeth Carlisle
Elizabeth W. Carlisle, Chairman
Associate Professor of Soil Science

I certify that I have read this study and that in my opinion it conforms to acceptable standards of scholarly presentation and is fully adequate, in scope and quality, as a dissertation for the degree of Doctor of Philosophy.

Robert E. Caldwell
Robert E. Caldwell
Professor of Soil Science

I certify that I have read this study and that in my opinion it conforms to acceptable standards of scholarly presentation and is fully adequate, in scope and quality, as a dissertation for the degree of Doctor of Philosophy.

Hugh L. Popenoe
Hugh L. Popenoe
Professor of Soil Science and Geography

I certify that I have read this study and that in my opinion it conforms to acceptable standards of scholarly presentation and is fully adequate, in scope and quality, as a dissertation for the degree of Doctor of Philosophy.

Frank N. Blanchard
Frank N. Blanchard
Associate Professor of Geology

I certify that I have read this study and that in my opinion it conforms to acceptable standards of scholarly presentation and is fully adequate in scope and quality, as a dissertation for the degree of Doctor of Philosophy.

Ariel E. Lugo
Assistant Professor of Botany

This dissertation was submitted to the Dean of the College of Agriculture and to the Graduate Council, and was accepted as partial fulfillment of the requirements for the degree of Doctor of Philosophy.

August, 1971

Asst Dean, College of Agriculture

Dean, Graduate School

8641 4